1993-04-01

Nuclear Structure Studied by Fluorescence Hybridization: Visualization of Individual Gene Transcription and RNA Splicing: A Thesis

Yigong P. Xing
University of Massachusetts Medical School

NUCLEAR STRUCTURE STUDIED BY FLUORESCENCE HYBRIDIZATION: VISUALIZATION OF INDIVIDUAL GENE TRANSCRIPTION AND RNA SPLICING

A THESIS PRESENTED
BY
YIGONG P. XING

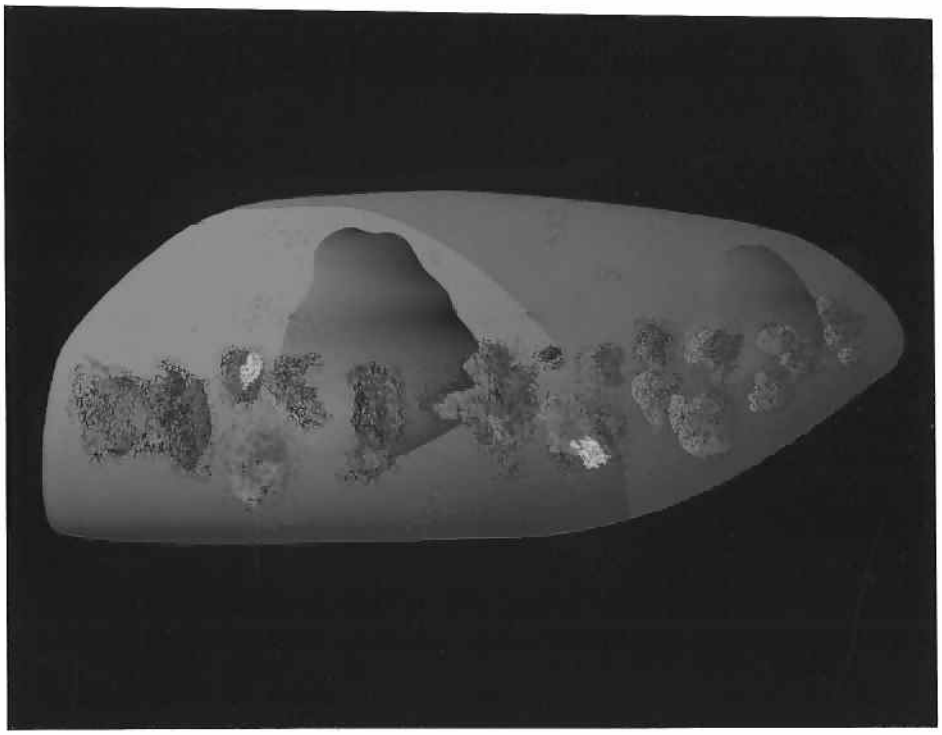

Submitted to the Faculty of the
University of Massachusetts Medical School in partial
fulfillment of the requirements for the degree of

DOCTOR OF PHILOSOPHY IN CELL BIOLOGY

April, 1993

COPYRIGHT NOTICE

Parts of this dissertation have appeared in separate publications:

Xing, Y. and J. B. Lawrence. 1991. Preservation of specific RNA distribution within the chromatin-depleted nuclear substructure demonstrated by *in situ* hybridization coupled with biochemical fractionation, *J. Cell Biology*, 112, 1055-1063.

Ewen, M. E., Y. Xing, J. B. Lawrence and D. M. Livingston. 1991. Molecular cloning, chromosomal mapping and expression of the cDNA for p107, a retinoblastoma gene product-related protein, *Cell*, 66, 1155-1164.

Brown, C. J., B. D. Hendrich, R. G. Lafreniere, J. L. Rupert, Y. Xing, J. B. Lawrence and H. F. Willard. 1992. The Human XIST gene: Analysis of a 17 kb inactive X-specific RNA that contains conserved repeats and is highly localized within the nucleus, *Cell*, 71, 527-542.

Xing, Y. , C. V. Johnson, P. Dobner and J. B. Lawrence. 1993. Higher level organization of individual gene transcription and RNA splicing, *Science*, 259, 1326-1330.

Xing, Y. and J. B. Lawrence. 1993. Molecular cytogenetics: Applications of fluorescence *in situ* hybridization (FISH) to chromosomal aberrations and cancer genetics, in *Chromosomes and Cancer: Causes and consequences of chromosomal aberrations*, Ilan Kirsch ed., CRC Press Inc. 3-28.

Xing, Y. , and J. B. Lawrence. 1993. Localization of specific genes and primary transcripts related to nuclear regions enriched in splicing factors, manuscript in preparation.

Xing, Y. and J. B. Lawrence. 1993. Nuclear distribution of RNAs from individual genes, *Trends in Cell Biology*. (in preparation)

NUCLEAR STRUCTURE STUDIED BY FLUORESCENCE HYBRIDIZATION:
VISUALIZATION OF INDIVIDUAL GENE TRANSCRIPTION AND RNA SPLICING

A THESIS PRESENTED
BY
YIGONG P. XING

Approved as to style and content by:

_____
Janet L. Stein, Chairperson of Committee

_____
Paul R. Dobner, Member of Committee

_____
Edward G. Fey, Member of Committee

_____
Susan A. Gerbi, Member of Committee

_____
Robert H. Singer, Member of Committee

_____
Jeanne B. Lawrence, Thesis Advisor

_____
Thomas B. Miller, Jr., Dean of Graduate
School of Biomedical Sciences

Department of Cell Biology
April, 1993.

This thesis is dedicated to my mother,
Dr. Shu-Jie Xing

ACKNOWLEDGMENTS

I would like to express my most sincere gratitude to my mentor, Dr. Jeanne B. Lawrence, for her patient, step-by-step guidance throughout my graduate studies at the University of Massachusetts Medical School.

I am greatly indebted to all the members of Dr. Lawrence' laboratory. Very special thanks to Dr. Kenneth Carter for his help and support and to John McNeil, Carol Johnson and Laurie Sullivan for their friendship and contributions to my thesis work. I thank Dr. Phillip Moen for his helpful suggestions in preparation of the thesis.

I would like to thank Dr. Robert Singer for encouraging my interest in cell biology and consistently providing important advice. I also wish to thank Drs. Paul Dobner, Edward Fey and Janet Stein for their suggestions to my thesis work.

I would especially like to thank Ms. Chris Dunshee for her excellent and patient assistance in photographic processing and Ms. Cindy Richard for her help during my studies in the Cell Biology Department. My appreciation is also extended to my fellow students in the Department of Cell Biology, whose friendship and scientific exchange made my graduate study life more colorful. I would like to thank the staff of the Graduate School Office, especially to Dr. Thomas Miller Jr., and Ms. Linda Dexter for their special assistance.

Finally, I would like to share the joy of this moment with my husband, Shan Lu, whose confidence in me and invaluable support during my graduate study have made it all possible and worthwhile.

TABLE OF CONTENTS

NUCLEAR STRUCTURE STUDIED BY FLUORESCENCE HYBRIDIZATION: VISUALIZATION OF INDIVIDUAL GENE TRANSCRIPTION AND RNA SPLICING

YIGONG P. XING
Thesis Advisor: Jeanne B. Lawrence, Ph.D.

ABSTRACT

The overall objective of this study has been to address some of the long-standing questions concerning functional organization of the interphase nucleus. This was achieved by using recently developed high-resolution fluorescence *in situ* hybridization techniques for a precise localization of specific DNA and RNA sequences in conjunction with immunocytochemistry and biochemical fractionation. This study is based on the philosophy that new insights may be gained by an approach that attempts to interrelate genomic organization, spatial arrangement of RNA metabolism, and nuclear substructure within the mammalian cell nucleus.

The nuclear distribution of an exogenous, viral RNA (Epstein-Barr Virus, EBV) within nuclear matrix preparations was studied by developing an approach which couples *in situ* hybridization with biochemical fractionation procedures. EBV RNA molecules accumulate in highly localized foci or elongated tracks within the nucleus of lymphoma cells. These RNA tracks were retained with spatial and quantitative fidelity in nuclear matrix preparations even after biochemical fractionation which removes 95% of cellular protein, DNA, and phospholipid. This provided direct evidence that the primary transcripts are localized via their binding to, or comprising part of, a non-chromatin nuclear substructure.

Then the nuclear distribution of RNA from an endogenous gene, fibronectin, was investigated using fluorescence techniques modified for more sensitive detection of endogenous RNAs within nuclear morphology. A series of *in situ* hybridization experiments were performed using different combinations of intron, cDNA, and genomic probes for RNA/RNA or RNA/DNA analysis in intact cells. Fibronectin RNAs were highly localized in the nucleus, forming foci or tracks. Both intron and exon sequences were highly

concentrated at the same site within the nucleus, indicating the presence of primary unspliced transcripts. Double-color hybridization using a nontranscribed 5' flanking sequence probe and a genomic DNA probe showed that the gene and RNA track for fibronectin were spatially overlapped, with the gene consistently towards one end of the track. These results provided evidence that the accumulation of RNA molecules occurs directly at or near the site of transcription, and further indicated a structural polarity to the RNA track formation with the gene towards one end. It was further discovered that within a single cell, cDNA probes produced longer tracks than those formed with intron probes, i.e. intron signals were generally confined to a smaller part of the track than the exon signals, indicating that splicing occurs within the RNA track. Additional experiments using poly(A) RNA hybridization or anti-SC-35 antibody staining combined with fibronectin RNA hybridization have shown that the fibronectin tracks were associated with recently discovered transcript domains enriched in poly(A) RNA and splicing factors.

To further determine whether other specific genes and RNAs are functionally organized within the nucleus, the nuclear distribution of several active or inactive genes was analyzed in terms of their spatial relationship to transcript domains. The results indicated that in addition to fibronectin, the genes or their primary transcripts from two other active genes, collagen and actin, were also closely associated with the domains. For both of these, over 90% of the gene/RNA sites were either overlapping or directly contacting the domains. In contrast, for two inactive genes, cardiac myosin heavy chain and neurotensin, it was found that both genes were separated from the domains in the majority of nuclei. Histone genes, which have several unique features, showed a relatively complex result with about half of the gene signals extremely close to the domains. Therefore, three actively expressed genes were demonstrated to be tightly associated with the domains and, moreover, their RNAs showed distinct and characteristic spatial relationships with the domains. In contrast, two inactive genes were not associated with the domains. One potential implication of these finding is that active genes may be preferentially localized in and around these transcript domains.

The nuclear localization of another RNA, XIST, standing for X-inactivation specific transcript, was studied because of its potentially unique

biological role. XIST is the only gene which is known to be expressed from the inactive human X chromosome but not from the active X chromosome, and was believed to be important in X inactivation. Using fluorescence *in situ* hybridization, it was found that XIST RNA was highly localized within the nucleus and always completely overlapped the Barr body which is the condensed, inactive X chromosome. The different fine distribution pattern of XIST RNA within the nucleus as compared to other protein coding RNAs suggested a unique function for this RNA, possibly involving a structural role in inactivating the X chromosome.

The final area of my thesis research was to study and acquire expertise in the applications of fluorescence *in situ* hybridization in gene mapping and cancer genetics. A retinoblastoma (RB)-related putative tumor suppressor gene, p107, was mapped to human chromosome 20 in band q11.2. Localization of p107 to 20q11.2 was of particular interest because of the correlation of breakpoints in this area with specific myeloid disorders such as acute nonlymphocytic leukemia and myelodysplastic syndrome. Other applications of *in situ* hybridization including the search for unknown genes at a known chromosomal breakpoint, detection of deletions, translocations or other chromosomal rearrangements associated with specific tumors were also explored and reviewed.

CHAPTER I

INTRODUCTION

A. Specific Aims

The overall objective of this thesis is to address some of the long-standing questions concerning the functional organization of the interphase nucleus. This study is based on the philosophy that unique insights may be gained by an approach that attempts to interrelate genomic organization with the spatial arrangement of RNA metabolism, and to relate both of these to nuclear substructure in the mammalian cell nucleus. The following are specific goals of this study:

1. To study the possible association of RNA transport and metabolism with nuclear structure by direct visualization of RNA before and after biochemical fractionation.

2. To investigate the spatial arrangement of gene transcription and RNA splicing for a specific cellular gene, including
   a. determining the distribution pattern of this specific RNA within the nucleus;
   b. relating the RNA distribution to the gene location;
   c. positioning introns and exons from this same gene within the individual RNA signals;
   d. relating the RNA signals to newly described pol II transcript domains.

3. To begin to assess the higher-level organization of several active and inactive genomic sequences within intact nuclei, with emphasis on the precise positioning of specific genes with respect to transcript domains.

4. To localize a unique transcript from a possible X chromosome inactivation related gene within the nucleus.

5. To acquire expertise in the application of fluorescence *in situ* hybridization to human genome mapping and disease gene identification.

B. Literature Review

The eukaryotic nucleus is involved in many aspects of cell function and is directly responsible for genome packaging, DNA duplication and cell division, differential gene transcription, RNA processing, and selective RNA transport of several major classes of RNA. In spite of the considerable progress in defining the basic molecular properties of the primary functions of the nucleus, our knowledge of how these processes are organized and regulated within the confines of nuclear structure is extremely limited.

A traditional view of the nuclear interior as a bag of chromatin immersed in a homogenous nucleoplasm which contains RNA molecules and protein factors is undergoing radical change. As has been noted for some time, there is a strong rationale for functional spatial organization within the nucleus (Comings, 1968, 1980). This rationale is based in part on the fact that the nucleus must perform numerous complex tasks, each of which requires a distinct biochemical machinery, and in part on the extreme density of the nucleoplasm with its theoretical limitation on diffusion (Jackson, 1991). In most higher eukaryotic cells, nearly all of the DNA (6×10^9 bp in the human) in the cell is sequestered in the nucleus but the nucleus occupies only about 10% of the total cell volume. A major function of the nucleus is to package this enormous length of genomic DNA in such a way that it is accessible for efficient and accurate replication and division during mitosis, and that individual genes are readily accessible to RNA polymerases and other proteins, resulting in the expression of only appropriate tissue specific genes (both housekeeping and cell type specific genes). Likewise, RNA transcripts from individual genes, which can be several microns long, must be packaged into ribonucleoprotein complexes that facilitate their extensive processing by poly(A) addition, RNA splicing and methylation. After these specific and precise steps, the RNA molecules must be selectively and rapidly transported out of the nucleus to the cytoplasm, where ribosomes begin translating the RNA into protein.

The functions of the eukaryotic nucleus are so complicated that it is logical to postulate that there is some structural organization of these functions. Electron microscopic examination of the nucleoplasm has revealed

that the nucleus has two types of chromatin material: the extended euchromatin visible in most areas of the nucleus and condensed heterochromatin, often clustered near the nuclear membrane and nucleolus (Fakan and Puvion, 1980). There is a correlation between the structural conditions of the genetic materials and their transcriptional activity. Heterochromatin is generally inactive. Euchromatin contains active genes but only a small portion of euchromatin is transcribed at any time (Lewin 1987a). Besides the euchromatin and heterochromatin, there are numerous fibrillar and granular RNP (ribonucleoprotein) components within the nucleus, but little functional information is available about them (Fakan and Puvion, 1980).

The nucleolus is probably the most obvious and well studied structural element in the eukaryotic interphase nucleus. It also establishes the precedent for the interrelated organization of the genome and RNA metabolism. Under the light microscope, nucleoli appear as solitary or multiple spherical bodies which occupy a substantial portion of the total nuclear space. In these highly specialized non-membrane-bounded regions, clusters of multiple copies of transcriptionally active ribosomal RNA (rRNA) genes are immersed in a cloud of ribosomal precursor particles of various stages of maturation (see recent review, Scheer and Benavente, 1990). The rRNA genes are from several different chromosomes (5 chromosome pairs in the human) which somehow become spatially associated to form this highly visible nuclear compartment. While still somewhat controversial, ribosomal DNA is believed to be localized specifically in contact with the "fibrillar centers" of the nucleoli and rRNA transcription occurs in the fibrillar cores (Thiry & Thiry-Blaise 1989) while the later steps of rRNA processing are thoughout to occur in the granular component of the nucleolus. It has been suggested that rRNA precursor molecules are synthesized, processed, and coordinately assembled with specific ribosomal and nonribosomal proteins to form preribosomal particles in an ordered manner and under defined topological conditions (Arroua et at. 1982; Thiry & Thiry-Blaise 1989; Scheer & Benavente, 1990).

However, much less is known about how transcriptionally active DNA sequences for the 50,000-100,000 protein coding genes and their respective

mRNA molecules distribute within the nucleus. Are they also concentrated in certain regions of the nucleus or do they spread homogeneously throughout the nucleoplasm? Answers to such fundamental questions are almost entirely lacking. A major reason that the nuclear interior has largely escaped our detailed scrutiny is due to the extreme density of its content. During the past decade, advances in the detection of specific nucleotide sequences within their cellular context, combined with ongoing research on the properties of the nuclear matrix, have just begun to give new insights into how the nucleus is functionally organized. Summarized below are many of the recent developments and ideas in this rapidly evolving field.

Gene transcription, RNA processing and nuclear organization

Of all the functions for which the nucleus is responsible, gene transcription and RNA processing have clearly undergone the greatest advances. Molecular biologists have begun to understand the fundamental mechanisms underlying the control of gene expression.

RNA synthesis begins when an RNA polymerase binds to a promoter DNA sequence. After forming a protein/DNA complex, RNA polymerase begins synthesizing RNA, extending its growing RNA chain in a 5' to 3' direction until it finishes the whole lenght of RNA molecule. Then, the newly synthesized RNA chain and the polymerase are released from the DNA. Three types of RNA polymerase, RNA polymerase I, II, and III have been identified (Murphy et al., 1989). Only RNA polymerase II transcribes the genes whose RNAs will be translated into proteins. Besides the RNA polymerases, other transcription factors are required to initiate transcription. RNA polymerase II first transcribes precursors of messenger RNA (pre-mRNA) in the nucleus. As pre-mRNAs are being synthesized, they are covalently modified at both 5' end and 3' end. The 5' end of the RNA molecule is capped by the addition of a methylated G nucleotide. The 3' end of most polymerase II transcripts is cleaved at a specific site. Immediately after cleavage, a poly-A polymerase adds 100 to 200 residues of adenylic acid to the 3' end of the RNA chain to complete the primary transcript. The pre-mRNA molecules for most genes are arranged in discontinuous segments--exons interspersed with noncoding

intron sequences. The formation of mature mRNAs requires the precise removal of intron sequences and joining of exons by RNA splicing. This step occurs within the cell nucleus and involves many protein components including snRNPs (small nuclear ribonucleoproteins) which are formed by U snRNAs (Uracil-rich small nuclear RNA) and polypeptide cores (Zieve and Sauterer, 1990). In vitro splicing experiments have shown that the snRNPs and pre-mRNA form a macromolecular complex known as a spliceosome (see review, Green 1989). Once primary transcripts are processed to mature mRNAs, they are transported to the nuclear periphery and exported to the cytoplasm via nuclear pore complexes. The means whereby the RNAs are transported through the dense nucleoplasm for selective translocation through the nuclear pores is essentially unknown (Agutter 1988; Green 1989).

Most of these studies have focused on the specific interactions between protein factors and DNA or RNA sequences, and how these interactions regulate gene expression. Despite the power of in vitro experiments using purified components, it is unlikely that they reflect exactly the complexity that exists in vivo.

Several experimental approaches have been used to determine where transcription occurs within the nucleus. In an early study, newly synthesized nuclear RNA in rat hepatocytes was pulse-labeled with [^{3}H]uridine for a short time (2 or 5 min) and studied by electron microscopy (Fakan et al., 1976). After labeling, the silver grains are predominantly associated with so-called perichromatin fibers distributed throughout the nucleoplasm. However, eighty percent of heterogeneous nuclear RNAs (hnRNA) is not polyadenylated (Lewin, 1975). The labeled signals by this method likely represent all classes of nuclear RNA, consisting largely of rRNA, undefined hnRNA and only 20% poly(A) RNA (Fakan and Puvion, 1980). This technique also poses another problem that it may not label the synthetic site, but a site of accumulation later in the pathway because transcription occurs so rapidly, ~1400 nucleotides/min (Shermoen and O'Farrell, 1991), that labeling for even 2-5 minutes may allow time for completed transcripts to travel from the synthetic site. In a very recent report, Jackson et al. (1993) studied the nuclear localization of transcription within encapsulated nuclei under conditions which allow transcription to occur more slowly than in vivo. They observed 300-400 Br-

UTP labeled transcription sites distributed throughout each nucleus. Again, a specific class of RNA cannot be identified by this type of labeling study and thus it is difficult to interpret these results in terms of the location of only active protein-coding genes since their site of transcription may be obscured by RNA synthesis from non-coding sequences.

A different approach, *in situ* nick-translation (Hutchison and Weintraub, 1985) is based on the increased DNase I sensitivity of active chromatin (Weintraub and Groudine, 1976) and its resultant preferential nick-translatability (Levitt et al., 1979). After a brief digestion with DNase I, cultured cell nuclei were nick-translated in the presence of biotinylated nucleotide analogues and the labeled regions located using fluorescently labeled streptavidin. Incorporation was found concentrated at the nuclear periphery in both chicken and mouse fibroblasts. Recently, using a similar nick-translation technique, it was shown that both normal and reverse-transformed CHO fibroblast nuclei are also labeled at the nuclear periphery while the transformed nuclei do not show such a distribution pattern (Krystosek and Puck, 1990). These studies are interpreted to reflect increased DNase sensitivity indicating active genes. However, they may reflect a higher concentration of DNA in the form of heterochromatin which is known to be at the periphery of the many nuclei (Lewin 1987a). It may also reflect increased penetration of the reagents into those regions. None of the above experiments directly locates transcriptionally active genes. It still remains to be proven that RNA synthesis readily takes place in these nuclear regions and firm evidence concerning this has been lacking.

Interest in the compartmentalization of RNA processing has been heightened by studies on locating snRNPs and other splicing factors within the nucleus. Using anti-Sm antibodies which recognize all of the major snRNPs except for U3 and other nucleolar snRNAs, it was found that the snRNP particles are mainly located in 20-50 speckles within the nucleus and are also present in lesser amounts in the surrounding nucleoplasm (Nyman et al., 1986; Spector, 1984; Spector, 1990). The SC-35 antigen, a non-snRNP splicing factor which is required for spliceosome assembly is also highly concentrated in those discrete nuclear regions (Fu and Maniatis, 1990; Spector et al., 1991; Carmo-Fonseca et al., 1991a; Carter et al., 1993; Huang and Spector, 1992). In

addition, as will be detailed below, poly(A) RNA has been found concentrate in these regions (Carter et al., 1991). Microinjected human β-globin pre-mRNA has been seen localized in 20-50 nuclear sites that are coincident with Sm speckles (Wang et al., 1991). It has been suggested that splicing activity can be restricted to those regions, but it is not clear whether these regions are merely sites of snRNP assembly or storage and the snRNPs active in splicing are actually distributed uniformly throughout the nucleoplasm. In amphibian oocytes, antibodies specific for snRNPs stain transcripts on lampbrush chromosomes, and at least three classes of extrachromosomal granules were found and termed A, B and C 'snurposomes' (Gall and Callan, 1989; Wu et al., 1991; reviewed by Gall, 1991). Type A snurposomes predominantly contain U1 snRNP while B snurposomes contain all the spliceosomal snRNPs. Type C can be stained with Sm antibodies and can have several B snurposomes on their surface. The relationship between the mammalian and amphibian oocyte staining pattern is at present completely unclear. In mammalian cells the situation is complicated further by the observation that in several cell types several snRNAs involved in splicing are highly concentrated in approximately 4 small nuclear foci, in addition to staining the snRNPs-rich domains spread throughout the nucleus (Carmo-Fonseca et al., 1991b). These foci have been further shown to correlate with coiled bodies, the dense spherical structures initially visualized by electron microscopy (Hardin et al., 1969; Carmo-Fonseca et al., 1992; Spector et al., 1992). U2AF (U2 auxiliary factor; Zamore and Green, 1991) which is a non-snRNP splicing factor has also been found colocalized with coiled bodies (Raska et al., 1991) but interestingly, not with the snRNP speckles. The function of coiled bodies also remains unresolved. They may have an important function in pre-mRNA metabolism but do not contain large amounts of SC-35 (Huang and Spector, 1992; Carmo-Fonseca et al., 1992) or poly(A) RNA (Carter et al., unpublished data) and may not be major sites of splicing. Therefore, it is still unclear where RNA splicing occurs within the nucleus.

DNA organization

Closely related to gene transcription is the topic of DNA organization

within the nucleus. Studies have shown that the DNA 2 nm double helix is first packaged with histone proteins as nucleosomes to form the 10 nm "beads on a string". Nucleosomes become more tightly opposed in the second level of packaging termed the 30 nm fiber, and it is this form of DNA filament which is believed to comprise DNA loop domains of approximately 100 kb (Weisbrod, 1982). However, additional forms of packaging must exist in order to condense 2 meters of linear human genome sequence approximately 200,000 times to fit within a 10 micron nuclear diameter.

An important observation which indicates a high degree of organization at a gross level is the reproducible pattern of dark and light staining bands on metaphase chromosomes. The Giemsa light bands correspond to chromatin that is gene-rich, early replicating, DNase sensitive and enriched in specific classes of repetitive sequences such as Alu (Manuelidis, 1984a; Korenberg and Rykowski, 1988; Goldman et al., 1984). While this clearly indicates some functionally related higher-level organization to the genome, it is not known at all how these bands are positioned at interphase and what their functional significance is. In the studies on replicating DNA, it was found that active genes are generally early replicating (Goldman et al., 1984; Herbomel, 1990) and that the early and late replicating DNAs have their characteristic and distinct clustered distributions at interphase (Nakayasu and Berezney, 1989), suggesting an organized and regulated replication of DNA within the nucleus.

Experiments using total chromosome hybridization and other approaches have shown that individual chromosomes can occupy discrete, relatively compact domains within the interphase nucleus (Cremer et al., 1982; Pinkel et al., 1988; Lichter et al., 1988; Manuelidis and Borden, 1988). However, our knowledge of how these chromosomes are arranged has not increased dramatically from the work of Rabl (1885) over 100 years ago, who suggested that chromosomes lie in a polarized "Rabl" configuration in newt nuclei, with centromeres towards one end and telomeres towards the other. In studies of *Drosophila* salivary gland polytene nuclei using state of the art 3-dimensional analysis, Sedat and colleagues found that centromeric DNA is attached to the nuclear membrane at one end and telomere DNA lies adjacent to the nuclear membrane at the opposite end of the nucleus, perhaps preserving the

orientation generated during anaphase (Agard and Sedat, 1983; Mathog et al., 1984). However in other cell types they did not find this same configuration (Hochstrasser and Sedat, 1987). Using *in situ* hybridization experiments, Manuelidis found a cell type-specific localization of centromeric sequences in cells of the mouse nervous system (Manuelidis, 1984b). In a recent report, it has been suggested that centromeres are located at the periphery of the nucleus and they move during S/G2 phase (Ferguson and Ward, 1992). Furthermore, analysis of the nuclear positioning of several human chromosomes in neuronal cells indicates specificity of their location in the interphase nucleus (Manuelidis and Borden, 1988). It has been proposed that the position of chromosomes, transcription, and RNA transport may be under strict regulation in a three-dimensional spatial manner (Blobel, 1985). It is suggested that specific genes are associated with particular nuclear pore complexes and the transcripts produced by that gene are "gated" to exit the nucleus by way of that pore complex.

Clearly, some degree of higher-level order is imposed on the chromatin organization in at least some somatic cells. The fact that very specific changes in cell-type specific nuclear morphology occur during development is consistent with the notion that nuclear organization may be important in differential gene expression. Higher-order chromatin folding may influence gene expression, possibly through gene suppression. The importance of chromatin organization is evident when the expression of chromosomal and extrachromosomal genes are compared. If a gene containing active promoter and enhancer elements is introduced into a cell, which contains the necessary activating factors, and maintained in an episomal state, respectable levels of expression are usually seen. In contrast, the same construct integrated into the host genome is most frequently repressed. P-element transformation in Drosophia and transgenic mice provide sophisticated means of stably introducing gene constructs into the chromatin of cells. However, highly variable levels of expression are seen (for example Palmiter and Brinster, 1986). There is some evidence that DNA elements distantly related (50-100kb away) can override this "chromosome position effect" and result in a position-independent, relatively normal expression of the inserted gene (Grosveld et al., 1987).

Possible structural basis for nuclear compartmentalization.

A number of different experimental strategies have been adopted to uncover the possible structural basis for nuclear compartmentalization. The results of these studies have suggested an underlying substructure, commonly termed the nuclear matrix, which is related to but distinct from the higher-level organization of DNA and RNA. However, since the nuclear matrix was isolated or directly visualized only following certain in vitro manipulations which destroy nuclear integrity, the existence of a nuclear matrix structure in vivo has been questioned.

In 1974, Berezney and Coffey reported the characterization of the "nuclear matrix" operationally defined as the residual nuclear material isolated from rat liver tissue by a sequential extraction method involving detergent (Triton X-100) treatment, nuclease digestion and high-salt extraction. This treatment removes most nuclear proteins, DNAs, RNAs and nuclear membrane phospholipid (Berezney and Coffey, 1974). The resulting structure, the nuclear matrix, is an insoluble, fibrogranular framework which resembles the nucleus in size and shape when examined by electron microscopy (Berezney and Coffey, 1977). A similar structure termed the "nuclear scaffold" which maintains the DNA in a folded conformation was observed by Laemmli and his associates using low-salt and detergent LIS (lithium 3,5-diiodosalicylate) to deplete histone and many other non-histone proteins in Drosophila and other types of cells (Mirkovitch et al., 1984). Later, Cook and his colleagues revealed a highly related structure they termed "nucleoskeleton" using Triton X-100 in a "physiological" buffer containing physiological salt concentrations to preserve gross structure and maintain DNA integrity (Jackson and Cook, 1985, 1988). In general, nuclear matrix preparations from different cells and tissues possess some common structural features: a peripheral lamina that represents a residual component of the nuclear envelope, the residual nuclear pore complexes that are embedded in the lamina, an extensive, extranucleolar granular and fibrous matrix structure containing RNA and protein, and the residual components of nucleoli. Importantly, it has been shown that the components of the matrix

are highly cell-type specific (Fey et al., 1988), although most of the specific proteins have yet to be identified and characterized.

.A large number of studies have been done to investigate the potential relationship of nuclear matrix and certain important nuclear functions (see review by Fey et al., 1991). While many studies support a role for the matrix in major nuclear functions, as described below, the results of these studies are to some extent controversial. For example, the specific association of transcribed genes with the nuclear matrix has been suggested. Pardoll and Vogelstein (1980) found that ribosomal DNA is associated with the matrix. In studies concerning the matrix association of a specific hormone-inducible gene, it was found that sequences adjacent to and within the ovalbumin gene are associated with the matrix of hen oviducts but not with the matrix of other tissues, and that the association of the same sequences reverses upon hormone withdrawal (Robinson et al., 1982; 1983; Ciejek et al., 1983). In contrast, other studies showed that heat shock genes are associated with the nuclear matrix structures prepared from Drosophila nuclei independent of transcriptional rate (Small et al., 1985).

Fixed transcriptional complexes that synthesize RNA have also been identified on the nuclear matrix (Abulafia et al., 1984; Jackson et al., 1981). Several studies have suggested that over 95% of newly synthesized hnRNA is associated with the nuclear matrix (Herman et al., 1978; Long et al., 1979; Mariman et al., 1982; Miller et al., 1978; van Eekelen and van Venrooij, 1981). Ciejek et al. (1982) found that precursor mRNAs are preferentially associated with the matrix as compared with the mature mRNAs. It was also suggested that small nuclear RNA species are recovered along with the nuclear matrix (Maundrell et al., 1981). It has been reported that almost all active RNA polymerase is retained within the residual chromatin after triton extraction and restriction endonuclease digestion (Jackson and Cook, 1985). However, other results suggested that RNA polymerases, both in their active and inactive forms, are not nuclear matrix associated (Roberge et al., 1988). Thus, in some cases the associations are still being questioned for whether they could be created artifactually. The unphysiological salt concentrations frequently used for isolating the nuclear matrix may cause nascent RNA or active polymerases to aggregate artifactually.

In addition, transcription factors are also co-isolated with the nuclear matrix. This has been shown for steroid receptors (Barrack, 1987) and proteins involved in the regulation of specific gene transcription (Getzenberg and Coffey, 1990; Ciejek et al., 1983; Ogata, 1990; Brotherton et al., 1991). Post-transcriptional RNA metabolism may also be influenced by nuclear structure. The matrix has been reported to contain assembled spliceosomes and is capable of processing exogenous substrates efficiently if provided with certain soluble protein factors (Zeitlin et al., 1989). A snRNP (small nuclear ribonucleoprotein particles) core protein has been found as a component of the nuclear matrix (Harris and Smith, 1988). These studies collectively suggested that the nuclear matrix may play a critical role in the synthesis and processing of mRNA.

DNA replication may also be associated with the nuclear matrix. It was found that there is a clustered arrangement of replication sites during S-phase of the cell cycle. The distribution of replication sites in nuclei of intact cells is the same as in nuclear matrix preparations (Nakayasu and Berezney, 1989). In agreement with this observation it has been shown that DNA polymerase alpha, primase, other replicative components and nascent DNA are also matrix-associated (Pardoll et al., 1980; Smith and Berezney, 1983; Jackson and Cook, 1986; Vaughn et al., 1990; Tubo and Berezney, 1987).

Although most of the nuclear machinery required for replication, transcription, and RNA processing appears to be associated with the operationally defined nuclear matrix, the full extent and true significance of these associations remains to be determined. More studies are needed to better define the nature of DNA/RNA-nuclear matrix associations and the actual role(s) of the nuclear matrix in these processes. A significant advance would be obtained if the same RNA/DNA associations observed after fractionation could be demonstrated in non-fractionated cells.

High resolution fluorescence *in situ* hybridization: A tool to study nuclear organization and genome mapping

Being a powerful approach, fluorescence *in situ* hybridization makes it possible to directly visualize the nucleic acid sequences within the

morphological contexts of individual cells, nuclei, or chromosomes. For many applications, this technology currently offers high hybridization efficiency and low background.

The early phase of *in situ* hybridization technology relied on autoradiographic detection of abundant sequences. During the past decade, several approaches were described to develop the nonisotopic detection techniques, including a method for direct labeling of fluorochromes to RNA probes (Bauman et al., 1981); the incorporation of biotinylated dUTP into DNA probes (Manning et al., 1975; Langer et al., 1981), detected by antibodies to biotin after hybridization to amplified polytene sequences (Langer-Safer et al., 1982), or direct attachment of enzymes (Renz and Kurz, 1984). Using improvements in the hybridization process, it has been demonstrated that a one-step fluorescent-avidin detection, without amplification or image-processing procedures, can detect single sequences as small as 5 kb by standard fluorescence microscopy (Lawrence et al., 1988). The same conditions can be used to detect smaller sequences of a few kilobases or less using digoxigenin-labeled probes.

One obvious and important application of the current advances in this technology is in the mapping of the human genome. The advent of single copy gene detection in both individual metaphase and interphase cells makes possible a new area of "molecular cytogenetics" whereby standard karyotypic analysis can be directly coupled with molecular biology. Using cytological hybridization, it is now possible to determine the loss or rearrangement of just a few kilobases of DNA anywhere within the genome. In the hunt for specific disease genes, the aberration resulting in nonidentical labeling of homologous chromosomes is very informative by this technique because a molecular cytogenetic defect in the gene itself might be revealed. Finally, in the area of cancer genetics, the capability of *in situ* hybridization for precise gene mapping will help to identify the chromosomal locus of putative tumor suppresser genes or oncogenes. The potential application of *in situ* hybridization in the area of human genetics and cytogenetics will be discussed further in Chapter VI.

In situ hybridization technology has also opened a door for investigations into the higher-level organization of the interphase nucleus.

In the past, the high density of nuclear content had made the study of nuclear organization rather difficult. Comprehensive analysis of a structure so densely packed with DNA, RNA and proteins clearly requires an approach which allows the precise localization of sets of related molecules within their cellular context. Research aimed at investigating the relationship between higher-order nuclear structure and function would benefit considerably from methods that permit the precise localization of a specific gene, its primary and spliced transcripts and the components of RNA metabolism machinery at the level of an individual cell. High resolution fluorescence *in situ* hybridization in combination with immunocytochemistry is exquisitely suited for this purpose.

The ability of fluorescence *in situ* hybridization to detect primary nuclear transcripts from expressed genes was first illustrated by the direct visualization of EBV (Epstein-Barr virus) viral RNAs (Lawrence et al., 1989; Raap et al., 1991). Specific EBV genes were visualized within interphase nuclei of infected cells (Lawrence et al., 1988). It was shown that the EBV genome is confined to the inner 50% of the nuclear sphere, suggesting a sequence-specific higher-level order within interphase chromatin (Lawrence et al., 1988). EBV specific RNA has consistently revealed a localized, often curvilinear, "track" type hybridization signal (Lawrence et al., 1989). This original observation suggests a highly ordered nuclear interior in which mRNA is not free to diffuse during some or all of its processing or transport within the nucleus. However, the EBV RNAs are abundant and stable within the nucleus and relatively easy to detect. The same hybridization method to cytogenetic preparations used for EBV RNA study showed no detection of endogenous RNA within the nucleus.

Using *in situ* hybridization, our laboratory has demonstrated that nuclear poly(A) RNA, which represents approximately 90% of all pre-mRNA (Puckett and Darnell, 1976; Nevins, 1983) concentrates primarily within 20-50 discrete "transcript domains" which often surrounded nucleoli (Carter et al., 1991; Carter et al., 1993). These Poly(A) RNA-rich domains are coincident with snRNP antigen clusters, with discrete regions of low DNA density, and are non-randomly distributed with respect to specific DNA sequences. These results raise questions as to whether the poly(A)/snRNP rich domains play a role in

mRNA transport and/or processing and possibly, whether these domains or the region immediately surrounding them are the sites of polymerase II transcription reflecting a clustering of active genes.

Despite the successful application of high resolution fluorescence hybridization in many different studies, it was necessary for me to further develop and exploit the potential of this technique to accomplish the goals of my thesis. Therefore, several new procedures have been further developed based on the previous methodology, including a) enhanced nuclear RNA preservation within intact cells and sensitive detection of nRNA; b) coupling biochemical fractionation with hybridization; c) single gene detection within nuclei of cells; d) simultaneous detection of specific DNA or RNA sequences; d) simultaneous detection of specific protein and DNA or RNA; and e) 3-D analysis of multiple nuclear components.

Summary

In summary, the cell nucleus is remarkable in the complexity of critical functions it must perform, and yet this complexity contrasts sharply with the simplified view of the nuclear interior which has persisted for many years. Evidently, we are only beginning to understand how the nucleus is organized and functions.

If genes are located non-randomly and RNAs are processed and transported according to some vectorial program, we can begin to think of the nucleus as an organized, integrated structure rather than a chaotic assortment of independent units. It is possible that additional, higher-level nuclear control mechanisms exist which can be as important for the selective retrieval of genetic information as the well-known mechanisms involving promoters, enhancers and transcription factors. However, our knowledge about higher-order control remains very limited.

Understanding the spatial organization of chromatin and nuclear processes such as transcription, RNA processing and RNA transport will enrich our knowledge of basic cell function and may well reveal new cellular control mechanisms. In this thesis study, an experimental approach that directly couples molecular and cytological information has been adopted,

based primarily on the use of high resolution fluorescence *in situ* hybridization. Several specific RNA transcripts from different genes were studied and the spatial arrangement of transcription and RNA splicing from a specific cellular gene was investigated. The nuclear locaions of active and inactive genes were also investigated with a emphasis on positioning them with respect to poly(A)/snRNP rich transcript domains. Also, a more critical test was applied to the association of nuclear RNA with the matrix by examining the spatial organization of specific RNAs in non-fractionated cells as well as in nuclear matrix preparations.

Obviously, it is impossible in one study to provide all the answers to fundamental, long-standing questions concerning the structure and function of the largest and most complex, but poorly understood organelle of the cell. It is hoped that information obtained from this study will help the black box of the nucleus to become more transparent.

CHAPTER II

Materials and Methods

The methods described in this chapter built on and substantially extended previous methodological work aimed at optimizing the preservation and sensitive detection of nuclear RNAs and DNAs by fluorescence microscopy (Lawrence et al., 1988, 1989, 1990, Johnson and Lawrence, 1991). Prior to beginning this thesis work, the existing methodology was appropriate for detection of highly abundant viral nuclear RNAs or overexpressed transfected sequences (Lawrence et al., 1989). Substantial development and new protocols were required to successfully detect nuclear RNAs from endogenous genes. Further modifications were required to apply these techniques to cells, such as fibroblasts and myoblasts, with extensive cytoplasms. In addition, new approaches for two color hybridization to DNA and RNA had to be demonstrated and applied, as well as new microscopic and computerized methods of imaging multiple colors in precise registration. In the interest of brevity, the many trials and errors involved in achieving successful technical experiments will be omitted and only the final protocols most frequently used described.

A. Cells

Rat fibroblast cells, RFL-6, and human fibroblasts, WI-38 and Detroit 551, were obtained from American Type Culture Collection.

The X chromosome aneuploid cell lines, GM04626 (47, XXX), and GM6061B (49, XXXXX), were provided by Dr. Huntington Willard (Standford University, Standford, CA).

Namalwa, an EBV infected cell line, was originally established from an African Burkitt lymphoma biopsy sample (Powell et al., 1979) and was provided by Dr. Elliot Kieff (The University of Chicago, Chicago, IL). B598 and BL2-B598 are EBV-infected lymphocytes and were provided by Dr. John Sullivan (University of Massachusetts Medical School, Worcester, MA).

RFL-6, WI-38 and Detroit 551 cells were grown as monolayers in DMEM

supplemented with 10% fetal calf serum (FCS) (Gibco Laboratories, Grand Island, NY) and 10 mg/ml gentamycin (Gibco Laboratories, Grand Island, NY). Namalwa, B598, and BL2-B598 cells were grown in RPMI 1640 medium supplemented with 10% FCS and 10 mg/ml gentamycin (Gibco Laboratories, Grand Island, NY). GM04626 cells and GM6061B cells were grown in aMEM containing 20% FCS and 100 unit/ml penicillin and 50 mg/ml streptomycin.

All of the above cells except Namalwa, B598, and BL2-B598 were plated in dishes containing autoclaved 1% gelatin-coated coverslips at a density of ~10^5 cells per 100 mm^2. Namalwa, B598, and BL2-B598 cells were grown in suspension. All cultures were maintained at 37°C in a 5% CO_2 humidified air atmosphere.

B. Probes and Antibodies

The EBV probes were provided by Dr. James Skare (Harvard University, Cambridge, MA) and represent BamH1 V fragments of the EBV genome (Skare and Strominger, 1980).

The rat fibronectin probes C1A1 and SX19-3 were gifts of Dr. Richard Hynes (MIT, Cambridge, MA). BBG-5'BR was provided by Dr. Jean Schwarzbauer (Princeton University, Princeton, NJ). The human fibronectin cDNA clone pHF-1 was provided by Dr. David Shapiro (St. Jude Hospital, Menphis, TN).

G1-4.9 was a gift of Dr. Pamela Norton (Brown University, Province, RI) and it contains a 4.5 kb non-transcribed 5' flanking sequences and part of the first exon of the rat fibronectin gene. This clone was digested with SacII and a 4.3 kb fragment only containing the 5' flanking sequences was excised and purified from the gel and named G1-4.9-5'.

The mouse collagen probe was provided by Drs. William Strauss and Rudolf Jaenisch (MIT, Cambridge, MA).

The beta actin probe P14T β17 and the human histone probe λHHG6 were gifts of Drs. Janet and Gary Stein (University of Massachusetts Medical School, Worcester, MA).

The cardiac myosin chain probe was obtained from Dr. Leslie Leinwand (Albert Einstein College of Medicine, Bronx, NY).

The neurotensin probe λHNT14 was a gift of Dr. Paul Dobner (University of Massachusetts Medical School, Worcester, MA).

The XIST gene probe G1A was provided by Dr. Huntington Willard (Standford University, Standford, CA).

The p107 probe was provided by Dr. David Livingston (Dana-Farber Cancer Institute, Boston, MA).

Oligo dT_{55} was provided by Dr. Krishan Taneja (University of Massachusetts Medical School, Worcester, MA).

Mouse monoclonal antibody anti-SC-35, in the form of a hybridoma cell tissue culture supernatant, was a gift of Dr. Tom Maniatis (Harvard University, Cambridge, MA).

C. Probe construction

The BBG-5'BR clone contains an 1.93 kb rat fibronectin insert which represents the complete first intron, second exon and part of the second intron of fibronectin gene. A 1 kb fragment only containing intron 1 sequences was excised with PvuII digestion, blunt-ended and inserted back into the original vector, pGEM2, from which all the previous intron/exon insert was removed by Bam H1 and Eco R1 digestion. The new intron only clone was named BBG-In and used as an intron specific fibronectin probe.

D. Cell Fixation and Biochemical Fractionation

For *in situ* hybridization experiments, RFL-6, WI-38, Detroit 551, GM04626 and GM6061B cells were first fixed as follows: cells were grown on the coverslips coated with 1% geletin. coverslips with attached cells were rinsed three times with Hanks solution (Gibco Laboratories, Grand Island, NY) at room temperature and incubated on ice in succession in cytoskeleton (CSK) buffer (100 mM NaCl, 300 mM sucrose, 3 mM $MgCl_2$, 10 mM PIPES, pH 6.8; Fey et al., 1986a) for 10-15 sec., CSK buffer plus 0.5% triton X-100 for 30 sec. and again in CSK buffer for 10-15 sec. Then 2 mM of vanadyl adenosine (BRL) was added to each of these buffers just before use to inhibit RNase activity. Cells were immediately fixed in 4% paraformaldehyde in 1X PBS (pH 7.4) at room

temperature for 5 min and stored in 70% ethanol at 4°C until use.

For biochemical fractionation and *in situ* hybridization experiments, the Namalwa, B598, and BL2-B598 cells were pelleted at 650 *g* for 5 min, resuspended in 1X PBS, and cytospun onto glass microscope slides at a density of $2X10^5$ cells/slide. Slides were fractionated first as described in next paragraph, air dried 5 min, fixed in 4% paraformaldehyde in 1X PBS for 5 min at room temperature and stored in 70% ethanol at 4°C. Alternatively, cells were put through a series of extraction and digestion procedures before fixation in paraformaldehyde and stored as described below.

For most biochemical fractionation experiments, cells were cytospun onto slides and fractionated according to Fey et al. (1986a). Alternatively, cells were fractionated first and then placed on slides. Cells were washed with 1X PBS at 4°C and incubated in CSK buffer with 0.5% triton X-100 for 10 min. Slides were then moved to an extraction buffer (250 mM ammonium sulphate, 300 mM sucrose, 10 mM PIPES pH6.8, 3 mM $MgCl_2$, 10 mM leupeptin, 2 mM vanadyl adenosine, and 5% triton X-100) for 5 min at 4°C. The chromatin fraction was removed from the remaining structure after digestion for 20-60 min at room temperature in a buffer similar to the CSK buffer but containing only 50 mM NaCl and 0.1-1 mg/ml bovine pancreas DNase I (Worthington Biochemical Corp., Freehold, NJ). DNase I digestion was terminated by putting slides into CSK buffer containing 0.25 M ammonium sulphate. The slides were fixed in 4% paraformaldehyde as described above.

The alternative fractionation procedure utilized was that described by Gallinaro et al., (1983). Cytospun slides were incubated in reticulocyte standard buffer (10 mM Tris-HCl pH 7.4, 10 mM NaCl, 1.5 mM $MgCl_2$) in the presence of 10 mM leupeptin for 10 min at 0°C. Samples were then washed in wash buffer one (10 mM Tris-HCl pH 7.4, 100 mM KCl, 1.5 mM $MgCl_2$, 0.25 M sucrose, 10 mM leupeptin). Washed slides were digested by 0.1 mg/ml DNase I for 60 min at room temperature. After digestion, samples were washed in wash buffer two (10 mM Tris-HCl pH 7.4, 400 mM KCl, 0.2 mM $MgCl_2$, 0.25 M sucrose, 10 mM leupeptin).

E. Probe preparation

Probes were nick-translated with biotin-16-dUTP or digoxigenin-11-dUTP (Boehringer Mannheim Biochemicals, Indianapolis, IN; BMB, in the following sections) by standard methodology. Briefly, 1 mg of double-stranded DNA for incorporation of biotin- or digoxigenin-nucleotide analogs was mixed with 10 ml of 10X nick translation buffer (0.5 M Tris-HCl, 0.1 M $MgSO_4$, 500 mg/ml bovine serum albumin and 1mM dithiothreitol), 10 ml of 600 mM each of dATP, dGTP, dCTP nucleotide, 6ml of either 1 mM biotin-16-dUTP or 1 mM digoxigenin-11-dUTP, 10 ml of 1-2 mg/ml DNase I (Worthington), 10 ml of DNA polymerase I (BMB), and H_2O to final reaction volume of 100 ml. Samples were incubated for 2-2.5 hours at 15°C and the reaction was stopped by addition of 1% SDS and by heating for 10 minutes at 70°C. Probes were ethanol-precipitated to remove free nucleotides and salt. The pellet was resuspended in water and stored at 4°C. Probes were sized and checked for analog incorporation by running them on a 1.5% agarose gel, transferring to nitrocellulose, and staining with either alkaline phosphatase-conjugated avidin or anti-digoxigenin (BMB) to assure that fragment sizes were in the range of 200-500 nucleotides (Lawrence and Singer, 1985; Singer et al., 1986; Lawrence et al., 1989). After nick translation, 20 mg each of sonicated salmon sperm and *Escherichia coli* tRNA were added for every microgram of probe.

Oligo dT (55 bases) was 3'-end labeled with biotin-16-dUTP (Bethesda Research Laboratories, Gaithersburg, MD) (Taneja et al., 1992). Briefly, probe (25 pM) in 50 ml was incubated with 25 mM of biotin-16-dUTP, 140 mM potassium cacodylate, 30 mM Tris-HCl, pH 7.6, 1 mM $CoCl_2$, 0.1 mM DTT, and 100 U terminal transferase (BMB). Samples were incubated at 37°C for 1.5 hour and then purified using a G-50 sephadex column.

F. Fluorescence *in situ* hybridization

For each slide, 50 ng of each probe plus 5 mg of competitor (if required) were lyophilized in an microcentrifuge tube. For detection of RNA, the slides were dehydrated through 70%, 95% and 100% ethanol and air-dried. For detection of DNA, the slides were first denatured in 70% formamide with 2X SSC at 70°C for 2 min and then immersed in 70% ethanol until all slides were denatured. They then were dehydrated in 95% and 100% ethanol and airdried.

Lyophilized probe was resuspended in 10 ml of 100% formamide and denatured at 75°C for 10 min. 10 ml hybridization buffer (2 parts 50% dextran sulfate, 1 part 10 mg/ml bovine serum albumin, 1 part 20X SSC, and 1 part double-distilled, deionized H_2O) was mixed into each tube, and the probe was then applied to the slide. The coverslips were covered and sealed with parafilm to maintain the humidity.

For simultaneous detection of the fibronectin gene and its RNA, several approaches were used, including hybridizing to DNA and RNA first, removing RNA by NaOH and then rehybridizing to detect the DNA only, or by attempting to saturate the RNA target first, then fixing, denaturing, and hybridizing to the DNA target. It was found that the method which gave the clearest and most reproducible results was to use a 5' flanking nontranscribed region probe to detect the DNA only and a transcribed sequence probe to target primarily RNA. This could either be done as a simultaneous or sequential hybridization.

Hybridization was performed at 37°C for a minimum of 3 hours to overnight in a incubator. Samples were rinsed for 30 minutes each in 50% formamide, 2X SSC at 37°C; 2X SSC at 37°C; and 1X SSC at room temperature. Slides were stained with fluorescent-avidin or Texas-red-avidin (10 mg/ml in 4X SSC, 1% BSA) for 45-60 minutes at 37°C and rinsed in 4X SSC, 4X SSC with 0.05% triton, and 4X SSC for 10-20 minutes each. Rhodamine or fluorescent conjugated antidigoxigenin (1:500; BMB) can be applied simultaneously with the avidin. Slides were then stained by either DAPI or propidium iodide. Samples were mounted in antibleach media (90% glycerol, 0.1% phenyline diamine in 1X PBS) and viewed with epifluorescence optics.

For poly(A) RNA and fibronectin RNA double hybridization, 5 ng biotin labeled dT55 probe in 10 ml of 30% formamide was denatured at 75°C for 10 min. 10 ml hybridization buffer was mixed into each tube, and the probe was then applied to the slide. Slides were incubated at 37°C for 2-3 hours and then detected by Texas-red avidin. After washing, slides were refixed in 4% paraformaldehyde for 10 min and rinsed in 1X PBS. This refixation step has been proved important for preserving the poly(A) RNA hybridization signals during subsequent hybridization (Carter et a., 1991). Samples then were hybridized with digoxigenin labeled fibronectin probe as described above.

For chromosome mapping, analysis was performed on metaphase

spreads of normal peripheral blood lymphocytes prepared by standard procedures. Slides were UV treated (365nm) for 1 hour and baked at 65°C for 4 hours just prior to hybridization. After rinsing in 1X PBS, slides were denatured and hybridized with DNA probes using *in situ* hybridization procedures described above.

G. Immunofluoresent staining

The antibody used, anti-SC-35, is against a spliceosome assembly factor (Fu and Maniatis, 1990). For simultaneous detection of an RNA or gene with SC-35, hybridization is performed as usual. It was found that in order to retain the hybridization signals during the immunofluoresent staining, it was important that the slides were refixed in 4% paraformaldehyde for 10 min at room temperature prior to antibody staining. Then, 30 ml of supernatant containing anti-SC-35 antibody was added to each slide. Cells were incubated with antibodies at 37°C for 45-60 minutes and then washed in 1X PBS three times. Rhodamine-conjugated donkey anti-mouse antibody (1:500) (Jackson Immuno Research, West Grove, PA) was used to detect SC-35 in the nucleus.

H. Cytogenetic preparations and chromosome banding

Cytogenetic preparations were made by standard methods. For normal peripheral blood lymphocytes, 10 ml of blood were collected in a heparin-coated tube and 5-10 drops were added to each 5 ml of prepared chromosome medium 1A (Gibco). After incubation for 72 hours at 37°C, 0.015 mg/ml Colcemid was added to the culture medium and incubation was continued for 30 minutes to 2 hours. Cells were then collected by pelleting and then 0.0075 M KCl was added until the total volume reached 5-10 ml. The tubes were incubated at 37°C for 17 minutes. After pelleting cells at 3000 rpm, almost all but 0.5 ml of hypotonic solution were removed and cells were resuspended in this remaining solution. Cells were fixed by addition of freshly prepared 3:1 methanol:acetic acid to 5-10 ml. The pelleting and fixing steps were repeated for 3 times. Cells were resuspended and dropped from a distance onto dry, ethanol-washed glass slides. Cells were then allowed to air-dry overnight and stored desiccated at -80°C.

Metaphase chromosomes were identified by banding with DAPI. To enhance chromosome elongation and banding, 3 mM BrdU was added to the culture 7 hours before harvesting to label late-replicating DNA.

I. Microscopy and image analysis

The data were analyzed primarily by standard fluorescence microscopy. Microscopes (Zeiss, Oberkochen, Germany) equipped with epifluorescent filters (Omega) were used. Detection of green and red fluorescence is routinely done using separate filter sets. However, for double-labeling experiments, the difference in opti cs between these filters results in a shift in the placement of the signals with respect to each other. This becomes particularly critical for applications where precise placement is essential, as in detailed studies of nuclear localization of gene and RNA or intron sequences and cDNA sequences. To avoid this problem, a dual-band filter set which allows simultaneous visualization of FITC-rhodamine or FITC-Texas red was used. The filter set consists a FITC (484-502 nm) / Texas red (578-593 nm) excitation filter and a FITC (515-540 nm) / Texas red (612-655 nm) emission filter with a compatable FITC-Texas red dichroic filter. The precise alignment of multiple nucleic acid sequences in two colors was achieved. Samples were visualized using 100X or 63X neofluor objectives.

Photography is done using Kodak (Rochester, N.Y.) Ektachrome 400 day light slide film for exposure of 1.5 min or more, or Ektar 1000 print film at 1-2 min exposure time.

Image analysis was done through a cooled CCD (charge-coupled device) camera (Photometrics Inc.). This camera is controlled from a Silicon Graphics workstation and the software from G.W. Hannaway and Associates was used to analyze and manipulate images. To obtain the accurate alignment of red and green images, beads that fluoresce in both colors were added in the slide-mounting medium. The images captured by CCD camera from separate filters were superimposed and aligned with these beads as positional reference markers.

For quantitation of RNA and DNA signals in Chapter III, images of the DAPI and the fluorescent signals were recorded with a CCD camera interfaced

with a digital imaging microscope and the intensity of signals was determined by computer analysis of the images. Fifty nuclei were chosen randomly for the intensity measurement by using a uniform box size for DAPI and the varied box for signals. Measurements of nonspecific background fluorescence were performed in the area free of cells using a box size similar to that for DAPI.

CHAPTER III

Nuclear Distribution of EBV RNA and Its Association with Nuclear Matrix

The fundamental question of whether mRNA precursors are synthesized in specific regions of the nucleus is unresolved and very little is known as to how transcripts destined for the cytoplasm are selectively transported from their site of synthesis to the nuclear pore. Relevant to these questions is the fact that the nucleus is an extremely viscous structure due to the enormous density of DNA, RNA, and protein that it contains. Hence it has been proposed that RNA is unlikely to be freely diffusing within this dense structure, but is more likely actively transported along a "solid-state" nuclear architecture (Agutter, 1985) and/or through channels in chromatin possibly connected to nuclear pores (Blobel, 1985).

During the past two decades a sizable body of literature has provided evidence for a nonchromatin nuclear substructure, the nuclear matrix or scaffold (reviewed in Nelson et al., 1986; Schroder et al., 1987; Verheijen et al., 1988; Fey et al., 1991). Numerous observations have suggested that this nonchromatin nuclear substructure may play a significant role in such fundamental processes as chromatin organization, transcription, RNA processing and transport, and DNA replication.

Despite an extremely large body of evidence accumulated since the chromatin-depleted nuclear matrix was first described (Berezney and Coffey, 1974), its existence in vivo and its specific association with nuclear RNA (nRNA) are not fully accepted. The concept of the matrix as a major structural component of the nuclear interior, with broad functional implications, has received little recognition as part of mainstream cell and molecular biology. While there may be several reasons for this hesitancy, a primary concern is that matrix structures visualized after nuclear fractionation may not accurately reflect structures that exist within intact cells, but could be an artifact of harsh preparation procedures, which trap or nonspecifically bind nuclear RNA. Because of the difficulty of investigating ultrastructure in extremely dense unfractionated nuclei, it is not possible to demonstrate that

the RNP-containing fibrillogranular structures visualized by resinless section (Fey et al., 1986a) electron microscopy in extracted nuclei also exist within nuclei of intact cells. This limitation has constituted a major obstacle to directly demonstrating *bona fide* in vivo counterparts of matrix structures. The precise localization of specific nuclear RNAs in both fractionated and unfractionated nuclei could contribute significantly to addressing a basic controversy which has long pervaded this field.

The work described in this chapter investigates the interaction of nuclear RNA with the nonchromatin nuclear substructure using a different approach than previous work. The experimental strategy was to couple the high resolution *in situ* hybridization methodology with nuclear fractionation procedures in order to visualize the distribution of a specific viral nuclear RNA both before and after nuclear extractions which remove the bulk of DNA, protein and phospholipid.

The viral RNA chosen for this study is the transcript from Epstein-Barr virus (EBV). EBV is a human herpes virus which is the causative agent of infectious mononucleosis. The EBV genome is stably maintained and partially expressed in growth-transformed B lymphocytes and tumor cells of two human cancers, nasopharyngeal carcinoma and Burkitt lymphoma. Latently infected cells usually contain multiple episomal copies of nonintegrated viral DNA. The episomal DNA is formed by covalent joining of the direct repeats that are at both ends of the linear EBV DNA (Dambaugh et al., 1980). Although episomal EBV DNA has been clearly demonstrated in latently infected cells, integrated EBV is also present. It has been found that the EBV genome is integrated into the chromosomal DNA of Namalwa cells (Henderson et al., 1983, Lawrence et al., 1989). Using fluorescence *in situ* hybridization technology, direct visualization of specific primary transcripts from EBV within nonfractionated nuclei has been reported (Lawrence et al., 1989). This work reveals a striking localization of specific viral transcripts within nuclei of Namalwa cells. Furthermore, the linear pattern of RNA signals becomes more obvious and the dramatic elongated structure is formed when the nucleus is swollen by hypotonic solution. The fact that the transcripts are tightly localized to well-defined "tracks" or "foci" and they are not disturbed or diffused in swollen nuclei suggests that nuclear viral RNAs are not free to diffuse, either because

of spatial constraints or, perhaps, because they are physically bound to some nuclear structure.

This model system provides an excellent opportunity to investigate whether a specific RNA can be visualized within nuclear matrix preparations. The objectives were: (*a*) to address a key point as to whether this RNA is localized due to spatial constraints between masses of chromatin or via association with nonchromatin nuclear substructure, and (*b*) to help resolve an important issue concerning the extent to which these fractionation procedures preserve structures which exist within intact cells, particularly the ribonucleoprotein filaments.

For three different virally infected cell types, two different nuclear matrix preparation procedures were evaluated which previously have been thoroughly characterized and reported to preserve hnRNA (Gallinaro et al., 1983). The primary procedure used (Fey et al., 1986*a*) has been very well characterized by electron microscopy, two-dimensional gel electrophoresis and assays of total RNA, DNA and protein retention. This fractionation procedure has been shown to remove >95% phospholipid, 94% of DNA, and 95% of cellular protein, while retaining 76% of nuclear RNA (Fey et al., 1986*b*).

RESULTS

The *in situ* hybridization procedures have been described in chapter II. DNA probes were labeled with biotin by nick translation and detected with fluorescent-avidin using epifluorescence microscopy. In this study, three different cell lines were used. The major part of the study was done using Namalwa human lymphoma cells which are latently infected with EBV and carrying two copies of the viral genome very closely integrated on one homolog of chromosome 1 (Henderson et al., 1983, Lawrence et al., 1988). Nuclear RNA distribution was also investigated in B958 cells productively infected with about 50 episomal viral genomes and in a second latently infected cell line (BL2-B958) carrying a single integrated viral genome. The primary probe utilized was the Bam HI V fragment of the EBV genome (Bam V) (Fig. 3-1) (Skare and Strominger, 1980; Lawrence et al., 1989), which was shown by previous studies to provide a good test system for the detection of

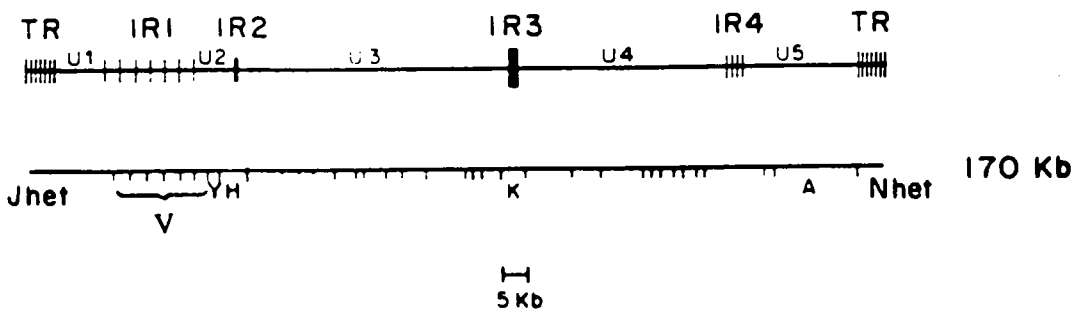

Figure 3-1. Physical map of the EBV genome indicating the BamH1 restriction fragments. The BamH1 V fragment was used for the study described in Chapter III. This map was modified from Henderson et al. (1983). The nomenclature is in accord with that of Skare and Strominger (1980).

EBV nuclear RNAs due to its size and relative abundance within the nucleus. Bam V sequences cover the 5' end of the genome and comprise up to 20 kb in the primary transcripts, but are extensively spliced to represent only 0.9 kb length of the mature mRNA (Van Santen et al., 1983; Dambaugh et al., 1986).

Comparison of nRNA Distribution within Intact Cells and Nuclei of Cytogenetic Preparations

Before considering the effect of nuclear fractionation procedures, it is instructive to compare the distribution of nuclear RNA in intact, paraformaldehyde-fixed Namalwa cells with nuclei of cytogenetic preparations. Previously reported work by Lawrence and her colleagues is based on cytogenetic preparations (Lawrence et al., 1989). Nuclei within cytogenetic preparations were swollen in hypotonic solution, fixed in methanol/acetic acid and placed onto glass slides. The diameter of the nucleus in this preparation was expanded to about 1.5-2 times that of paraformaldehyde-fixed intact, nonswollen cells (Fig. 3-2, A and B).

Fluorescence *in situ* hybridization was performed on both intact cells and cells from cytogenetic preparations using the Bam V probe. In both types of preparations, the viral transcripts were detected in the majority of the cells. The fluorescence signals were tightly restricted to a single site (occasionally two sites), with the accumulated transcripts forming a clearly defined focus or elongated linear track (Fig. 3-2, A and B). Previous analysis demonstrated that these tracks extended from the nuclear interior where the viral genome is localized (Lawrence et al., 1989). The average amount of nuclear signal per nucleus was roughly 300 copies of the Bam V sequence (Lawrence et al., 1989). While the nRNA formation tended to be elongated in both types of preparations, the track was consistently more linear and often dramatically elongated in the swollen nuclei of cytogenetic preparation (compare Fig. 3-2, A with B). This comparison provides the initial insight into the relationship between nuclear RNA distribution and nuclear structure in that the more elongated nature of the tracks within swollen nucleus suggests that the RNA may be attached to, or comprise, a nuclear structure that becomes distended during osmotic swelling. If the primary transcripts were free to diffuse, it would be expected that the cytogenetic preparations would result in less,

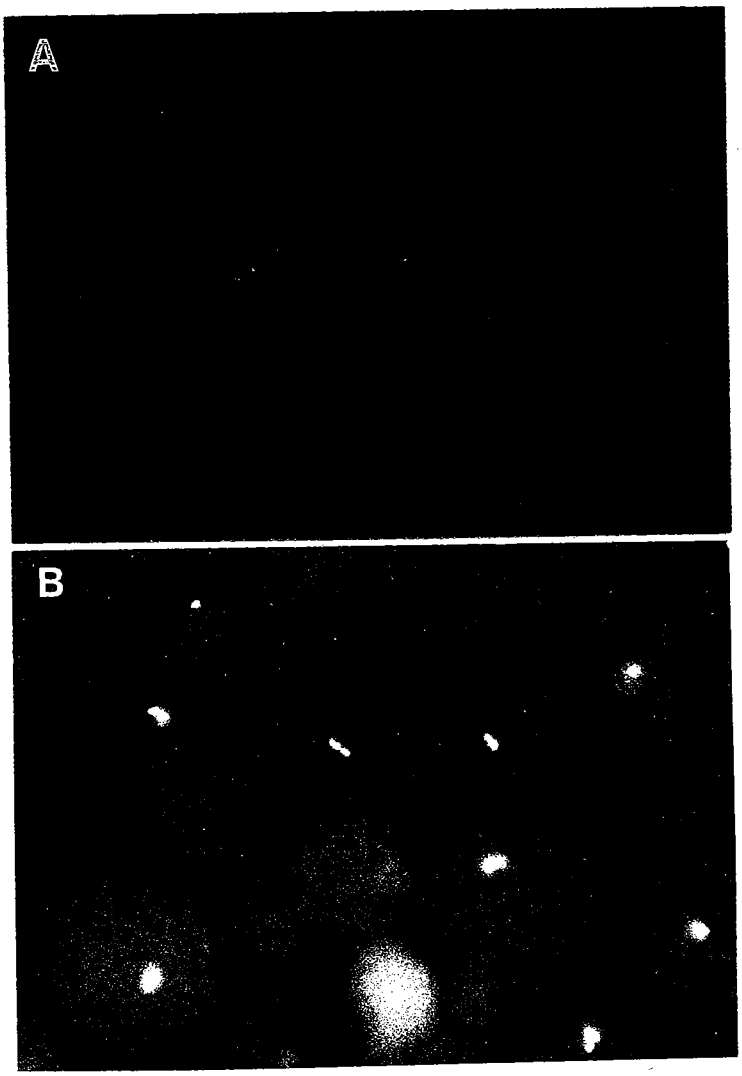

Figure 3-2. Detection of nuclear viral RNA within cytogenetic preparations and intact cells. Biotinylated probes for EBV Bam V RNA were hybridized in situ to latently infected Namalwa lymphoma cells and specific hybridization detected with fluorescein-avidin (*yellow*). Cellular DNA was not denatured prior to hybridization. Nuclei were stained with propidium iodide (*red*). (A) Hybridization to cytogenetic preparation of Namalwa cell nuclei, in which the RNA tracks have a particularly elongated configuration. (B) The EBV Bam V RNA tracks in nuclei of paraformaldehyde-fixed intact Namalwa cells. Exposure, 1.5 min.

rather than more, pronounced localization. Another line of evidence of the tight binding of this nRNA within the nucleus comes from the previous observation that nuclear transcripts are stably retained after methanol/acetic acid fixation and hybridization, conditions shown to result in loss of 80-90% of cytoplasmic mRNAs (Lawrence and Singer, 1985).

Effects of Detergent Extraction on nRNA Distribution

The effects of fractionation procedure on RNA distribution was first tested on the cells treated with detergent. Cells were extracted by Triton X-100 and then fixed by paraformaldehyde. *In situ* hybridization was performed on both untreated and detergent treated cells.

As shown in figure 3-3, A, when DAPI or propidium iodide was used to stain the total DNA in the nucleus, nuclei of unextracted cells revealed a solid, evenly dense appearance with a well-defined nuclear border. The EBV Bam V RNA hybridization signal was observed in >90% of nuclei, with the accumulated RNAs forming either linear, twisted, or focal structures, and occasionally the signals were branched. The possibility that the signals represent the detection of the EBV genome can be excluded because: (*a*) the nuclear DNA in these experiments was not denatured and, therefore, does not hybridize under the conditions used (Lawrence et al., 1989, 1990); (*b*) after digestion with RNase prior to hybridization, signals were completely absent in nondenatured samples; (c) previous work showed that signals were removed by actinomycin D and are specific to transcribed EBV sequences (Lawrence et al., 1989).

The first step in nuclear fractionation was to treat cells with Triton X-100 as specified in Chapter II, thereby permeabilizing the cell membranes and releasing soluble cellular components. As previously described (Fey et al., 1984, 1986*a*), this extraction removes phospholipids and 70% of soluble cell proteins but does not affect the DNA content. Light microscopic observations showed that the pattern of propidium iodide and DAPI staining of the extracted nuclei was not noticeably different from that of the intact cell (compare Fig. 3-3, A with B). *In situ* hybridization demonstrated that the EBV nuclear transcripts were detected after Triton extraction in almost all nuclei. Further, the overall appearance and intensity of the nuclear RNA tracks within the

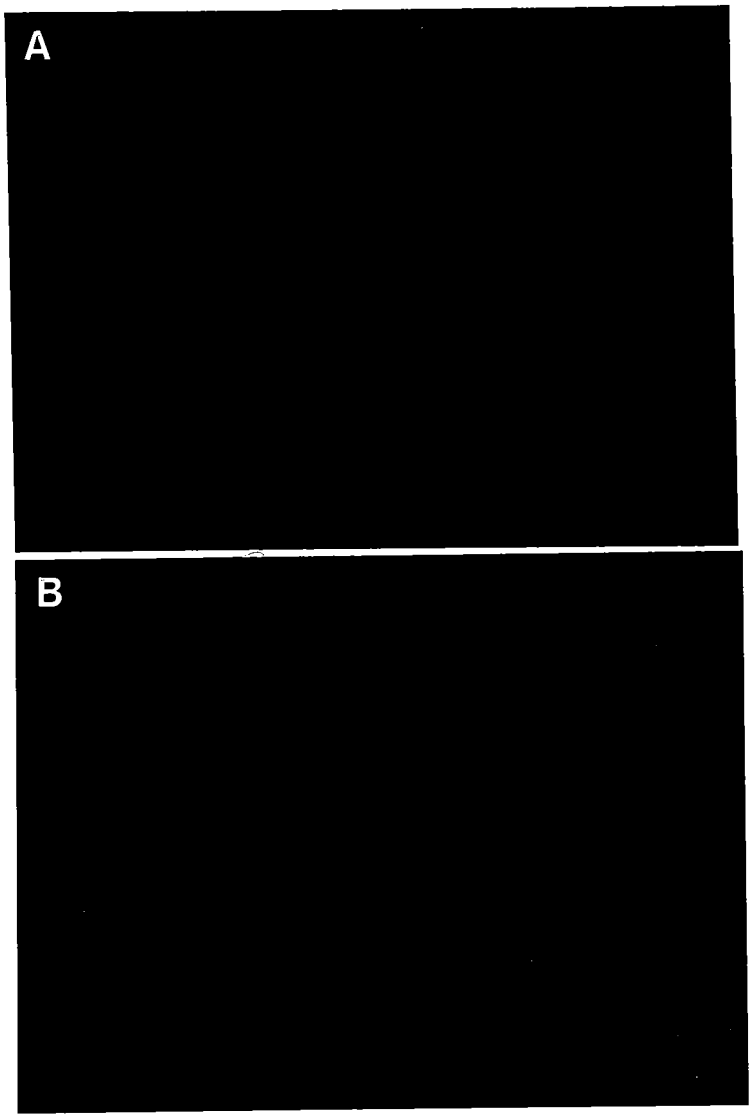

Figure 3-3. Nuclear viral RNA tracks within intact cells and detergent treated cells. EBV Bam V RNA in latently infected Namalwa cells were hybridized with biotinylated probes and detected with fluorescein-avidin. Nuclei were stained with propidium iodide. (A) Tracks of EBV RNA in intact Namalwa cell nuclei. (B) Hybridization to EBV Bam V RNA in nuclei of cells extracted with Triton X-100 for 5 min. Exposure, 1.5 min.

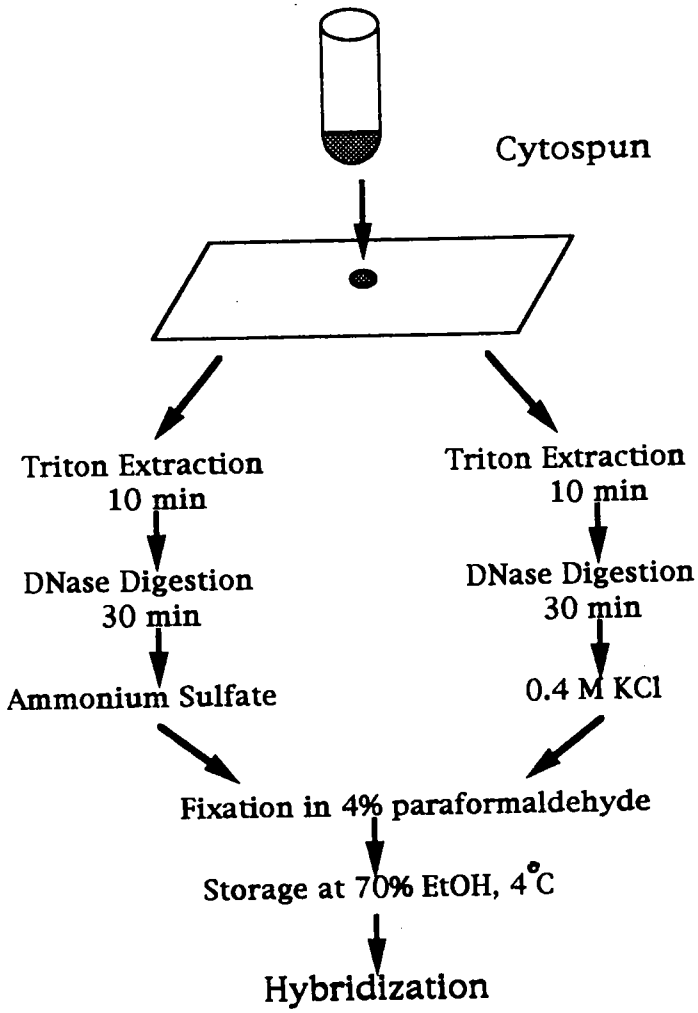

Figure 3-4. Schematic figure to show the steps involved in the procedure of nuclear fractionations.

extracted nuclei (Fig. 3-3, B) were identical to those of the intact cell nuclei (Fig. 3-3, A). Hence Triton extraction does not alter the retention or localization of this nRNA. The stable localization of nRNA after Triton treatment may be due to its association with underlying structure or due to its position between the densely packed DNA.

RNA Localization in Nuclei Fractionated with Detergent, DNase, and Ammonium Sulfate Extraction

A much more extensive fractionation of the nucleus was then undertaken after detergent extraction. After Triton treatment, chromatin was digested with RNase free DNase I and eluted with ammonium sulfate in the presence of RNase inhibitors (Fey et al., 1986*a*) (Fig. 3-4). Chromatin was cut principally between nucleosomes and the digested DNA and associated proteins were then eluted by ammonium sulfate. It has been shown by several biochemical studies that in addition to removing most of the DNA and phospholipid, this procedure removes >95% of histones and 70% nonhistone nuclear proteins. Studies using one- and two-dimensional gels have shown the remaining nuclear fraction to contain a specific but heterogeneous set of nonhistone proteins (reviewed by Nelson et al., 1986; Schroder et al., 1987; Verheijen et al., 1988).

The results of DAPI staining and *in situ* hybridization on these fractionated cells are shown at Figure 3-5. The intensity of DAPI staining, which is directly proportional to DNA content (Coleman et al., 1981), is greatly diminished in the fractionated nuclei and indicates the removal of DNA content in these cells (compare Fig. 3-5, A with C). The very pale residual DNA stain is evenly distributed throughout the nuclei. With propidium iodide, which stains both DNA and double-stranded RNA, the interior of the nuclei appears devoid of staining after fractionation with about one to four solid stained, round shaped bodies remaining in each nucleus (Fig. 3-6, A). Based primarily on morphology, the large dense structures observed in matrix preparations by electron microscopy are considered to be nucleoli (Fey et al., 1986*a*). That these dense bodies are nucleoli was confirmed by several lines of evidence observed in our experiments. First, while consistently observed after propidium iodide staining of both DNA and double-stranded RNA (Barni and

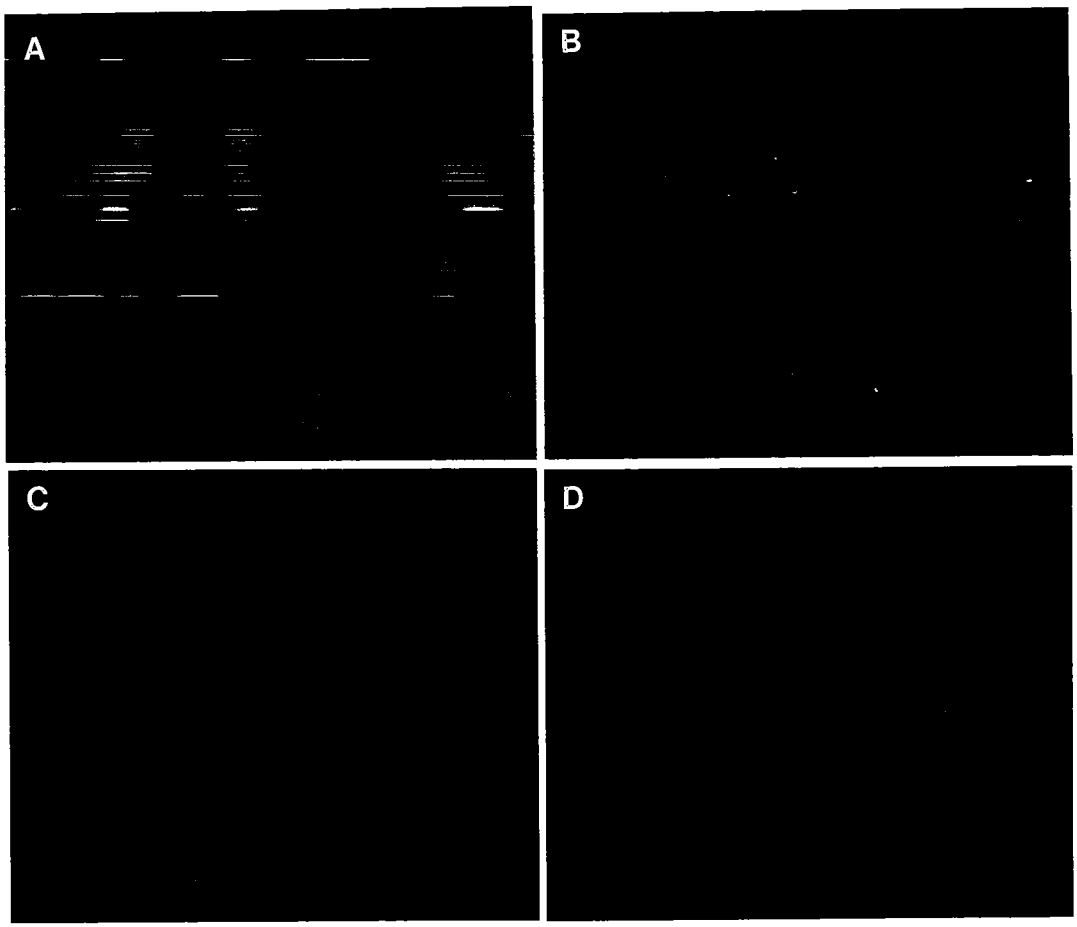

Figure 3-5. Fluorescent detection of total DNA and nuclear viral RNA within Triton extracted cells and cells prepared by nuclear matrix fractionation. (A) DAPI fluorescence staining of Triton-extracted Namalwa cell before fractionation gives extremely bright fluorescence intensity of total nuclear DNA. Exposure, 20 s. (B) Hybridization of Bam V probe to RNA in the same nuclei shown in A. Exposure, 1.5 min. (C) Same as A except that cells were fully extracted with DNase and ammonium sulphate. Exposure, 20 s. Loss of DAPI fluorescence indicates loss of total DNA. (D) Detection of RNA by Bam V probe in the nuclei shown in C. Exposure, 1.5 min. Note the great decrease of DAPI intensity in the DNased nuclei and the indistinguishable fluorescence intensity and morphological characteristics of the specific RNA signals in fractionated and unfractionated nuclei.

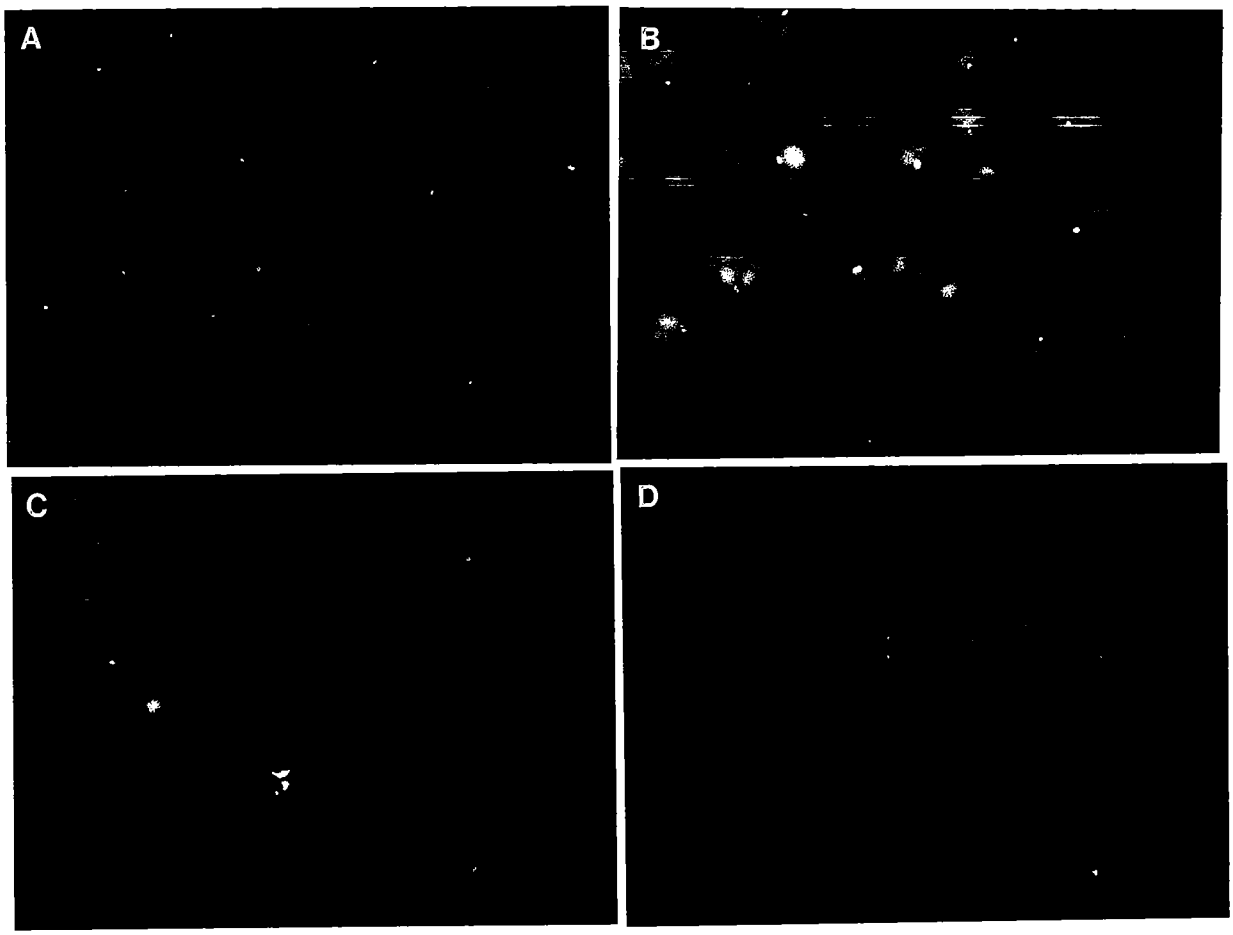

Figure 3-6. Fluorescence localization of nuclear viral RNA within Namalwa cells fractionated by different protocols. All fractionations used the DNase and ammonium sulphate procedure except for (D). Tracks of EBV RNA detected by the Bam V probe (yellow) were shown in nuclei of extracted cells stained with propidium iodide (*red*) (A) or stained with acridine orange (*orange*) (B). Nucleoli remain in the matrix fraction and are stained by both propidium iodide and acridine orange. (C) shows tracks of RNA in the cells fractionated in the suspension and then cytospun on to glass slides. (D) Similar results were also obtained in cells detergent-extracted, DNased and eluted with 0.4 KCl instead of ammonium sulfate. Exposure, 1.5 min.

Gerzeli, 1985), fully extracted nuclei stained for just DNA with DAPI exhibit uniform dim fluorescence (Fig. 3-5, C). Second, RNase H-digested samples stained with propidium iodide revealed a clean, empty nuclear interior with no dense nucleolar bodies. Finally, acridine orange of total RNA in extracted cells showed bright staining nucleoli of similar size, shape, and number (Fig. 3-6, B). Therefore, in addition to providing evidence that these solid stained bodies are nucleoli, these results demonstrate that the ribosomal RNA itself is well preserved at its expected site within the preparation.

In situ hybridization was then applied to determine how removal of the bulk of the nuclear contents, including lipids, soluble and insoluble proteins, and DNA, would affect the retention and moreover, the distribution of a specific mRNA precursor. Results were unambiguous, with the nRNA tracks still clearly observed in the "empty" nuclei (Fig. 3-5, D; Fig. 3-6, A and B). One or two tracks or foci were present in almost every nucleus, as in intact or Triton-extracted nuclei. The formations of nRNA were structurally indistinguishable from those in unfractionated nuclei. In addition, the fluorescence intensity of the nRNA tracks or foci was essentially the same as in nuclei before digestion.

The above experiments were repeated numerous times and the results are reproducible and consistent. For most of the experiments, fractionation was performed with cells cytospun onto glass slides. To exclude the possibility that the nRNA may have attached to the glass by some unknown mechanisms and remained after the fractionation, cells were extracted by the same steps in suspension and then the extracted cells were cytospun onto glass slides. Similar hybridization results were obtained with the cells extracted in suspension as that on glass (Fig. 3-6, C). To assure that DNase conditions were optimal for chromatin removal, the effects of DNase concentration and digestion time were examined. Two different enzyme concentrations (0.1 or 1 mg/ml) were used for 20, 40 or 60 minutes digestion. In all samples, the general appearance and density of the nucleus were similar and the fluorescence hybridization signals were identical. This indicates that the DNase I digestion reaction was rapid and essentially complete in 20 min, hence the 60 min digestion used in most experiments was more than sufficient for removal of bulk DNA. In contrast, when cells were treated with RNase A

before hybridization as a negative control, the hybridization signals were completely absent.

To address whether these results could be reproduced with a different matrix isolation procedure, a second method was used with 0.4 M KCl elution (Gallinaro et al., 1983) instead of ammonium sulfate. In general, very good retention of nRNA tracks and foci were observed using this procedure (Fig. 3-6, D). Therefore, retention of the RNA within the matrix fraction is not unique to the ammonium sulfate protocol.

Quantitation of DNA and RNA Retention

Results of the visual analysis described above were clear cut, in that RNA hybridization signals were not noticeably less intense after fractionation while nuclear DNA staining was greatly reduced. Removal of nuclear DNA is a critical and uniformly accepted criterion for preparation of the nuclear residue or "matrix". To provide an objective confirmation and quantitation for these results, DNA loss was measured by [^{3}H]thymidine labeling and specific RNA hybridization signals were quantitated using microfluorimetry in large numbers of individual cells before and after fractionation. As shown in Figure 3-7, there was extremely little intercell variation within one experiment. For two experiments with a total of 12 samples radioactively labeled by [^{3}H]thymidine, an average of 85% of labeled DNA was removed by the digestion procedure described above. This result was further confirmed by a different strategy, using cells that had been fully extracted in suspension and then cytospun onto slides, in which 86% of DNA was removed. Quantitation of specific hybridization signals was made possible by the use of quantitative microfluorimetry using digital imaging microscopy. The intensity of fluorescent signals after hybridization to the viral RNA was quantitated in over 50 randomly selected individual nuclei in both fractionated and unfractionated preparations. The nRNA tracks in the cells before and after DNase treatment were virtually identical in their average fluorescence intensity (Fig. 3-7). Remarkably, 96% retention of the specific nuclear RNA was higher than the 76% retention reported for total hnRNA by this procedure (Fey et al., 1986*a*).

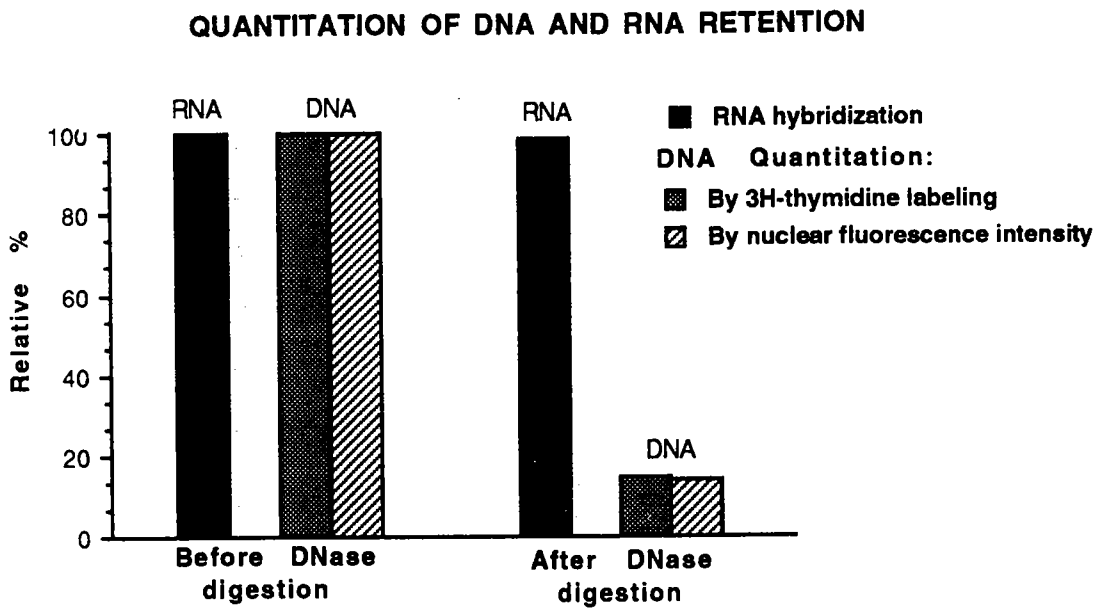

Figure 3-7. Quantitation of nRNA and DNA retention in nuclei of Namalwa cells. For quantitation of DNA removed by fractionation, cells were labeled for 24 h with 10 μCi/ml [^{3}H]thymidine and counted in a scintillation counter. Eight slides in each group with or without DNase I digestion were measured from two experiments. For quantitation of RNA hybridization signal and DNA intensity with DAPI, digital image processing was used. The total fluorescence units of either fluorescent hybridization signals or total DNA staining was measured by microfluorimetry in 50 randomly selected nuclei for each group, and corrected for background fluorescence as described under Methods (Chapter II).

Localization and Retention of Viral nRNA in Other Permissively and Latently Infected Cell Types

To determine if the localization of this viral RNA and its stability and retention throughout these procedures are specific to the cell line studied, two other EBV-infected cell lines were analyzed. A second latently infected cell line BL2-B958 with a single integrated viral genome exhibited a distribution of nuclear transcripts indistinguishable from Namalwa cells and a similar retention of nRNA after fractionation. More interesting results came from cell line B958, which was permissively infected and carries numerous episomal viral genomes. The RNA hybridization pattern is very different from that of Namalwa cells. In each nucleus, there are many well-defined tracks of nRNA detected by the Bam V probe throughout the whole nucleoplasm (Fig. 3-8, A). Hence, each of numerous active episomal genomes apparently produces an nRNA track. When nuclear fractionation is applied to these cells, results of hybridization show that these foci or tracks are completely retained after nuclear fractionation (Fig. 3-8, A). It can be concluded, therefore, that the primary transcripts from nonintegrated DNA are also physically bound within nuclear substructure.

The vast majority of B958 cells had many sites of localized transcripts within their nucleus, as illustrated in Fig. 3-8, A. However, a small fraction (3-5%) of the cells had extremely bright fluorescence with the highest concentrations more evenly distributed throughout the nucleus (Fig. 3-8, B). This is consistent with the frequency of cells in these cell line that enter a highly productive state. It was of interest, therefore, that the majority of RNA produced in these cells was also retained within the nuclear matrix fraction. It appears that the results observed are not unique to the Namalwa cell line or to latently infected cells, but represent a common property of different cell lines and cells in different states of expression for EBV nRNA.

Visualization of nRNA in the Same Cells before and after Fractionation

The above results strongly indicate that the RNA studied is quantitatively retained within fractionated nuclei, with no apparent change in morphology or distribution of the specific RNA tracks. An especially convincing demonstration that native ribonucleoprotein filament structures

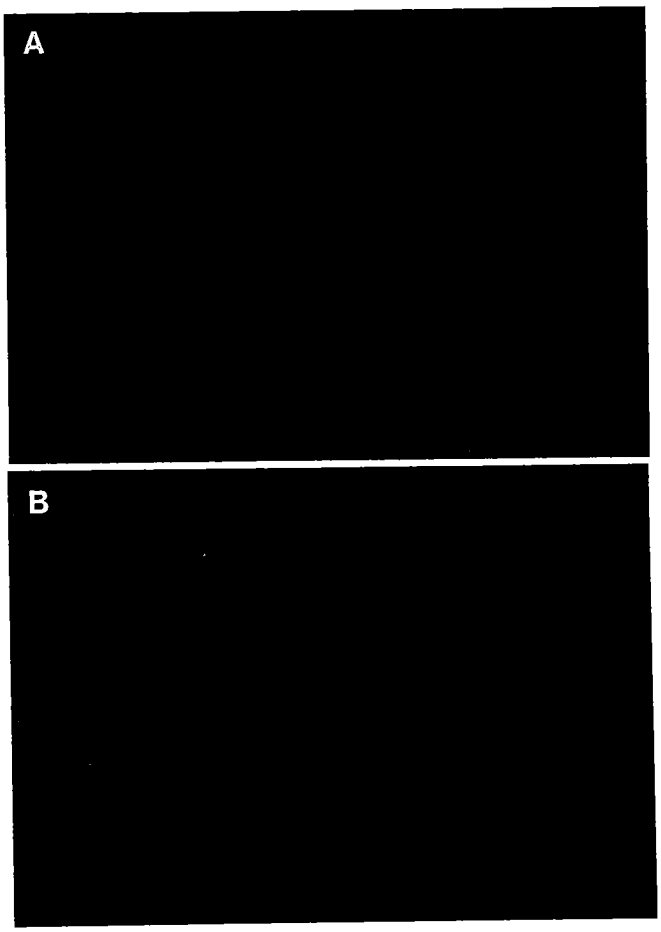

Figure 3-8. Fluorescent detection of nuclear viral RNA within fractionated B958 cells. Nuclei were stained with propidium iodide (*red*). These cells carry numerous episomal genomes and exhibit many viral RNA foci or tracks (*yellow*) which are retained with the nuclear matrix fraction (A). A small fraction of B958 cells had extremely strong hybridization throughout the nuclei and some cytoplasmic signal. These high concentrations of signals were illustrated in the fractionated cells (B).

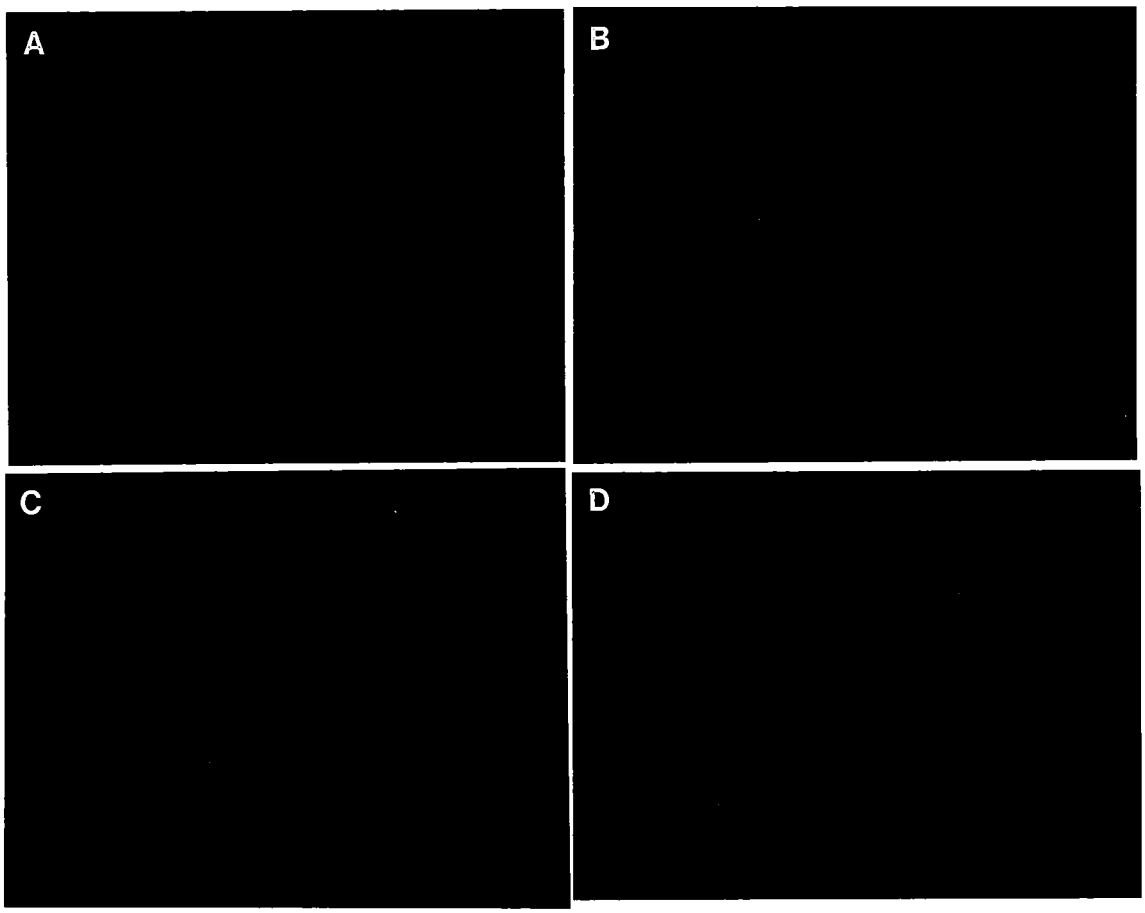

Figure 3-9. Fluorescence localization of nuclear viral RNA within the same EBV infected Namalwa cells before (A) and after (B) fractionation. Note the identical position of the nRNA tracks after fractionation. It is important to note that the fluorescein hybridization signal is diminished only due to bleaching during prephotography as demonstrated by quantitation of nRNA and DNA retention (Fig. 3-7). The propidium staining, in contrast, does not fade during photography due to different properties of this dye. The same nRNA tracks in nuclei of B958 cells before (C) and after (D) fractionation. Again note any diminution of fluorescein (yellow) signals is due to fading during prephotography. Nuclear staining indicates that the DNase digestion conditions used were effective after very brief fixation and hybridization.

remain unperturbed in the chromatin-depleted nucleus would be to visualize these structures in the same cell both before and after fractionation. This would further address whether the track of RNA could be maintained within the matrix preparation by virtue of attachment at one end, for instance, to the nuclear lamina or pore. Experiments were designed to address whether the RNA formation shifts position during fractionation.

Hybridization was performed and fields of cells photographed and marked. Samples were then fractionated by Triton treatment, DNase digestion and salt elution as described above. The same cells were then relocated and photographed to compare with the RNA distribution before fractionation. As illustrated for Namalwa cells in Fig. 3-9, A and B and B958 cells in Fig. 3-9, C and D, the nuclear staining with propidium iodide indicates that the fractionation procedure, which includes an extensive DNase digestion, was still very effective in removing nuclear DNA despite the prior brief fixation and hybridization. Results show clearly that for both cell types the RNA signals are not only still present, but are essentially identical in appearance and position. Neither end of the RNA tracks showed any displacement after DNase digestion, further confirming that they are held by or form substructures within the chromatin-depleted nucleus. It is important to note that the decreased intensity of the fluorescent signals after fractionation is due to the fading that occurs when the slide is exposed to light for the first photograph (before fractionation). On the same slide, hybridization signals in areas that were not exposed to light showed similar intensity before and after digestion, as documented by the quantitative studies described above. It was a consistent and striking observation that, by procedures that might be expected to be harsh or disrupting and that systematically remove the bulk of the nuclear contents, these formations of specific nRNA show no indication of movement or loss.

DISCUSSION

The work in this chapter provides direct visual evidence supporting the retention of a specific nuclear RNA within the chromatin-depleted nuclear substructure. The novel approach used here allows not just quantitation of the

RNA, but a qualitative evaluation of its spatial distribution before and after nuclear fractionation. Nuclear matrix literature frequently acknowledges the difficulty of unequivocally demonstrating that the RNP-containing structures observed by electron microscopy are not created during nuclear extraction in low or high ionic strength salts (Schroder et al., 1987; Agutter et al., 1985; Jackson and Cook, 1988; He et al., 1990). A direct critical test of this is made possible by the work described here. The RNA studied was unequivocally retained within the nonchromatin nuclear substructure, with no appreciable change in either the quantitative or qualitative appearance of the nRNA track. Retention of nuclear RNA formations in fractionated nuclei was observed in three different virally infected cell types using two different matrix isolation procedures. Quantitative image processing and microfluorimetry were used to confirm that close to 100% of the EBV nRNA present within intact nuclei still remained after nuclear fractionation, whereas at least 85% of DNA was removed. These results demonstrate that native RNP distribution is preserved throughout these procedures and further indicate that the striking localization of the nRNA within the nucleus is a consequence of its binding to or comprising internal structures which prevent free diffusion. Results of this coupling between high resolution hybridization and nuclear fractionation corroborate a body of work based on biochemical and ultrastructural studies supporting the existence of a nonchromatin nuclear structure with which hnRNAs are intimately associated.

Previous results from Lawrence et al. (1989) demonstrating a highly localized RNA track suggested that the nRNA is either associated with nuclear structure, or perhaps compressed into narrow spaces or "channels" between masses of chromatin. Results presented here demonstrate that the bulk of the chromatin can be removed from the nucleus, and the nRNA maintains its position, hence the nRNA is not localized by spatial constraints confining it to a channel. The RNA signals observed are much longer than the dimension of the gene, which is below the resolution of the light microscope and produces just a tiny point signal, therefore the RNA is not simply bound via its association with MARs within the gene. Although it is possible that the nRNA track or focus is tethered at one point to the nuclear lamina (or pore) that

remains in the matrix preparation, the nRNA tracks cannot be directly attached along their length to the lamina because previous work demonstrated that they extend into the nuclear interior where the viral genome is localized (Lawrence et al., 1989). This observation has been confirmed by confocal microscopy and three-dimensional analysis on suspension cells (Bauman and Lawrence, manuscript in preparation). The conclusion that the primary transcripts are "bound" to a nuclear substructure is not intended to exclude the possibility that the RNPs actually comprise this substructure, as has been suggested previously (Fey et al., 1986a, Nickerson et al., 1989). It is possible that the nuclear RNAs studied constitute part of the matrix "core filaments" (He et al., 1990), however further investigations would be required to establish this.

The nuclear RNA studied is transcribed from the EBV genome and codes for a low abundance cytoplasmic nRNA for EB nuclear antigens expressed in both latently and productively infected cells. Hence, in all three infected cell lines investigated the nRNA is processed and transported to the cytoplasm. However, the target sequences represented in the mature nRNA are very small relative to the primary transcript (0.9 vs. 21 kb), diffusely distributed, and much less abundant (three molecules per cell, Dambaugh et al., 1986), and thus are less detectable in the cytoplasm. The localization of the primary transcripts and their retention within the matrix preparations are not properties peculiar to a given EBV-infected cell line, but were demonstrated in three different cell lines, including latently and productively infected cells. Interestingly, the B958 cell line carries numerous episomal genomes, each of which is in a bound state unperturbed by nuclear fractionation. Thus RNAs produced by episomal as well as integrated genomes are physically associated with the nonchromatin nuclear substructure. It is interesting to speculate that the abundance of viral RNAs in the nucleus relative to the cytoplasm of nonproductively infected cells could reflect control of expression or processing related to release from the nuclear matrix.

It cannot be assumed that the viral model system will be representative of primary cellular transcripts in general, however these results provide evidence that this specific RNA is localized by virtue of its association with substructure. Regardless of whether the term nuclear matrix is used to

describe the remaining structure, the significant point is that the striking morphological localization of this nRNA is independent of bulk DNA and extensive protein and lipid extraction. The fact that the RNA distribution is precisely preserved in a form indistinguishable from its in vivo distribution makes it unlikely that it is merely entrapped or aggregated within the nuclear fraction. If this were the case, we would expect that some quantitative or spatial alteration of its distribution would have been discernible. A general conclusion, independent of the model system used, is that carefully characterized nuclear fractionation procedures (Fey et al., 1986a; Gallinaro et al., 1983) can preserve, with a remarkable fidelity, the distribution of a specific primary transcript.

While some types of nuclear RNA may have primarily a structural role, the functional significance of pre-mRNA association with the matrix is in all likelihood directly related to transport or processing, or both. The rapid and selective exit of RNA from the nucleus very likely requires some form of vectorial transport, for which the matrix may provide the framework (see review by Agutter, 1988). There is an increasing awareness of cellular compartmentalization in facilitating cell biochemical functions (for example the binding of enzymes involved in electron transport within the mitochondrial membrane). The possibility of a role for a nonchromatin substructure or matrix in RNA processing is made stronger by evidence that association of RNA processing components with the nuclear matrix fraction can significantly increase the speed of these reactions (Zeitlin et al., 1989). In keeping with the consideration that the RNAs themselves may comprise this substructure, it is possible that pre-mRNA molecules from a given gene somehow associate or interact with each other so as to promote an ongoing chain of transcription, processing and transport. This is consistent with the observation that inhibition of transcription with actinomycin D appears to halt the extension of previously transcribed EBV RNAs toward the nuclear periphery (Lawrence et al., 1989).

The experimental approach demonstrated here, because of the advantage of allowing visualization of specific RNAs or DNAs before and after fractionation, should be broadly applicable to a host of questions concerning the interrelationship of nuclear structure with RNA transport and processing,

and with chromatin organization. The ability to precisely localize single genes or their primary transcripts, as well as more abundant sequences, is in itself a powerful approach to studies of nuclear organization. The work presented here demonstrates the feasibility and value of wedding this approach with various biochemical fractionation procedures in order to unravel the underlying structural and organizational principles of the nucleus and chromosome.

CHAPTER IV

Nuclear Distribution of the Fibronectin Gene and Its RNA

Studies on the nuclear distribution of transcripts from Epstein-Barr virus provided the initial insights into the structural and functional organization of pre-mRNAs in the nucleus. While the EBV model system has been excellent for revealing new aspects of nuclear organization and structure, it cannot be considered representative of endogenous gene expression within the nucleus.

A given cell nucleus, expressing several thousand housekeeping and tissue specific genes, must accurately transcribe, process and transport RNA through a nuclear interior densely packed with chromatin, and it must do so in a highly selective way. Several major classes of RNA, including tRNA, rRNA, snRNA, and mRNA, are metabolized by distinct sets of enzymes. Moreover, the nucleus somehow discriminates between processed and unprocessed RNAs, and exports only functionally appropriate molecules such as mature mRNA.

Very little is known about the distribution of specific pre-mRNA metabolism within the interphase nucleus. Although rRNA is easily visualized within the nucleolus by *in situ* hybridization or by general RNA dyes such as propidium iodide and acridine orange, the intranuclear distribution of other RNAs, such as mRNA and snRNA remains unsolved. Several recent observations have heightened the interest in the spatial organization of pol II transcripts. The results of an *in situ* hybridization study with radioactively labeled probe have indicated that intron sequences in acetylcholine receptor (AChR) mRNA preferentially localize around the nuclear periphery (Berman et al., 1990). However, a recent report using a similar method found that AChE (acetylcholine esterase) intron sequences distribute randomly throughout the nucleoplasm (Tsim et al., 1992). Total nuclear poly(A) RNA has been shown to accumulate within 20-50 discrete transcript domains that coincide with the location of snRNPs (Carter et al., 1991; Carter et al., 1993). These snRNPs were previously reported to exhibit a clustered nuclear distribution (Spector et al., 1984; Fakan et al., 1984) coincident with the spliceosome assembly factor SC-35

(Fu and Maniatis, 1990). The concentration of microinjected human β-globin pre-mRNA within these 30-50 regions (Wang et al., 1991) different from the distribution patterns observed for several viral RNAs (Lawrence et al., 1989; Lawrence et al., 1990; Raap et al., 1991) and for c-fos RNA synthesized in vivo (Huang and Spector, 1991).

Visualizing the nuclear distribution of an RNA gives important inside into the organization of that RNA, such as whether it is randomly distributed, concentrated in specific regions, or is localized to a specific site, possibly through association with nuclear substructure. However, without further analysis to identify the biochemical processes occurring at a given site, locally concentrated RNA molecules can only be assumed to reflect some unknown rate-limiting step in RNA transport or metabolism. In the study presented in this chapter, the nuclear distribution of RNA from an individual endogenous gene, fibronectin, was studied in detail. A combination of intron, cDNA, and genomic probes was used to visualize the intranuclear distribution of fibronectin RNA. Further, this distribution is investigated relative to sites of transcription and processing and to large domains enriched in poly(A) RNA and splicing factors. Fibronectins are high molecular weight glycoproteins involved in cell adhesion, morphology and migration. The size of the fibronectin gene is about 70 kb and its mature RNA is about 9 kb (Patel et al., 1987; Schwarzbauer et al., 1987). The gene is made up of multiple small exons and the primary transcripts are alternatively spliced (Tamkun et al., 1984; Schwarzbauer et al., 1987). The fibronectin gene is expressed in many different cell types including fibroblasts and myoblasts (Hynes, 1983). The large size of the gene and the wide expression in different cell types made fibronectin an ideal system to study the nuclear distribution of specific cellular RNA.

RESULTS

Fibronectin RNA Is Highly Localized as A Focus or Track in the Nucleus.

To determine if fibronectin RNA is diffuse or localized within the nucleus, the fibronectin RNA was first detected by hybridization of a 6.5 kb rat genomic DNA probe C1A1 (Fig. 4-1) to rat fibroblasts RFL-6 or myoblasts L6

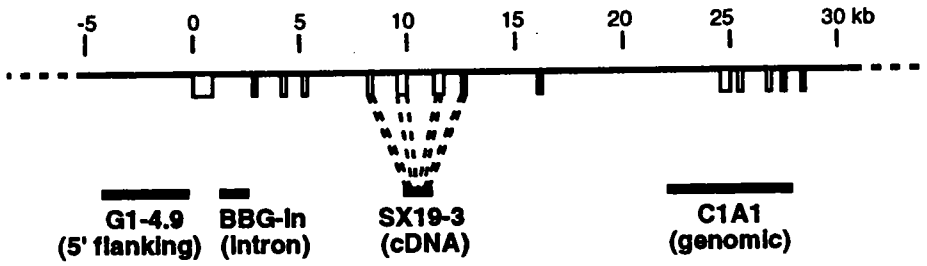

Figure 4-1. Map of partial rat fibronectin gene (~30 kb) and hybridization probes for fibronectin RNAs. The scale is marked in kilobases from the transcription initiation site. The black bars indicate the fibronectin probes, and the open boxes indicate exons.

grown in monolayer. The probe was labeled by either biotin or digoxigenin using nick translation. After a 3-16 hours hybridization, at least one site of bright fluorescent signal was found in the nuclei of about 60-80% of the cells, with less intense diffuse signal within the cytoplasm (Fig. 4-2, A). Among these positive nuclei, 55% showed one site of signal, 38% two sites and 7% three or four sites per nucleus. Human fibronectin RNA was later detected in two types of human fibroblast cells, Detroit 551 and WI-38, using probe pFH-1, and similar results were obtained as in the rat fibronectin system. Several pieces of evidence indicated that the detected signals were accumulated fibronectin nuclear RNA and not DNA of the fibronectin gene. First, the samples were not denatured before hybridization and hence cellular DNA was not available for hybridization (Lawrence et al., 1989; Johnson and Lawrence, 1991). Second, in cells treated with actinomycin D for 3-5 hours the hybridization signals were no longer visible. Third, previous work using RNase digestion had shown that signals detected under similar conditions were accumulations of RNA (Lawrence et al., 1989; Xing et al., 1991).

Most interestingly, in many nuclei the concentrations of fibronectin RNA frequently were more elongated than focal, forming "tracks" up to about 6 microns long (Fig. 4-2, B). In some cells, the tracks were found to be extended through several planes of focus. The distribution of the foci or tracks appeared random and was not concentrated in the periphery of the nucleus. Both the length and orientation of tracks with respect to the X-Y and Z axes were highly variable.

The accumulation of fibronectin RNA detected with the genomic probe could represent unprocessed transcripts, mature mRNAs, or possibly intron sequences that had been removed from the primary transcript. To differentiate the above possibilities, cDNA (SX19-3) and intron specific (BBG-In) probes (Fig. 4-1) were used for hybridization. Using identical labeling schemes, both cDNA and intron probes hybridized to just one or two focal sites within the nucleus in most of the cells. By using different haptens to label intron and cDNA probes, the intron and exon distributions were compared within the same cell. As illustrated in figure 4-3, the intron and cDNA probes localized to the same nuclear foci, indicating the presence of unspliced transcripts.

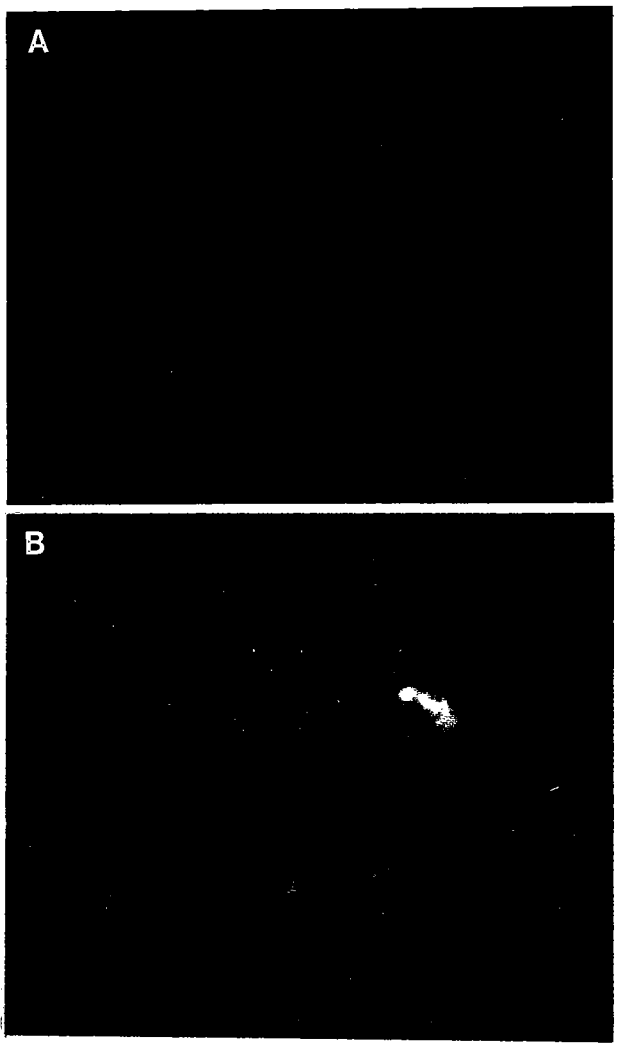

Figure 4-2. Detection of fibronectin RNA in rat RFL-6 fibroblast cells. Fibronectin RNA was hybridized with digoxigenin-labeled genomic probe C1A1 and the specific hybridization was detected with fluorescence conjugated anti-digoxigenin antibody. (A) Low magnification of unselected cells with fibronectin RNA foci or tracks. Most of the nuclei have one or two intense sites of hybridization. (B) High magnification of a cell with a highly localized and elongated RNA track within the nucleus.

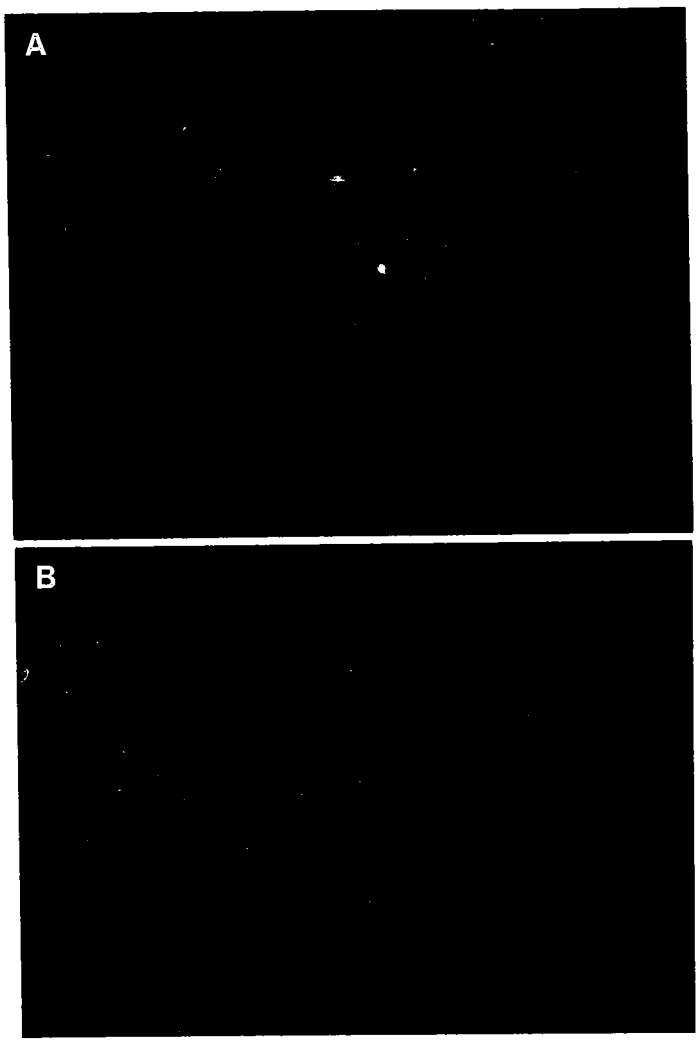

Figure 4-3. Hybridization of fibronectin primary transcripts in rat RFL-6 fibroblast cells. (A) Fibronectin RNA was hybridized with digoxigenin-labeled, intron specific probe BBG-In and detected with a rhodamine-conjugated antibody to digoxigenin. (B) Fibronectin RNA was hybridized with the biotin-labeled, exon-specific cDNA probe SX19-3 and detected with fluorescein isothiocyanate (FITC)-avidin in the same cells shown in (A).

In addition to highly localized foci or tracks, cDNA probe hybridization also showed diffuse, less intense fluorescence signal in the cytoplasm indicating the existence of mature fibronectin RNA in the cytoplasm (Fig. 4-3, B). For intron probes, in addition to bright fluorescent foci or tracks there was a dimmer, slightly punctate fluorescence dispersed throughout the nucleoplasm excluding the nucleolus, with essentially no label in the cytoplasm (Fig. 4-3, B). This dimmer "intron" signal may suggest that the excised intron sequences are free to diffuse throughout the nucleus and was further supported by similar results obtained using a neurotensin intron probe in PC12 cells (Xing et al., 1993). The relative uniform distribution of dimmer fibronectin intron signal is in contrast to a previous study for the AChR intron using autoradiography which reported a concentration of signals around the nuclear periphery (Berman et al., 1990), but agrees with a very recent autoradiographic study (Tsim et al., 1992),

These results from *in situ* hybridization to fibronectin RNA in fibroblast cells provide direct visual evidence for individual RNA accumulations within the nucleus. The high sensitivity of this technique allows the expression of a single gene in each cell to be studied. After the other experiments in this chapter were completed, additional studies were done to see if there is any change in the nuclear distribution pattern of a gene transcript when the gene becomes more active. Fibronectin RNA distribution within the nucleus was studied in the cells with or without TGF-β treatment. Previous biochemical and molecular studies on the cellular responses to TGF-β have shown that the level of fibronectin protein expression was increased after TGF-β treatment and the main regulation of this increase was at the transcriptional level (Ignotz et al., 1987).

Rat fibroblast cells before and after TGF-β treatment were hybridized with genomic fibronectin probes. The results indicated that the percentage of cells in which fibronectin nuclear RNA signal were detected was increased in TGF-β treated cells from 60% to 90% as compared to untreated cells (Fig. 4-4, C); the portion of the cells which had two RNA tracks or foci was increased also (32% to 63%); and finally, careful examination of individual RNA trackshowed they were brighter and often appeared longer than the signals in control cells

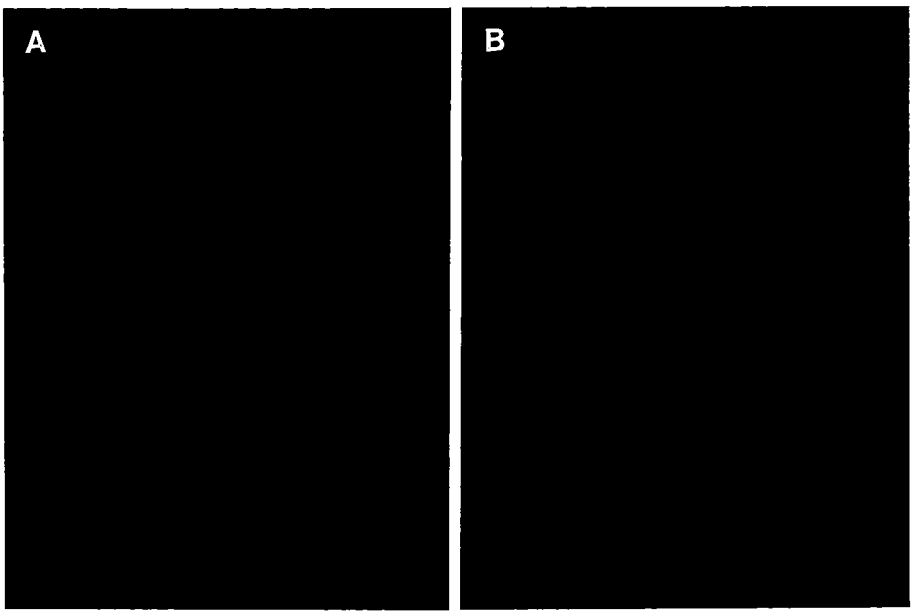

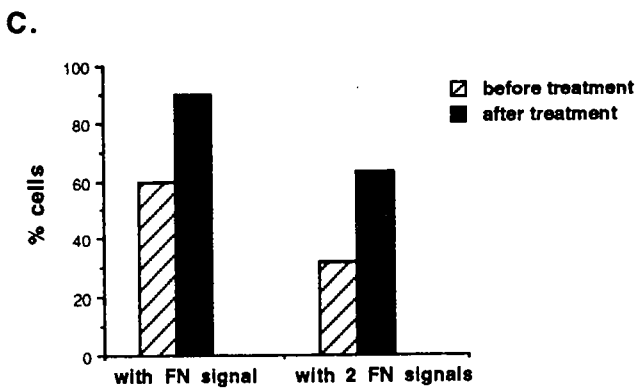

Figure 4-4. Effect of TGF-β on the expression of the fibronectin gene in rat fibroblasts. Fibronectin RNA was hybridized with genomic probe and detected with a FITC-conjugated antibody to digoxigenin in the serum starved cells before (A) and after (B) 6 h TGF-β treatment. Note the increased intensity of RNA signals in the nuclei of treated cells compared with that of non-treated cells. (C) Quantitation of fibronectin RNA detection in nuclei of rat fibroblasts with and without TGF-β treatment. Cells were incubated with or without 500 pM TGF-β in the culture medium for 12 h before the fixation. The number of RNA signals was counted in 210 randomly selected cells for each group.

(Fig. 4-4, compare A with B).

The Site of the Gene Is Closely Associated with the Site of Accumulation of Its Transcripts.

Localized accumulation of specific nuclear RNAs may represent the site of any rate limiting step along the progression from transcription through processing to ultimate translocation through nuclear pores. To determine at which step the RNAs become concentrated and whether the RNA accumulation co-localizes with the site of transcription, it is necessary to examine the spatial relationship of fibronectin gene and its RNA track. Several approaches to this were tested, and ultimately this was achieved by simultaneous visualization of the fibronectin gene and its transcripts using a 4.3 kb probe (G1-4.9-5') for the nontranscribed 5' sequence immediately flanking the fibronectin gene to detect the position of the gene (Fig. 4-1). It was labeled with digoxigenin. The genomic DNA probe C1A1 was used to detect RNA and was labeled with biotin. The slides were heat denatured before hybridization and the gene and RNA signals were visualized using different color detections. The gene signals revealed a very small spot-like focus in the nucleus. Two different analytical methods were used to verify the precise registration of different color fluorescence images. One is done by utilizing a single filter that allows simultaneous visualization of red and green with no optical shift, and the second utilizing separate red and green images which were captured by a CCD camera and then were aligned and superimposed. To obtain accurate alignment of red and green images, beads that fluoresce in both colors were added in the slide-mounting medium. Observed through the double-color filter, it was obvious that the gene signal and the RNA focus or track were spatially coincident (Fig. 4-5). For 88 nuclei with the gene signals detected, 86% of the gene signals overlapped with the RNA signals. Furthermore, in 88% of elongated RNA accumulations the gene was clearly positioned at or near one end of the track. This polarity could even be found in the gene position within the focal RNA accumulation (Fig. 4-5, B and C).

These results provide evidence that the accumulation of RNA molecules occurs directly at or near the site of transcription, and further indicate a structural polarity to the RNA formation, with the gene and transcription

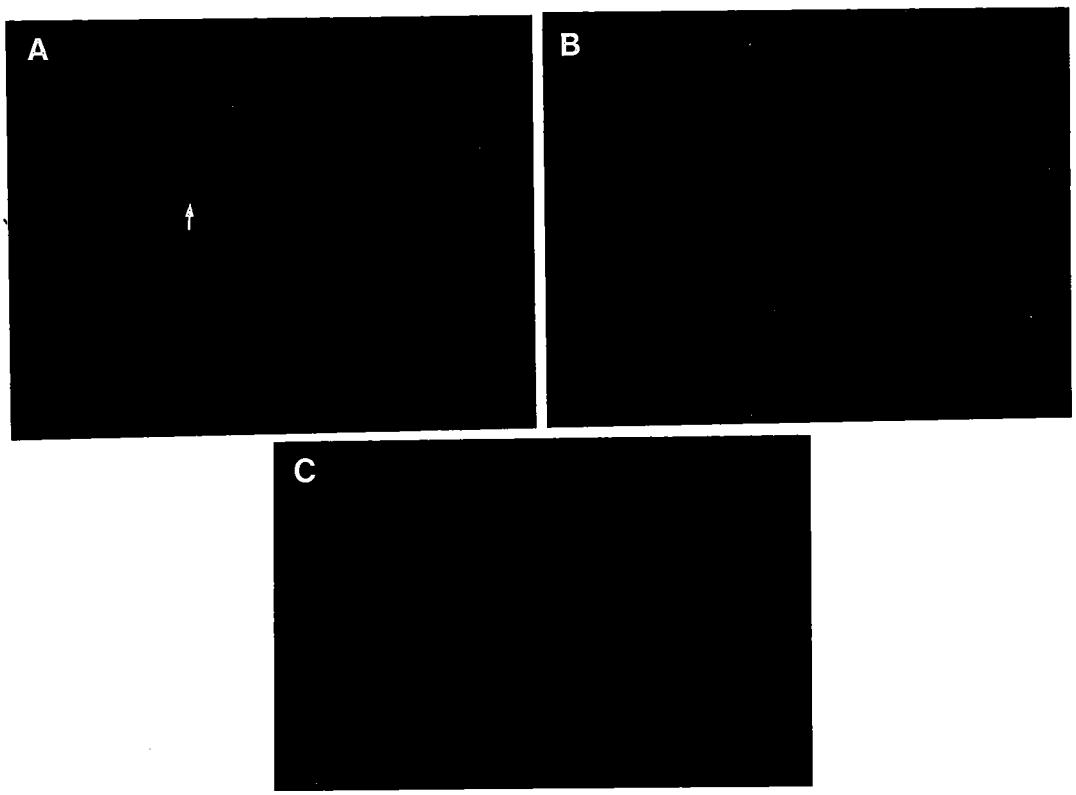

Figure 4-5. Localization of fibronectin RNA tracks relative to sites of transcription. The nuclear location of the fibronectin gene and its primary transcripts were shown by dual-label hybridization on RFL-6 cells. Probe G1-4.9, which contains 4.3 kb of nontranscribed 5' flanking sequence of the rat fibronectin gene, was labeled with digoxigenin (red, rhodamine). The RNAs were hybridized with a biotinylated C1A1 genomic probe (green, FITC). Fixed cells were denatured and hybridized as described in Chapter II. The photomicrographs in (A) and (B) were taken through a dual-band filter that allows precise alignment of red and green fluorescence (arrow denotes the gene signal). The image in (C) was captured by a CCD camera from separate filters superimposed and aligned with multicolor fluorescence beads (lower left) as reference markers. The insert shows two additional examples at high magnifications.

towards one end of the track.

RNA Processing Is Spatially Coupled with Transcription.

From biochemical and molecular studies, it has been known that RNA splicing involves several steps and probably occurs co-transcriptionally or shortly after transcription. However, little was known about the higher-level spatial relationship between processing and transcription. It was not clear whether RNA processing could occur at the site of transcription or RNA was synthesized at the site of transcription and then shipped to another nuclear location for processing. The observation of the accumulation of primary fibronectin transcripts at the site of transcription did not in itself answer this question. A priori different explanations exist for the RNA accumulations at the site of transcription: they could represent a build-up of newly synthesized transcripts prior to transport elsewhere for processing; or they could represent an "assembly-line" of transcripts actually undergoing processing at or near the transcription site.

To discriminate the above fundamentally different models, a close examination of RNA accumulations with two-color hybridization using intron and cDNA probes became necessary. A 1 kb intron sequence BBG-In and a 1.2 kb cDNA probe SX19-3, which is 3' to the intron sequence within the fibronectin gene (Fig. 4-1), were used to achieve this goal. The fluorescence signals obtained from these two probes in the same cells were visualized simultaneously by using a red-green dual color filter or alternatively by computerized superimposition of red and green color images captured with a CCD camera. For both analytical techniques, identical results were obtained. The simultaneous intron and cDNA probe hybridization revealed a two-color track or focus within the nucleus when directly viewed under the double color filter. One part of the track was found to have mixed colors representing both intron and cDNA detection, the other part showed only the color of cDNA hybridization (Fig. 4-6A). When using single color filters to examine the intron and cDNA hybridization signals separately, it was clear that the cDNA signal was present throughout the whole length of the track and in contrast, the intron signal was confined only to a small part of the track (Fig. 4-7). In 90 randomly selected fibronectin RNA tracks, 84% of the cDNA hybridization

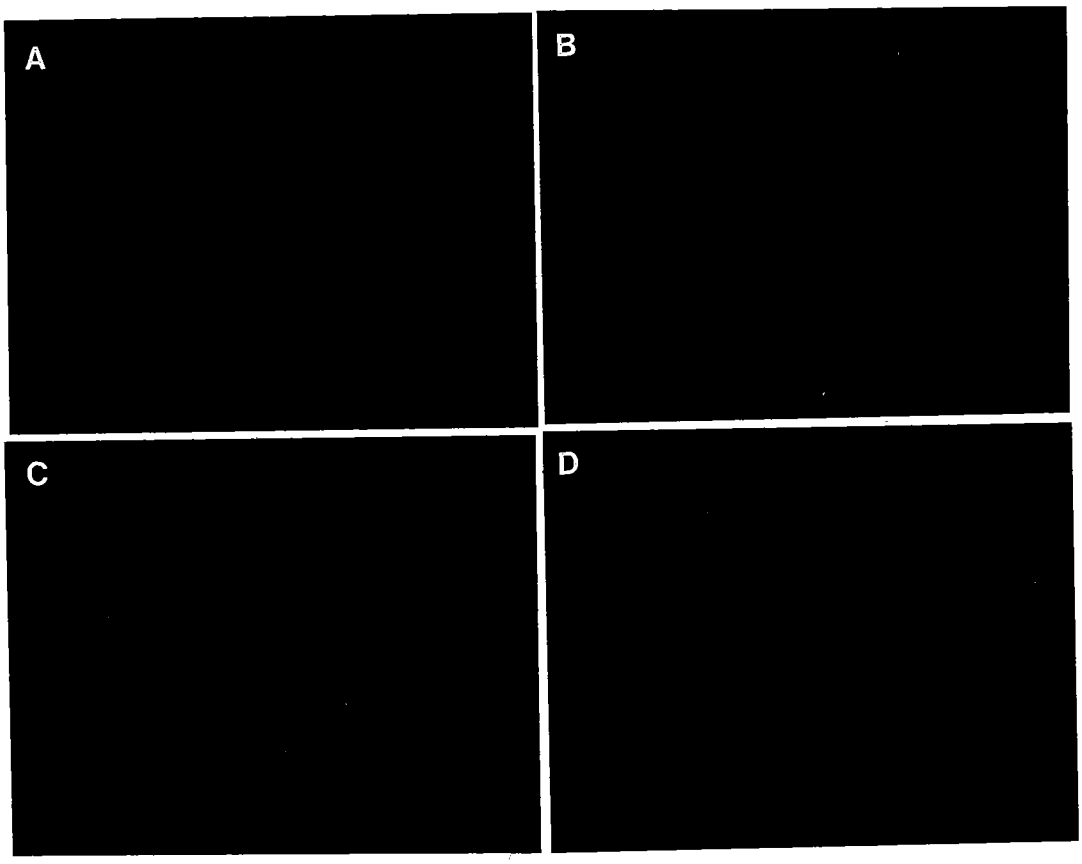

Figure 4-6. Localization of fibronectin RNA tracks relative to sites of splicing. (A) Fibronectin gene transcripts detected by the biotinylated intron probe BBG-In (green, FITC) and by the digoxigenin labeled cDNA probe SX19-3 (red, rhodamine). The cDNA signal extended further than the intron signal. (B) Reverse labeling to (A) (BBG-In, digoxigenin, rhodamine; SX19-3, biotin, FITC). (C) Simultaneous hybridization of two probes for the same sequence (C1A1) one labeled with biotin and the other with digoxigenin show no color separation. (D) Both intron and exon probes were labeled with biotin and detected by Texas-red avidin and FITC avidin.

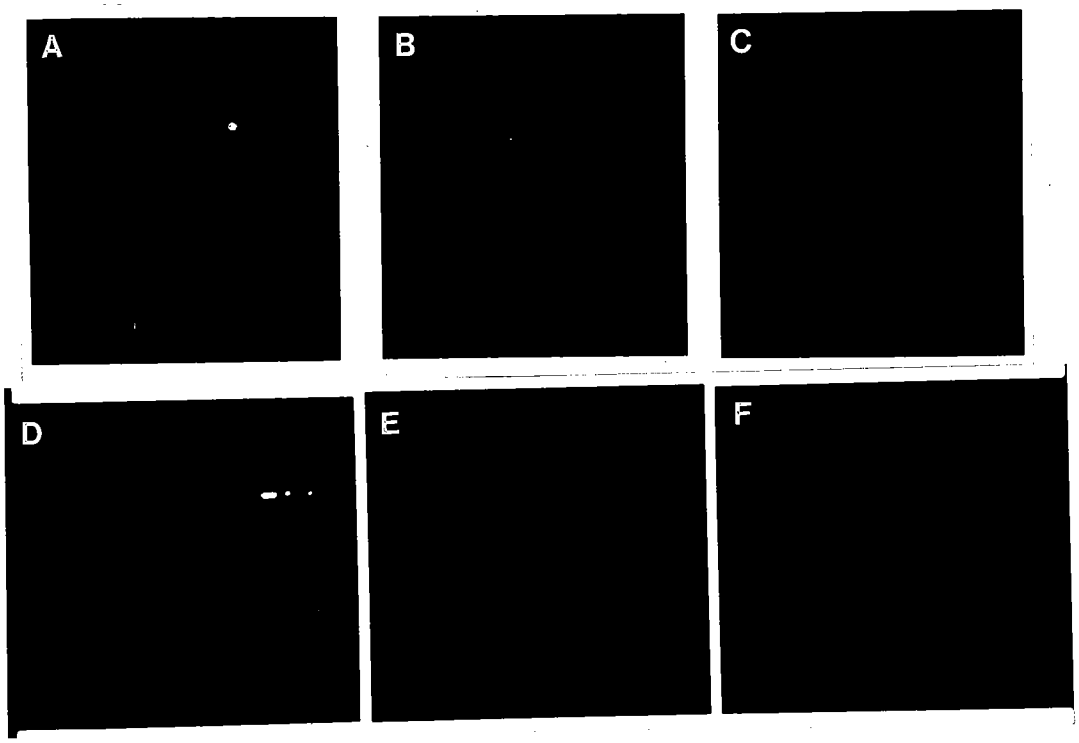

Figure 4-7. Digital images of fibronectin RNA tracks captured with a CCD camera. Signals from digoxigenin labeled intron (B and E, rhodamine) and biotinylated cDNA probe (C and F, FITC) were captured separately and superimposed (A and D) on a computer using alignment beads which fluoresce in both colors in the same field. The exon sequences extend through the whole length of the track.

signals were longer than those produced by the intron-specific probes. In the rest of the tracks, signals produced by the cDNA and intron probe were of the same apparent length.

To confirm that the color separation of a track was not due to some artifact created by certain combinations of fluorochromes, intron and cDNA probes were labeled with reverse colors. Regardless of the labeling scheme the signals made by the cDNA probe were consistently longer than with the intron probe (Fig. 4-6, B).

To further confirm that the two color track was not due to optical shift of the different fluorochromes, a single genomic fibronectin probe was labeled by both biotin and digoxigenin and detected by red and green colors, or cDNA and intron probes labeled by biotin and detected by two different colors. For both types of experiments, only a mixed orange color could be seen throughout the whole length of the track (Fig. 4-6, C and D). There was no separation of the colors in any of these control experiments, indicating that the two color track observed by intron and exon double color hybridization was clearly not due to an optical shift for either of the two methods of analysis used.

The two color track created by the absence of intron sequences in part of the track or focus defined by the cDNA probe indicates that the removal of intron sequences occurs within this accumulation of RNA. These results further suggest that the splicing process is spatially ordered within the track.

Specific RNAs Are Associated with Transcripts Domains in the Nucleus.

Having demonstrated that accumulations of fibronectin RNA reflect the sites of both transcription and splicing, further analysis was undertaken to determine if the individual fibronectin RNA tracks associate with the poly(A)/snRNP rich transcript domains and, if so, the frequency and nature of their spatial relationship. Two different overlapping markers were used to define the "transcript domains": biotinylated oligo d(T) probes to detect regions concentrated in poly(A) RNA or, alternatively, indirect immunofluorescence to detect SC-35 antigen. The detection of both fibronectin RNAs and domains in the same cells was done by hybridization of fibronectin transcripts first and followed by fixation and subsequent detection

of poly(A) or SC-35. Since the anti-SC-35 antibody does not react with rat cells, human fibroblast cells and human fibronectin cDNA probes were used.

Quantitative analysis of over one hundred cells was done by direct microscopic visualization through a dual-band filter, or by superimposing computer images of optically sectioned cells captured by a CCD camera. The results showed a variable but clearly non-random spatial relationship between fibronectin RNA foci or tracks and the larger domains enriched in processing components and poly(A) RNA (Fig. 4-8). As illustrated in figure 4-9, the percentage of cells in four categories representing different types of spatial association was determined. "Total overlap" indicates that the whole length of the RNA track or focus was completely within the domain; "partial overlap" indicates only part of the RNA track overlaps the domain; "in contact" means that one end or just one side of the RNA track appears to directly contact the domain; and "separate" indicates that there is no visible association or connection between the RNA signal and domains. The analysis performed by two independent investigators showed that the majority (88%) of the RNA tracks or foci were associated with poly(A) rich domains, although the specific positioning varied from cell to cell. Approximately 43% of fibronectin RNA tracks or foci partially overlapped with poly(A) RNA rich domains, 37% immediately juxtaposed the domain, and 8% totally overlapped with domains. Only a small fraction (12%) appeared separate, although often very close. This association between the fibronectin RNA tracks or foci and larger transcript domains is thought to be specific for the following reasons. First, the nuclear volumes of both individual fibronectin RNA tracks or foci and transcript domains are small; poly(A) transcript domains have been estimated to occupy approximately 5% of the whole nuclear volume by using potics allowing 0.5 μm resolution at z axis (Carter et al., 1993) and specific RNA accumulations occupy significantly less, no more than 1%. Hence the frequency with which the RNA track and domains would spatially associate based on random location is extremely small. Second, in negative controls in which non-transcribed centromeric sequences were hybridized simultaneously with poly(A) RNAs, it was found that the satellite DNAs are totally non-coincident with poly(A) domains (Carter, et al., 1991).

When another marker, SC-35 antibody, was used to define the transcript

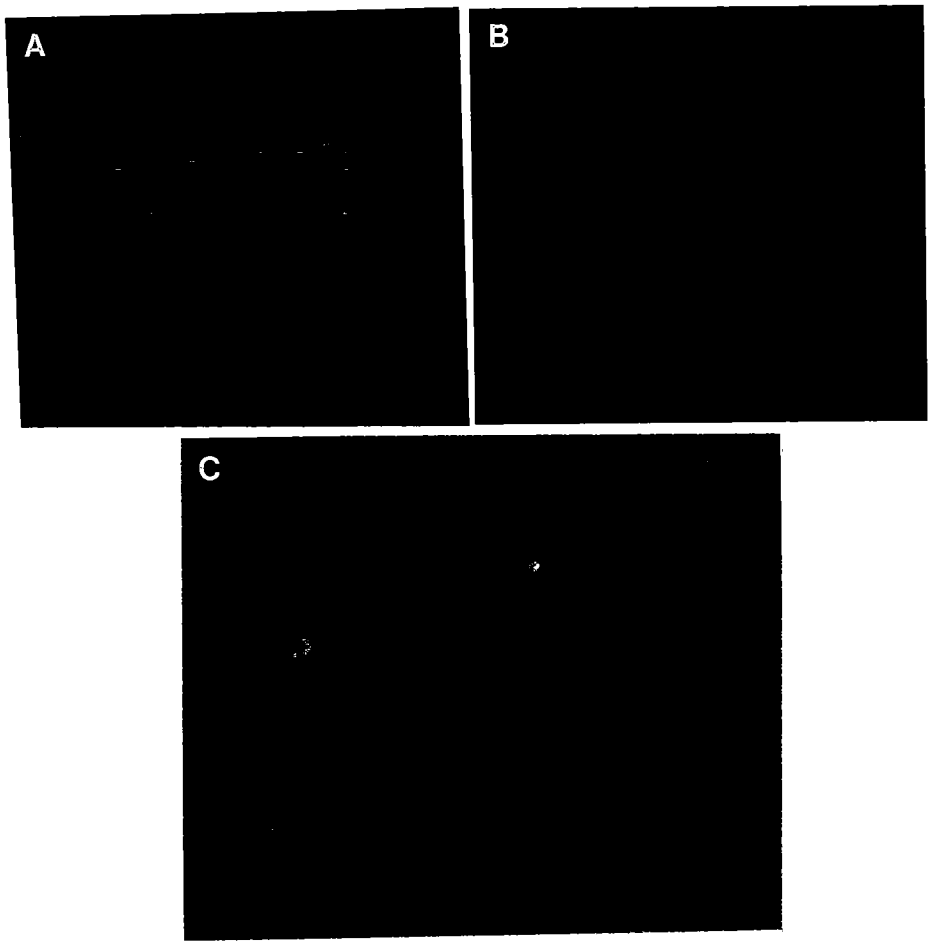

Figure 4-8. Localization of fibronectin RNA tracks relative to larger transcript domains. (A and B) Standard photomicrographs showing the location of the fibronectin RNA tracks or foci relative to transcript domains visualized using antibodies to SC-35 in WI-38 fibroblasts. The digoxigenin labeled 2 kb pFH-1 human cDNA probe was detected using FITC anti-digoxigenin (green) and anti-SC-35 using rhodamine (red) conjugated donkey anti-mouse antibody. (C) Location of the fibronectin RNA tracks relative to transcript domains visualized by poly(A) RNA hybridization using a biotinylated dT55 probe. Signals were detected using FITC conjugated anti-dig for the pFH-1 cDNA probe and Texas-red avidin for poly(A) RNA.

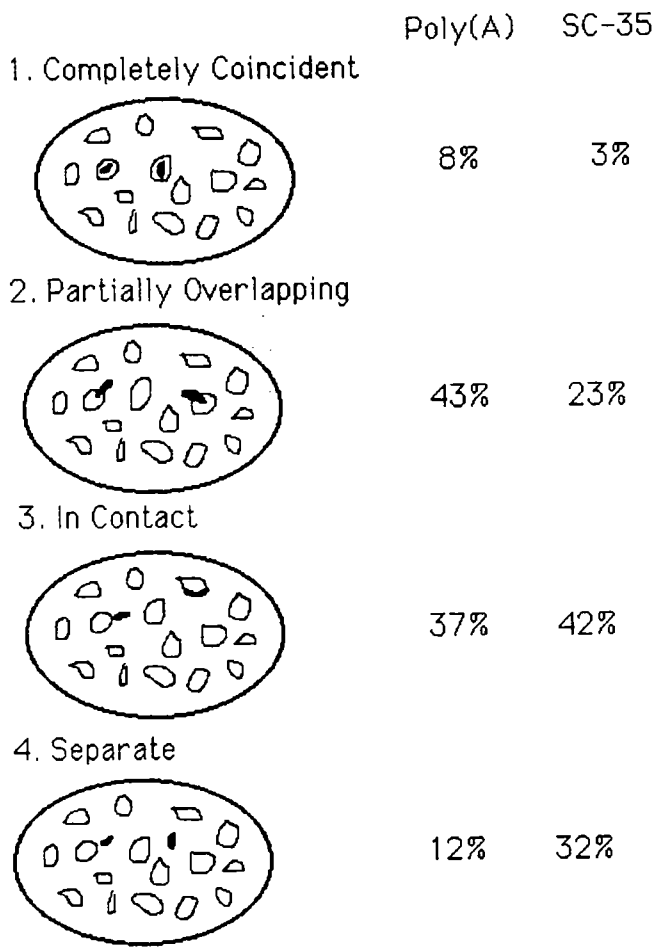

Figure 4-9. Quantitative summary of the spatial relationship between fibronectin RNA foci or tracks and transcript domains. Four nuclei represent four different categories. Open circular structures in each nucleus represent signals from deoxy$(T)_{55}$ hybridization or antibody staining of SC-35 domains. Patched areas represent signals from pFH-1 hybridization to human WI-38 fibroblasts. Nuclei (n=130) were scored by two independent investigators. The first three categories represent different positional relations of tracks or foci that were associated with transcript domains, totaling 88% for poly(A) RNA and 68% for SC-35. If tracks and domains did not appear to be associated with each other, they were scored as separate (regardless of the distance between them). This analysis was performed with optics (Zeiss Neofluor 100, 1.4 numerical aperture) that allow 0.5 μ Z axis resolution. In addition, several cells were serially sectioned in 0.2 μ optical steps.

domains, the result of colocalization of fibronectin RNA track and domains was similar but slightly different from the result of poly(A) domains. The majority of RNA signals were associated with SC-35 rich domains even though the fraction of fibronectin RNA tracks scored as separate from a visible SC-35 domain increased to 32.4%. This can be explained by the previous observation that SC-35 forms a smaller inner core within the poly(A)-rich domains (Carter et al., 1993). Therefore, a certain percentage of tracks may overlap with the periphery of poly(A) domains and be adjacent to but not contacting the SC-35 core.

To assess whether the fibronectin RNA accumulations extended to the nuclear envelope or were more internally positioned, direct microscopic inspection of many cells was done by using high-resolution optics. The result indicated that RNA tracks or foci were localized in the internal portion of the nucleus. This result is further confirmed in five different optically sectioned cells in which fibronectin RNA accumulations were in the same internal focal planes as the highly concentrated SC-35 or poly(A) rich regions, which have been shown to lie in a single horizontal layer just below the midline of the nucleus some distance from the nuclear envelope (Carter et al., 1993). The cover of this thesis shows a model of the topology of fibronectin RNA tracks related to transcript domains and the nuclear interior.

Although recent work has shown that transcript domains are areas enriched in snRNP proteins which contain accumulations of pol II transcripts (Carter et al., 1991), the actual site of either active splicing or transcription within the nucleus has not been previously demonstrated for any non-ribosomal gene. The results presented here provide the first and direct evidence that active splicing of fibronectin RNA occurs in close association with transcript domains. Since these results show that transcription occurs very close to splicing, gene transcription may also be closely associated with the larger poly(A)/snRNP rich domains.

DISCUSSION

Using high resolution fluorescence *in situ* hybridization, fibronectin RNA synthesis as well as splicing and the relationship of these with overall

nuclear structure have been studied. Several lines of evidence are found to support the higher-organization of the nucleus and provide insight into the relationship of RNA metabolism and nuclear structure.

Different combinations of genomic, cDNA, intron specific probes and anti-SC-35 antibody were utilized for DNA/RNA, RNA/RNA and RNA/protein detection. The experiments allow the simultaneous visualization of a gene and its transcripts, intron sequences and exon sequences from this same gene, or individual gene transcripts and larger poly(A)/SC-35 rich domains within individual cells. A highly localized nuclear concentration of fibronectin RNA was observed, and most nuclei showed one or two distinct sites of intense hybridization. The localized RNA signals frequently formed an elongated "track" up to 6 micron in length and both the length and orientation of tracks with respect to the x-y and z axes were highly variable. Intron and exon probes were hybridized to the same focus or track in the nucleus indicating the concentrated RNA signals represent the accumulation of primary transcripts. Double hybridization to both DNA and RNA demonstrated that 86% of the detected gene signals overlapped RNA accumulation sites. Furthermore, in 88% of elongated RNA tracks, gene signals were positioned at or near one end of the track. This indicates that the fibronectin RNA accumulation forms from the site of transcription and extends well beyond the dimensions of its gene. Hybridization of cDNA probes produced signals which were longer than those formed by the intron-specific probes in at least 84% of cells. Intron signals were never observed longer than cDNA signals on the same track. Therefore, splicing clearly occurs within this RNA track as shown by this unambiguous, spatial separation of intron-containing and spliced transcripts. The transcription/processing site of the fibronectin gene, is associated with poly(A) rich transcript domains in over 88% of cells, with the majority positioned adjacent to the inner SC-35 core.

The highly localized nuclear focus or track of the primary transcripts from the fibronectin gene is consistent with our previous observations on EBV viral RNA which demonstrated a dramatic localization of viral RNA tracks, most elongated in swollen nuclei of cytogenetic preparations (Chapter III). Studies from other groups have also shown localized nuclear RNA from the human cytomegalovirus (HCMV) gene (Raap et al., 1991), the c-fos gene

(Huang and Spector, 1991) and the delta transcript (Kopczynski and Muskavitch, 1992). Most of the RNAs observed in these studies form a focus instead of elongated track, similar to the observations of neurotensin RNA (Xing et al., 1993), c-fos RNA (Huang and Spector, 1991), nascent transcripts of the Drosophila Ubx gene (Shermoen and O'Farrell, 1991) and HCMV viral RNA (Raap et al., 1991). The detectability and different distribution patterns seen for different nuclear transcripts are likely related to the size of the primary transcript, level of transcription, extent of processing and the efficiency of transport.

In previous electron microscopic studies on ribosomal RNA gene transcription in amplified nucleoli of Drosophila melanogaster, it was found that the clusters of RNA strands are extended from DNA template in a tandemly-repeated array which is described as a "Christmas tree" (Miller and Beatty, 1969). However, the elongated RNA tracks observed in our fibronectin gene expression system are not likely to represent this "Christmas tree" because the length of the gene is generally below the resolution of the light microscope and hence would produce just a point signal of fluorescence (Lawrence et al., 1988; Lawrence et al., 1990; Trask et al., 1991). The much longer RNA hybridization signals in this study reflect an accumulation of many RNA molecules extending well beyond the dimension of the gene.

Since specific RNA tracks were initially described, it has been suggested by indirect evidence that they may overlap the site of transcription (Lawrence et al., 1989, 1990; Raap et al., 1991; Huang and Spector, 1991). However, in none of these studies was the site of a gene and its primary transcripts visualized simultaneously in order to demonstrate directly the site of transcription. The clear overlap between the fibronectin gene and its RNA accumulation demonstrates that we are directly visualizing the site of transcription. A recent similar finding from our lab provides evidence that collagen RNA tracks also form at the site of transcription (Strauss et al., 1993). The polarity of the fibronectin gene and its RNA track argues that unprocessed RNA molecules accumulate from the site of transcription. The accumulation of RNA at or near the site of transcription may reflect the fact that the speed of synthesis of primary transcripts is high relative to subsequent processing steps which appear to be rate limiting.

Our results indicate that allelic genes from homologous chromosomes are often both transcriptionally active and spatially separate, forming two tracks or foci in each nucleus. TGF-β stimulation of fibronectin transcription increased the percentage of positive cells (from 60% to 90%), the percentage of nuclei containing two signals (from 32% to 63%) and the intensity of each individual signal. This result could reflect the sensitivity limit of our fluorescence *in situ* hybridization procedures, in that the nuclear RNA from each gene in non TGF-β treated cells may not always be detected if expressed. It is not clear whether the increased detection in TGF-β treated cells reflects more genes being transcriptionally active or whether the detection efficiency of each RNA track has been increased due to greater abundance (intensity).

Splicing of introns from the primary transcripts occurs directly within the accumulation of RNA. There is a discrete spatial separation of transcripts containing and lacking a specific intron along what may be an "assembly-line" beginning at the site of transcription (Fig. 4-10). There is evidence both for and against the cotranscriptional splicing of pre-mRNAs. Observing the transcripts of the chorion genes in Drosophila, which were amplified about 16 fold over the normal diploid level during oogenesis, Osheim et al. had shown that the spliceosomes are associated with nascent transcripts (Osheim et al. 1985), and in some cases, the splicing of the nascent transcripts can be directly visualized by E.M. (Beyer and Osheim, 1991). In contrast, for some mammalian mRNAs, the unspliced transcripts could be isolated in the poly(A) fraction, indicating that splicing is post-transcriptional (Nevins, 1983). Based on the dimensions of the track and the separation of intron containing and intron absent portions within a track, our results are most consistent with the post-transcriptional splicing model. However, the intron probe used in our study covered only one of many introns (the 1st intron) of the fibronectin gene and the cDNA probe span four exons (the 5th-8th exons) downstream of our intron probe. Hence, the intron-lacking part of the RNA track only reflects the removal of that specific intron. It has been suggested that the introns of ovomucoid pre-mRNA are removed in a preferred order (Lewin, 1987b). However, it is unclear for fibronectin pre-mRNA as for most pre-mRNA, if the splicing machinery prefers to remove all the introns in one primary transcript first and then initiate the next splicing step to another

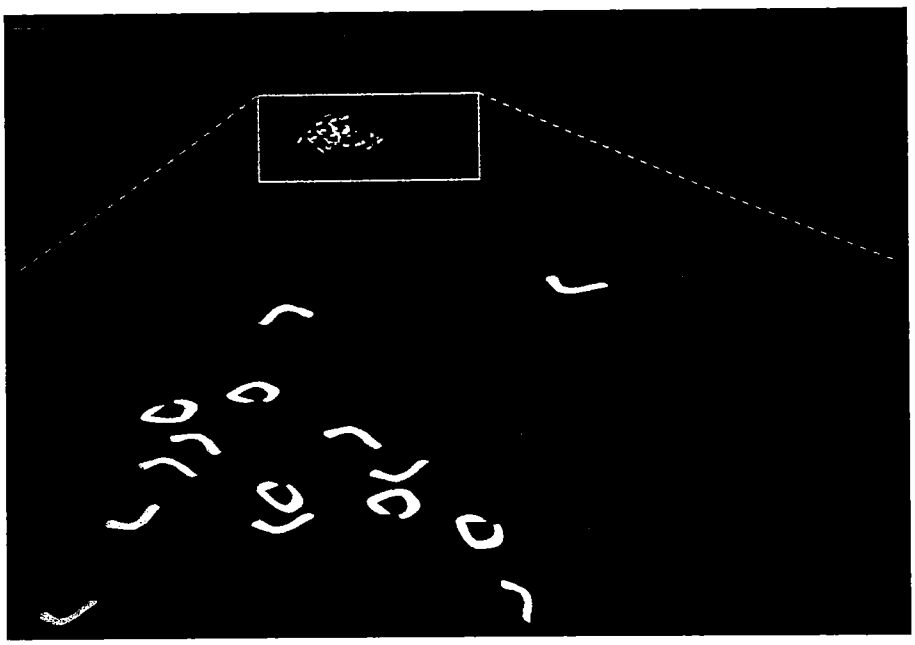

Figure 4-10. Schematic model for the ordered assembly of transcripts within the fibronectin RNA track. This model suggests that transcripts at different stages of processing are concentrated in different areas along a processing track at varying distances from the gene. The red structure represents the DNA frame. During splicing, the unprocessed transcripts do not appear to be freely diffusing but rather may be physically associated with an insoluble nuclear substructure. A simplified version of the primary transcript is shown, with a single intron indicated in white and exons indicated in green. The exon probe used in these experiments is high-lighted with yellow to indicate its position 3' to the intron probe (white). This model shows the RNA track oriented with the intron-containing transcripts closest to the gene, although this has not been directly demonstrated.

primary transcript.

The clear order within one fibronectin RNA track strongly supports the association of unspliced and spliced transcripts with nuclear substructure. For example, the nuclear matrix as shown by the EBV RNA study (Chapter III) might be the possible structural basis for this localization. Further investigations to determine if the fibronectin RNA track is also preserved after matrix fractionation should be very informative in this regard.

In contrast to primary and mature transcripts, excised introns for some RNAs may diffuse freely. The study of neurotensin RNA by *in situ* hybridization has indicated that excised intron sequences are free to diffuse in the nucleoplasm in induced PC-12 cells (Xing et al., 1993). The observation is not caused by hybridization to repetitive RNA or DNA, since it is absent in noninduced cells, and is only apparent in induced cells expressing bright fluorescent nuclear foci of neurotensin RNA. Similarly, hybridization with genomic or intron probes for fibronectin RNA frequently showed more nucleoplasmic staining. The apparent free diffusion of intron sequences, in contrast to the discrete localization and structural association of primary transcripts and the splicing process suggests that the spliced intron may not be associated with nuclear substructure. This is in very good agreement with two previous studies using biochemical fractionation and RNA Northern blot analysis (Zeitlin et al., 1987; Coleclough and Wood, 1984). These studies indicated that the excised introns are easily extracted from the nucleus, whereas the primary transcripts as well as the processed mRNA remain insoluble within the matrix fraction. The high sensitivity of the techniques used here, coupled with the possibility that excised introns may be more abundant than believed from studies of detergent extracted cells, have allowed us to visualize the distribution of these less concentrated sequences, in addition to the localized areas of highly concentrated RNA. However, it should be noted that the presence of punctate nucleoplasmic intron signals of fibronectin RNA was not as consistently evident as for neurotensin. The possible explanations for this inconsistency include: a) the abundant cytoplasm around and over nuclei within monolayer fibroblasts and myoblasts necessitated that cells be briefly triton extracted which may preferentially release excised intron sequences from the nucleus (Zeitlin et al., 1987), and b)

as contrasted with non-extracted PC12 cells which have very little cytoplasm and were flattened by cytospinning, the presence of fibronectin mRNA in the fibroblast perinuclear cytoplasm made it more difficult to evaluate whether there was a low concentration of introns throughout the nucleoplasm.

Sites of both transcription and processing of fibronectin RNA overlap or juxtapose large, internally localized transcript domains. This is consistent with previous results which indicated that both poly(A) RNA (Carter et al., 1991) and c-fos RNA (Huang and Spector, 1991) concentrate in these regions. Results presented here indicate that transcription and RNA splicing are associated with transcript domains, hence it is unlikely that these larger domains exist exclusively for the assembly or storage of spliceosomes. It remains to be determined, however, how the RNA track is oriented relative to both the domain and the nuclear envelope. It would be interesting to know which end of the track is closer to the domains, the end proximal to the gene or the end distal to the gene.

The results presented in this chapter suggest an important possibility that active genes are specifically positioned with respect to the domains. Based on the number, relative size and intensity of signal for poly(A) RNA domains versus specific RNAs, it appears likely that each transcript domain reflects the transcription and/or processing activity for numerous genes. If other active genes are found preferentially positioned relative to these domains, it will imply a higher-level genomic organization which may have profound implications for the regulation of gene expression. Although actual sites of transcription and splicing were not identified, the demonstration that c-fos transcripts accumulate near snRNP-rich domains soon after gene induction (Huang and Spector, 1991) is consistent with this model, as are some of the recent results from our lab localizing primary transcripts from other genes (Coleman and Lawrence, in preparation and Chapter V).

In the previous report, it was suggested that the EBV viral RNA "tracks" may represent either a processing or transport pathway (Lawrence et al., 1989). While work presented in this chapter does not specifically address transport, it provides direct evidence that splicing is occurring within the fibronectin RNA formation. Although some transport of RNA is likely to occur along this track, perhaps simultaneous with processing, the observation that

fibronectin RNA tracks or foci did not generally extend to the nuclear envelope leaves open the possibility that transport of mature mRNA, which is quite rapid, occurs through more than one route or even by free diffusion.

The contrast between the highly localized distribution of endogenously synthesized nuclear RNAs with the much broader, more diffuse distribution pattern of microinjected pre-mRNAs (Wang et al., 1991) indicates different pathways that the two types of RNA take and underscores the potential importance of structural association for RNAs synthesized in vivo. RNAs synthesized in vivo accumulate close to their transcription site and undergo splicing at this site. In contrast, large amounts of exogenous microinjected pre-mRNAs do not accumulate at the site of gene but rapidly move throughout the nucleus and distribute widely in any snRNP rich centers they contact. Obviously, it is important to investigate more genes and their nuclear RNAs to fully understand the integration of nuclear structure and function. What our results clearly indicate is that genes and their pre-mRNAs synthesized in vivo can exhibit not only higher-level nuclear organization, but also a functional association with underlying substructure.

CHAPTER V

One of the major implications of the fibronectin studies (Chapter IV) was that specific genes and RNAs may be functionally organized within the nucleus. To determine the extent to which this may be generalizable, more genes and RNAs were studied. In this chapter, additional results concerning the localization of specific RNAs and their respective genes within the nucleus are presented. In part I, data on five protein coding genes from work that is still ongoing is presented. In part II, the distribution of an atypical and interesting nuclear RNA from the XIST gene, which apparently does not code for a protein is investigated. Results presented in this chapter are not intended to be conclusive and a more thorough analysis will certainly yield a better understanding of nuclear organization.

PART I: Nuclear Localization of Specific Genes and/or RNAs Relative to SC-35 Rich Domains

The results of the fibronectin RNA study provide initial evidence for functionally relevant nuclear organization. The localization of the fibronectin gene and its RNA indicate that both transcription and splicing of at least some specific RNAs are preferentially associated with larger transcript domains. One implication of this finding is the possibility that transcriptionally active genes could be clustered in interphase nucleus near sites which facilitate RNA metabolism. One way to test this hypothesis is to directly examine and compare the nuclear locations of specific sequences of several different genes. Information about the nuclear positions of these genes in either the active or inactive state will help determine whether observations made in the fibronectin system can be generalized.

The distribution of three active and two inactive genes were studied, all in the same cell type. Experiments were done under conditions which allow simultaneous detection of genes and transcript domains in two different colors. The genomic probes for these genes were labeled with digoxigenin and hybridized to intact human diploid fibroblasts, while transcript domains were

visualized by immunofluorescence with anti-SC-35 antibody. Among the specific genes studied are actin, collagen, cardiac myosin heavy chain, neurotensin and histone.

RESULTS

Experimental results were analyzed largely by standard light microscopy using a dual or triple-band filter. Once a successful experiment is obtained, the relative positions of genes in many cells can be analyzed fairly quickly, using a high numerical aperture objective which has a depth of field of approximately 0.5 microns. Because objects further apart than this appear to be out of focus, some three-dimensional information can be obtained in this way. Cells were scored by two independent investigators in the following categories, completely coincident, in contact (directly adjacent), or separate.

Like the fibronectin gene, the collagen gene which is about 40 kb in size is also highly expressed in the fibroblast. Paraformaldehyde fixed human fibroblast cells, Detroit 551, were heat denatured as described in Chapter II and a 17 kb mouse genomic probe to collagen type I was used for hybridization. This probe effectively detects the human mRNA due to high homology of the coding region (Strauss et al., 1993). Most frequently, two (range 1-4) hybridization signals with either focal or track-like structures were observed within the nucleus (Fig. 5-1, A). Compared to the tiny spot of a typical single-copy gene signal, the size and shape of the observed collagen hybridization signals clearly suggested that they represent the detection of collagen RNA instead of just the collagen gene. That the signal was predominantly if not entirely RNA was confirmed in other experiments in which nuclear DNA was not denatured (Johnson and Lawrence, personal communication) and the collagen signals remained essentially unchanged.

To investigate the relationship between collagen RNA and transcript domains in the nucleus, SC-35 antibody was used again to stain the domains. Cells which had both collagen RNA and transcript domain signals were scored under the microscope through a dual-band filter. About 96% of the RNA signals (n=73) were totally overlapping with SC-35 domains and the other 4% partially overlapped domains. It is important to note that the vast majority of

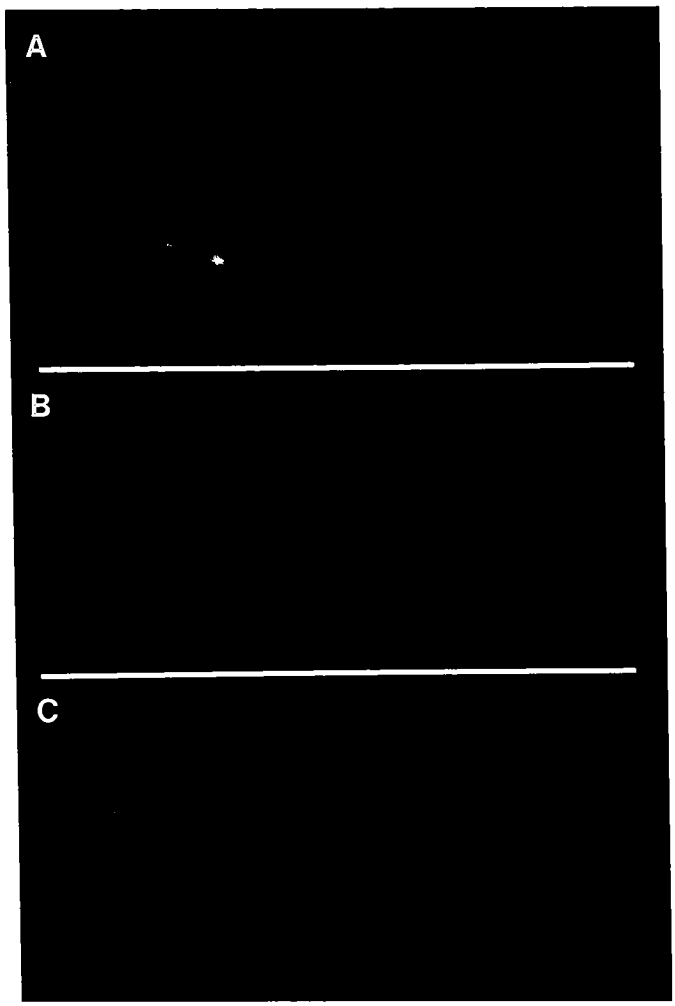

Figure 5-1. Detection of collagen RNA and transcript domains. Human Detroit 551 fibroblasts were hybridized with digoxigenin labeled mouse genomic collagen probe. Transcript domains were stained with anti-SC-35 antibody. (A) Specific hybridization was detected by FITC conjugated anti-digoxigenin antibody and SC-35 staining by rhodamine conjugated donkey antibody. (B) Nuclear distribution of collagen RNA shown in red (rhodamine). (C) Transcript domains visualized with FITC anti-dig (green).

collagen RNA signals totally overlapped with the transcript domains. In contrast, the association of fibronectin RNA with transcript domains was in this respect less complete [totally overlapping (3%), partially overlapping (23%), in contact (42%) and separate (32%)]. Collagen RNA signals that were well separated from SC-35 domains were not observed at all (Table 5-1).

An interesting aspect to the collagen RNA results is that many RNA signals were found which had a similar size and shape to their associated domains (compare Fig. 5-1, B with C). However, the RNA was often much more concentrated in one part of the domain, whereas the SC-35 staining did not show this intensity difference. Careful examination indicated that in most (~80%) of cases each RNA signal did not completely occupy the whole area of the SC-35 domain, consistent with the possibility that each domain may be formed by RNA from more than one gene (see Discussion).

It has been shown from the fibronectin model system that the site of the fibronectin gene is located immediately next to the RNA track. In a study from our lab using transgenic mouse cells, the simultaneous detection of RNA from an inserted collagen gene and sequences from the flanking vector also indicated that the collagen gene and its RNA were extremely close (Strauss et al., 1993). Therefore, it is reasonable to assume that the site of the collagen gene is very closely associated with the transcript domains. However, the detailed spatial relationship between the collagen gene and domains remains to be determined. The gene could be localized either at the center or just at the border of the domains.

To further expand these observations, the human beta actin gene was studied. A 14 kb genomic probe, p14T β-17, which conatins the human beta actin gene (~6 kb) was similarly hybridized to human fibroblasts, Detroit 551, in which the actin gene is actively expressed. The results showed one or two tiny signals in the nucleus (Fig. 5-2), consistent with detection of a single-copy gene. Non-denatured control samples indicated that nuclear RNA from the actin gene was not readily detected in these experiments (see Discussion), therefore the gene was studied directly. The detection of only one site of the gene signal in some nuclei probably reflects the fact that hybridization efficiency is not 100%, and is considered unlikely to represent somatic pairing since interphase gene mapping studies indicate that homologous chromosomes

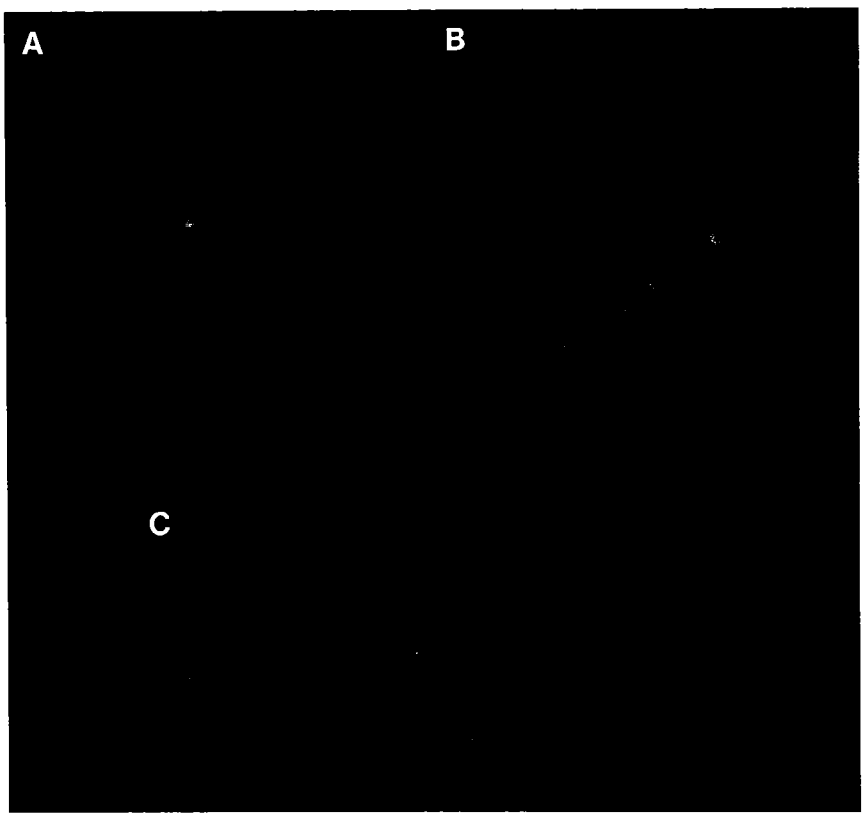

Figure 5-2. Distribution of the actin gene and transcript domains within the nucleus. (A and B) Actin gene in Detroit 551 cells was hybridized with a digoxigenin labeled human genomic β-actin probe and detected by FITC conjugated anti-digoxigenin antibody. SC-35 antibody staining was detected with rhodamine conjugated antibody. The association of the actin gene is clear in figures A & B. There are one gene signal can be seen in A and two in B. Figure C illustrates a more difficult to interpret cell, in which one actin signal is associated with a very small domain, and the other is close to but not in contact (not associated) with another small domain.

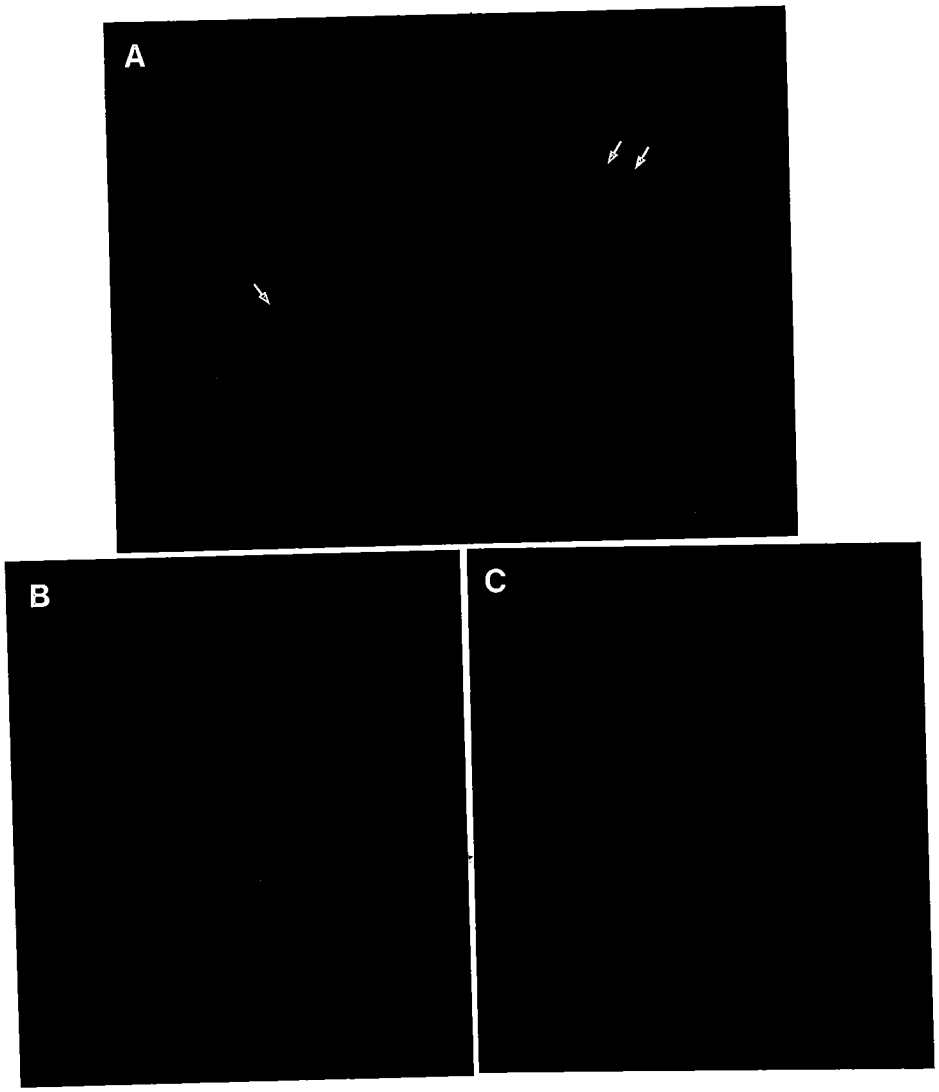

Figure 5-3. Localization of neurotensin and histone genes with respect to transcript domains within the nucleus. (A) Neurotensin gene was visualized by a digoxigenin labeled probe and detected with rhodamine (red). Transcript domains were detected by anti-SC-35 antibody (FITC, green). The neurotensin genes are generally separated from SC-35 domains and at the nuclear periphery (see arrows). (B and C) Histone gene was hybridized with a digoxigenin labeled probe and detected by FITC conjugated anti-digoxigenin antibody. Anti-SC-35 antibody staining was detected with rhodamine conjugated antibody.

are widely separated (Lawrence et al., 1990, Trask et al., 1991). Through a dual-band filter, the location of the gene and its relationship with SC-35 domains were studied and over 100 gene sites in 80 cells were randomly chosen and scored. 90% of the actin gene sites were directly adjacent to the domains, i.e. localized at the edge of the domains with no visible separation from them (Fig. 5-2). 4% of the gene sites totally overlapped (inside) the domains and 6% were separate from the domains (not in direct contact) (Table 5-1). An important observation, as also seen for collagen, was that if two visible gene or RNA sites were found in one nucleus, generally they were not associated with the same domain but with two different domains. The size of the domains with which the actin gene associated was variable. It was also noted that, as observed in two dimensions, there was no tendency to localize near the nuclear periphery. The close association became even more obvious in cells whose nuclei had relatively few transcript domains, yet the gene signals were still attached to the domains which occupied a small volume of the nucleus. As previously discussed, poly(A) domains only make up about 5% of nuclear volume and specific gene/RNA signals appear to represent no more than 1% of the total nuclear volume, hence the probability of random association between these two is very negligible.

Next, the inactive genes were studied. The first was the human cardiac myosin heavy chain (cMHC) gene which is expressed exclusively in the cardiac muscle (Lompre et al., 1984; Saez et al., 1987). The relationship of the cardiac myosin heavy chain gene with transcript domains was investigated in fibroblasts, in which the gene is expected to be inactive. The data show that 90% of cardiac myosin heavy chain gene signals did not associate in any form with SC-35 domains and only 10% were in direct contact with the domains (Table 5-1). The distance from most of the gene sites to the nearest domains was variable but generally not very close. Since this data on cMHC is based on just twenty cells, it will need to be extended to a larger cell sample to confirm the results. However, results thus far clearly indicate that the gene is not associated with the domains and positioned quite differently than either collagen or actin.

A second inactive gene, neurotensin, was then investigated. Neurotensin is actively transcribed only in certain types of neural cells

	ASSOCIATED		SEPARATE
	Overlapping	Contacting	
Collagen RNA	100	0	0
Actin gene	7	87	6
Histone gene	11	43	46
Neurotensin gene	1	10	89
cMHC gene	0	10	90

Table 5-1. Quantitative summary of the spatial relationship between different genes and/or RNA and transcript domains. For collagen, 135 signals were scored; actin, 155; histone, 122; neurotensin, 154; and cardiac myosin heavy chain (cMHC), 20. Data are expressed as the percentage of signals counted.

(Kislauskis et al., 1988). For this sequence, 91% of over 100 gene signals were found to be separated from the transcript domains within nuclei of fibroblasts (Fig. 5-3, A; Table 5-1). The rest of the signals (9%) were either in contact at the edge or overlapping the domains. Interestingly, in the case of neurotensin it was clearly observed that there was a preferential localization of this inactive sequence at the nuclear periphery, with slightly over half of the signals being in the rim, just under the nuclear envelope, from an area in which transcript domains are excluded (Carter et al., 1991, 1993).

Finally, the histone gene was studied. This gene is transcribed in fibroblasts, most actively but not exclusively during S-phase (Baumbach et al., 1987). The genomic probe used for the study represents the H3 and H4 histone gene cluster (Sierra et al., 1982). The results of the histone gene experiments gave a relatively complex picture (Fig. 5-3, B and C). About 46% of the gene sites were separated from the domains, 11% overlapped and 43% were extremely close but not contacting the domains (Table 5-1). While these results still suggest a possible preferential association or positioning, the results were not as clear cut as for the other four genes described above.

DISCUSSION

Information as to where specific protein-coding genes reside within the nucleus has been almost entirely lacking in previous literature. A few observations have been reported; it was noted that the neu oncogene is consistently localized in the central region of lymphocyte nuclei; whereas the dystrophin gene sequences are very close to the nuclear envelope even in male cells in which the X chromosome is not inactivated (Lawrence et al., 1990). In this study, the nuclear position of different active and inactive genes was examined in detail relative to specific, functionally relevant reference points, the poly(A) RNA/splicing factor rich transcript domains. If transcript domains are centers involved in RNA processing and, possibly, transcription, it becomes compelling to assess how specific genes are positioned with respect to these centers. They provide not only internal reference points, but reference points with defined functional implications.

The results clearly demonstrated that in addition to fibronectin, two

other active genes (actin and collagen) are closely associated with transcript domains such that their genes or primary transcripts either totally or partially overlap with domains. In contrast, the non-transcribing genes (cardiac myosin heavy chain and neurotensin) do not show preferential association with the domains. The results of another gene, histone, paint a different picture with about half of the gene sites separate and half very close to the domains.

An interesting feature of these findings is the variant but characteristic patterns of spatial association with transcript domains that different active genes or their transcripts showed. In a previous report, c-fos RNA is found associated with the SC-35 domains (Huang and Spector, 1991). Although the specific spatial relationship is not detailed, from the image presented the RNA also appeares to be at the periphery of the domains. In our study, essentially all the collagen RNA sites totally overlapped with the associated domains. In contrast, fibronectin RNA revealed a more complicated association with transcript domains with most tracks either only partially overlapping or immediately juxtaposing the domains (Table 5-1). This suggests that some RNAs/genes might have a preferred position relative to the domains. However, it is unknown whether such a preferred localization has any direct functional linkage to gene expression. Would the different locations within a domain reflect different levels of transcription or RNA splicing for specific genes? It is noted that the average size of collagen nuclear RNA signals is bigger than that of fibronectin RNA, which may indicate that more collagen RNA is synthesized or accumulated before or during splicing. More analysis on the association of transcript domains with other genes/RNAs will be necessary to address these questions.

The study of the actin gene showed a peripheral position of this gene along the edge of transcript domains. It is possible that actin gene transcription occurs just at the outer edge of the transcript domains and then the primary actin transcripts are spliced within the domains. In the case of collagen, since this gene was not directly localized without its RNA, it was not possible to identify the exact sites of the collagen gene with respect to the domains. This gene could be in the center or at the edge of the domain as is the actin gene. The exact location of the fibronectin gene relative to the domains

is also unknown. In future studies, RNase or NaOH could be used to remove collagen RNA so that the exact location of collagen genes within transcript domains could be visualized.

In sharp contrast with the close associations between transcript domains and these actively expressed genes, the result from the human cardiac myosin heavy chain gene and the neurotensin gene, which are both inactive in fibroblasts (Saez et al., 1987; Lompre et al., 1984; Kislauskis et al., 1988), revealed that the vast majority of two gene signals were located outside and separate from the transcript domains (Table 5-1). The localization of inactive neurotensin sequences at the nuclear periphery is consistent with a periphery distribution of inactive heterochromatin within the nucleus (Lewin, 1987a). Collectively, our results do not support the view that active chromatin is localized at the periphery, to facilitate RNA transport through the pores (Hutchinson and Weintraub, 1985; Blobel, 1985; Krystosek and Puck, 1990).

Histone genes pose several unique features as compared to other protein coding genes. Histone gene expression is regulated with the cell cycle with increased transcription during S-phase, but a low level of transcription throughout the cell cycle (Baumbach et al., 1987). Histone transcripts are neither poly-adenylated nor spliced (Stein et al., 1984). These considerations may be relevant to the observation that the histone genes had a pattern of association with transcript domains different from either the active or inactive genes. In our experiments, overall the histone genes had a low percentage of direct overlap with the transcript domains, but a high percentage of gene signals in close proximity with domains. In future work, it will be interesting to see whether the gene positions change during S-phase of the cell cycle.

The reason that we failed to detect obvious localized actin transcripts in the fibroblast nucleus remains unknown. In several experiments targetting only RNA, there was no detectable level of actin RNA signals in the nucleus. In a few experiments a dim punctate fluorescence was observed. It was excluded that the probe was defective or the cells were generally poor in RNA preservation. The possible explanations of the lack of visible concentrated actin RNA signals in the nucleus may include: a) the speed of processing actin

RNA precursor is very high and there is no detectable accumulation of actin gene transcripts in the nucleus; b) the pathway of actin gene transcription and RNA processing might be different from fibronectin and collagen, e.g. transport or processing of actin transcripts may be more diffuse or the RNA released by Triton extraction; c) detection of RNA was obscured by the presence of diffuse RNAs containing repetitive elements in the nucleus. The third is favored currently because it has recently been shown that competition of repetitive sequences allowed another specific RNA to become detectable (Clemson, personal communication). Also, in hybridization of actin probe to cells in which cellular DNA had been denatured and repetitive hybridization competed, the gene signal often appeared to be slightly larger than typically obtained for a single-copy gene, and may have contained an RNA component, and this will be tested in future studies for actin RNA detection. Although extensive attempts to detect histone RNA were not made, the fact that an obvious RNA signal was not observed is consistent with the unusual nature of histone RNA which is very small, unspliced and known to exit the nucleus with exceptional high speed (Stein et al., 1984).

The above analysis on nuclear positions of different genes within a given cell type provides initial insight into potential functional implications of cell-type specific changes in nuclear organization. It is not coincidental that the distributions of three genes which are actively expressed in fibroblast cells are tightly associated with the transcript domains. If this result is further confirmed with more studies, it would suggest that the association of a gene with the transcript domain(s) may well serve to facilitate the expression of that gene, or possibly contribute to its regulation. However, such an association need not be essential for expression of all genes, since other preliminary results from the Lawrence lab indicate that foci of nuclear RNA from the human dystrophin gene are not associated with SC-35 domains, whereas within the same cells MHC primary transcripts are (Coleman and Lawrence, unpublished observations). However, it should be noted that the dystrophin gene is unusually big (2 megabase pairs; Koenig et al., 1987) and experiments thus far have targetted only a small part (10 kb) of this primary transcript.

Since there appear to be few transcript domains relative to the number

of active genes in a nucleus, it will be important to determine directly how many genes may be associated with each detectable "transcript domain". While there are approximately 20-50 transcript domains with a diameter ranging from 0.5 to 3 mm (Carter et al., 1993), there is much less concentrated signal for poly(A) RNA and splicing components throughout the nucleus, which sometimes appears as tiny spots or fibrils. Hence, at this time it is not possible to predict how many different primary transcripts might be associated with the concentrated centers we term "transcript domains". The results presented in this chapter strongly support the conclusion that transcript domains are directly involved not only in RNA processing, but in transcription, since evidence indicates that both collagen and actin gene transcription occurs directly at the edge of the domain or in its center. Therefore, for both collagen and actin, these results demonstrate an even closer spatial relationship between transcription and the domain than was shown for fibronectin (Chapter IV). The results with collagen RNA, in particular, raise the question of whether highly concentrated regions of splicing components could form on the nascent transcripts produced from a single highly active gene. While this cannot be ruled out, several points currently are not consistent with this as the general explanation for transcript domains: 1) fibronectin RNA concentrates not in the SC-35 region, but next to it, therefore the RNA could not have caused the accumulation of SC-35, 2) in general, the concentration of a nuclear RNA does not correlate well with the concentration of SC-35, 3) the number of transcript domains appears to be much smaller than the expected number of active genes per cell (approximately 2000 to 5000), 4) the fluorescent poly(A) signal detected with a small oligonucleotide probe in each domain is generally more than the signal observed with a larger probe targetting several kb of the specific RNA.

The specific association of actively transcribed genes with transcript domains has the important implication that there may be another level of gene expression control, in addition to the direct interaction between transcription factors and certain DNA sequences. The fact that changes in cell-type specific nuclear morphology occur during development (Weiss, 1983) is consistent with the notion that nuclear organization is important in differential gene expression. As a whole, development is characterized by a

progressive restriction in the competence of cells to express their entire genomes. While the complex, highly orchestrated regulation of gene expression necessary to construct an entire organism may eventually be explained in terms of combinatorial schemes of transcription factors, it is also plausible that genes become specifically organized during development in ways that either increase or decrease their competence to respond to transcription factors or the transcriptional machinery. It will be important to study the same genes in different states of expression and the study of this question in the muscle cell system is currently ongoing in the our laboratory.

The possible structural foundation for the relationship between genes and transcript domains could be a nuclear substructure, e.g., the nuclear matrix. Current evidence suggests that interactions of chromatin with the nuclear substructure are important in the transcriptional control of gene expression (Farache et al., 1990; Vaughn et al., 1990, de Jong et al.; 1990; Fey et al., 1991) Using high salt extraction procedures, histones are extracted from chromatin to reveal distended loops of DNA which create a "halo" around and outside the residual nuclear matrix (Vogelstein et al., 1980; Mirkovitch et al., 1988). In a study of the relationship between the DNA loop/scaffold and specific genes by *in situ* hybridization to halo preparations, several transcriptionally active sequences were found positioned at the base of the loop associated with the residual matrix, whereas several inactive sequences were on the extended portion of the loop (Gerdes and Lawrence, in preparation). This differential structural association of active versus inactive genes is consistent with a role for the matrix in spatially organizing DNA. Finally, in this regard it is of interest that in another study, SC-35 has been found tightly bound to the nuclear matrix in the presence of high salt and this association remains under the treatment of DNase I or RNase A (Spector et al., 1991). Hence the high concentration of SC-35 in "transcript domains" may be structurally independent of the high concentration of gene transcripts in this region.

PART II: Localization of XIST RNA within the Nucleus

All the RNAs discussed so far are transcribed from protein coding genes which only make a very small portion of the total RNAs synthesized within the nucleus. There is a large amount of RNA synthesized in the nucleus of eukaryotic cells which remains in the nucleus without being transported to the cytoplasm (Lewin, 1975). The functions of these non-protein coding RNAs may be important but for the most part remains a mystery. In the following section, the nuclear distribution of one such potential RNA, XIST RNA, is studied.

XIST RNA is synthesized from a gene located at the X-inactivation center. X inactivation is the process by which mammals compensate for the presence of an unbalanced dosage of X chromosome-linked genes between sexes. The X inactivation process is a unique *cis*-limited regulatory event which occurs early in mammalian development to transcriptionally "switch off" genes on one of the pair of X chromosomes in females (Lyon, 1961; Brown and Willard, 1992; Grant and Chapman, 1988). Although the mechanisms of the X inactivation process are far from being understood, systematic studies of inactivation patterns in females carrying X chromosome aberrations (mainly X-autosomal translocations) have provided strong evidence of an "X-inactivation center" (*XIC*) located in Xq13 (Russell, 1963; Lyon, 1971; Cattanch, 1975; Brown et al., 1991b). This same region is further implicated in the processe of X inactivation by the observation that it is required for the formation of a visible Barr body (Therman et al., 1974), the heterochromatic region found at the periphery of the nucleus which corresponds to the inactive X chromosome (Barr and Carr, 1962; Daly et al., 1977).

An important advance has been recently made through the cloning of a gene, XIST (Xi-specific transcript), which maps to the *XIC* region (Brown et al., 1991a). This gene has the unique feature of being expressed from the inactive X chromosome, but <u>not</u> from the active X chromosome, while other genes known to escape X-inactivation are active on both X chromosomes. The coincident location of XIST with the XIC and the exclusive expression from the inactive X chromosome suggest that XIST has a role in X inactivation.

Human XIST cDNAs containing at least eight exons and 17 kb of *XIST* cDNA have been isolated and sequenced (Brown et al., 1992). It has been shown that XIST RNA is alternatively spliced and at least some of the XIST RNA is poly-adenylated (Brown et al., 1992). The gene spans 35 kb of genomic DNA within the region of the XIC and does not contain any significant conserved open reading frames, and thus does not appear to encode a protein (Brown et al., 1992). The absence of a protein product encoded by the XIST gene suggests that XIST-encoded product is a cis-acting RNA molecule involved in X inactivation, e.g., in the formation of the heterochromatic Barr body.

The unique nature of XIST RNA and its possible structural function in X inactivation make it a very attractive candidate for the study of nuclear RNA distribution. The subcellular location of XIST transcripts was analyzed by nuclear and cytoplasmic fractionation and it is found that XIST RNA localized predominantly if not entirely to the nucleus (Brown et al., 1992). To attempt to determine the subnuclear distribution of XIST RNA within the nucleus, fluorescence *in situ* hybridization analysis was performed.

RESULTS

A 9 kb genomic probe G1A was labeled by nick-translation with digoxigenin-dUTP and hybridized to diploid female human fibroblasts (WI-38) under conditions which allow RNA but not DNA hybridization (see Chapter II). Consistent with the subcellular fractionation experiments, hybridization signals were predominantly nuclear. The signals were highly concentrated at a single subnuclear location (Fig. 5-4, A). Just one site of hybridization was observed in over 97% of nuclei, in contrast to RNAs produced from autosomal genes, such as fibronectin and collagen, which commonly showed two signals. In 46, XX female cells, the two homologous X chromosomes are usually separated widely within the nucleus of fibroblast (Lawrence et al., 1990), indicating that the observed site of XIST RNA is not produced by RNAs from alleles on both X chromosomes. Strikingly, these nuclear hybridization signals were highly localized to a site corresponding precisely with the position of the heterochromatic Barr body which is detected at the periphery of the nucleus by DAPI staining (Fig. 5-4, compare A with B), indicating a highly specific association of XIST transcripts with the inactive X chromosome.

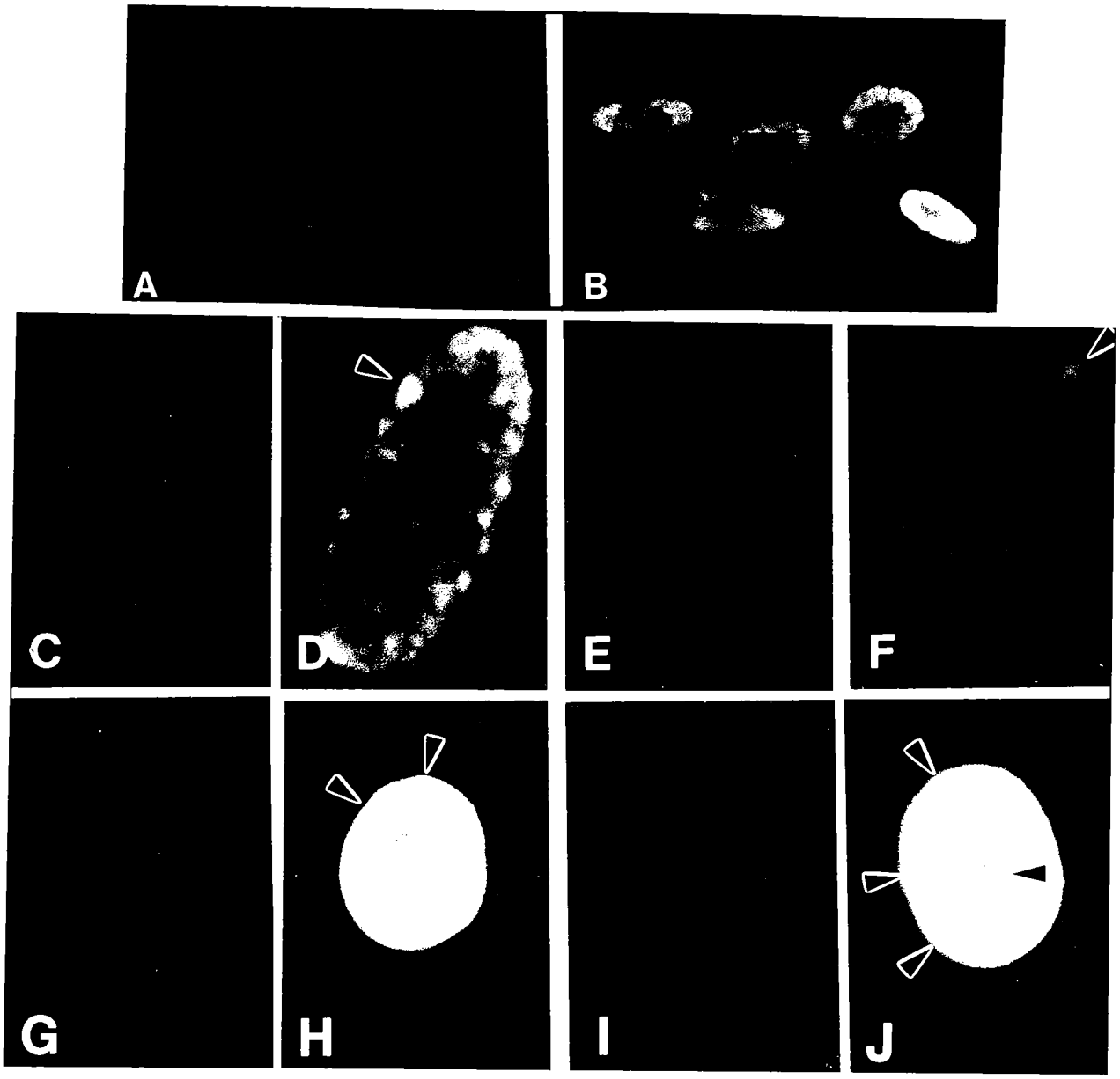
A
B
C
D
E
F
G
H
I
J

Figure 5-4. Hybridization of XIST RNA within human diploid and aneuploid cells. Digoxigenin-labeled probes for XIST RNA were hybridized to nondenatured cells and specific hybridization was detected with FITC-conjugated anti-digoxigenin antibody (green). Nuclei were stained with DAPI (blue). (A) a low magnification view of several WI-38 cells showing the consistent detection of a single site of concentrated XIST RNA within each nucleus. (B) DAPI staining of (A). (C) and (E) show higher magnification views of XIST RNA signals concentrated within individual WI-38 nuclei, demonstrating that they colocalize with the condensed Barr body (arrow) evident by DAPI staining as shown in (D) and (F), respectively. (G and I) Multiple XIST RNA signals were detected in the nuclei of 47,XXX cells (G) and 49,XXXXX cells (I), respectively. The location of Barr bodies revealed by DAPI staining is apparent in (H) and (J).

In normal male cells which have no inactive X chromosome, no XIST hybridization could be detected. However, in aneuploid cells carrying multiple X chromosomes, for which it is well established that one X chromosome becomes active and the rest are inactive (Gumbauch et al., 1963; Gartler and Riggs, 1983), the number of labeled nuclear XIST RNA sites was always one less than the total number of X chromosomes. Thus, cytological hybridization detected XIST transcripts localized at two nuclear sites (Fig. 5-4, C and D) within 91% of nuclei in a 47, XXX cell line and at four sites (Fig. 5-4, E and F) in 63% of nuclei in the 49, XXXXX cell line. In both cell lines, these sites were consistently coincident with Barr bodies visualized by DAPI staining.

Because of the potentially unusual character of this RNA, it was of particular interest to examine the fine distribution of the localized XIST RNA signal. The distribution pattern of XIST RNA within the nucleus is compared with the patterns of other cellular RNAs, fibronectin and collagen. Unlike other cellular RNAs studied, XIST RNAs do not generally form a highly condensed focus or track in the nucleus. Instead they appeared as many tiny fluorescent dots which cover a small area overlapping with the location of the Barr body, i.e. they appeared to be more broadly and diffusely distributed than "foci" or "tracks" of the other individual RNAs studied and may have a shape similar to the Barr body (Fig. 5-5). These spots are not distributed evenly in that region, sometimes part of the region is more intensely labeled than the rest.

The striking association of XIST RNA with the Barr body, its different distribution pattern within the nucleus, and the fact that it does not appear to code for a protein (Brown et al., 1992) raised an important question: whether the nuclear XIST RNA signal represents a "typical" primary transcript which will be transported elsewhere for its function, or whether it may function via some stable association with the X-chromosome possibly contributing directly to its heterochromatinization. Experiments have been initiated to address this, with intriguing preliminary results. To determine if XIST RNA was stably associated with the inactive X, cells were treated with actinomycin D for 6 hours. XIST RNA signals were still observed in most of the nuclei with a similar distribution pattern to that in the untreated cells except that some

Figure 5-5. Simultaneous detection of XIST RNA and fibronectin RNA within human fibroblast cells. XIST RNA was hybridized with biotin-labeled probe (red, rhodamine) and fibronectin RNA with digoxigenin-labeled probe (green, FITC).

signals were slightly weaker. For comparison, fibronectin nuclear RNA was studied at the same time and the result showed that fibronectin nRNA was not visible in the cells after actinomycin D treatment. Using another approach, hybridization experiments with intron and genomic DNA probes of XIST within the same cell showed that genomic probe was detected at the sites of RNA signals but the intron sequence was not present at detectable level at these sites. However, more analyses will be required and is ongoing to confirm this result.

DISCUSSION

The analysis of a unique nuclear RNA, XIST RNA, showed a highly localized signal in the nucleus of female cells but not male cells, and this nuclear distribution of XIST RNA was found to concentrate in a site coincident with the Barr body. The expression pattern and overlap between XIST RNA and the Barr body strongly support the findings of molecular biology studies indicating that XIST RNA was only produced by the inactive X chromosome. The results also indicate that in cells with multiple X chromosomes, all but one X expresses XIST RNA. There consistently appeared to be a close structural association of XIST molecules with the inactive X chromosome.

The experimental results described here do not distinguish between XIST RNA at the site of transcription or, possibly, XIST RNA at a site of deposition. However, the facts that the XIST transcripts are relatively stable within the nucleus, may not code for protein, and appear to localize over a broader region of the inactive X than the concentrated transcriptional focus or track, suggest that XIST transcripts, after synthesis and processing, may become stably associated with the Barr body. However, further study is required to demonstrate this and to clarify whether XIST RNA is associated with the entire inactive X chromosome or whether it is confined to a particular region on the X, perhaps the XIST locus itself, and/or elsewhere within the critical XIC region. Future experiments will be required to examine the detailed distribution of XIST RNA and to compare it in the same cells with RNAs produced from other transcriptionally active genes, especially including those X-linked genes that escape inactivation and are transcribed from both active

and inactive X chromosomes.

The function of XIST RNA is unknown. That XIST expression is completely concordant with X inactivation clearly suggests that XIST is either involved in, or directly influenced by, the process of X inactivation. One hypothesis is that XIST may function in X inactivation as a structural RNA molecule. Results here make the hypothesis more favorable since the different distribution pattern and actinomyocin D response of XIST RNA suggest that XIST RNA may have a different function than protein coding RNA, possibly playing a role in regulating X chromosome inactivation.

The current results are also consistent with the cis-action of the X-inactivation center, as local chromatin structure spreading from XIST, rather than a potentially diffusible substance as the agent of inactivation. The *cis*-limited nature of X inactivation is much more readily explained by an RNA with limited capacity for diffusion than by a protein that would have to be translated in the cytoplasm and then transported back into the nucleus. For example, such an RNA could serve a number of plausible roles: (*i*) to induce facultative heterochromatin formation as part of the cis-limited spreading of inactivation (by analogy with position effect variegation) (Henikoff, 1990); (*ii*) to facilitate critical protein-DNA interactions on the inactive X, either early in development at the time of initiation of X inactivation or constitutively in somatic cells, perhaps involved in the maintenance of the inactive state through interaction with methylated DNA-binding proteins; (Boyes and Bird, 1991; Lewis et al., 1992); or (*iii*) to sequester the inactive X within the nucleus, for example as part of the Barr body. It should be noted that the XIST RNA does undergo processing, which may or may not require that its transcripts move from their site of synthesis on the X chromosome. Interestingly, preliminary results indicate that XIST RNA is not associated with SC-35 domains (Lawrence and Coleman, unpublished observation).

Despite the fact that the full characterization of the XIST gene and transcripts will be required to understand the mechanism of the inactivation of the X chromosome, the unique expression feature and nuclear distribution pattern of XIST RNA make it an attractive model for the possible functions of nuclear RNA other than encoding proteins. Evidence indicates that there is a very large fraction of RNA within the nucleus that does not code for protein

and has no known function (Lewin, 1987b). For a long time, this large amount of RNAs synthesized in eukaryotic cells has often been considered "junk". Perhaps in the future, it will be possible to unmask a real function of these molecules. The unique distribution pattern of XIST RNA compared with other known protein coding RNAs opens a new pathway to study their potential roles in cellular activities.

CHAPTER VI

Gene Mapping by Fluorescence *In Situ* Hybridization: Mapping of the Putative Tumor Suppressor Gene, p107, to Chromosome 20

Fluorescence *in situ* hybridization procedures that directly couple molecular and cytological information have recently had a surge of success in powerful new applications. Pivotal to these advances has been technological improvements that allow the precise visualization of single gene sequences within individual metaphase and interphase cells. Using this technique it is now possible to detect just a few kilobases of deleted or misplaced DNA anywhere within the genome. These improvements have important implications for human gene mapping as well as for investigation into the occurrence, causes, and consequences of chromosomal aberrations. To obtain experience in gene mapping and cytogenetics, a tumor suppressor gene candidate had been mapped to chromosome 20. In this chapter, the data of that study will be presented in combination with brief excerpts of a review which I participated in (Xing and Lawrence, 1993) on the recent progress in this rapidly developing area.

Metaphase and Interphase Gene Mapping

An obvious and important application of the ability to detect single copy genes with fluorescence *in situ* hybridization is to map the human and other genomes. The resolution of fluorescence as well as the speed and efficiency of this approach is far superior to previous autoradiographic techniques which have a limit of resolution on the order of 10^4 or 10^5 kilobases. While autoradiography has had some advantage in sensitivity over fluorescence, it has been found that fluorescent signals as small as a few kb can be detected without amplification of biotinylated probes (Lawrence et al., 1988) (Fig. 6-1, A). However, in most genomic mapping today, the need is not to detect smaller probes, but larger ones. It is very important to show that genomic probes containing repetitive elements could be used. This was initially reported using competition with Cot-1 DNA for detection with peroxidase and interference

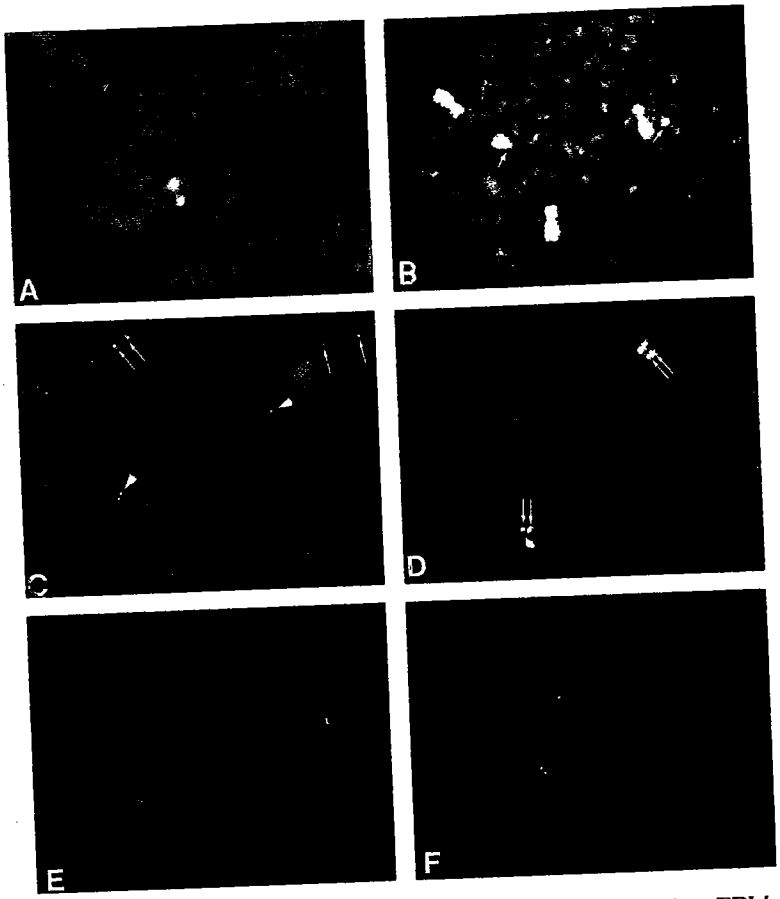

Figure 6-1. (A) Hybridization to an 18-kb target within the EBV genome, using biotin-labeled probes and a one-step fluorescein-avidin detection. Chromosomes are stained with propidium iodide. (B) Hybridization of a chromosome-7 library to a tetraploid cell line carrying a translocation involving this chromosome. Two normal chromosomes 7 and two derivative chromosomes (arrows) are observed. (Photograph contributed by K. Wydner and L. Sciorra. Department of Pediatrics, Diagnostic Genetics, University of Medicine and Dentistry of New Jersey-Robert Wood Johnson Medical School) (C) Hybridization of a chromosome-1 sequence to cytogenetic preparations of the Namalwa cell line, illustrating how a cytogenetic abnormality is evidenced by the nonidentical labeling of sister homologues. Note that three signals, rather than two, are observed within the interphase nucleus. (D) Simultaneous hybridization to neu (erB2) and nerve growth factor receptor cosmid clones which are closely linked and frequently resolvable along the length of less-condensed metaphase chromosomes. On more-condensed chromosomes, they may only be resolvable across the chromosome width. (E and F) Dystrophin sequences separated by ~700 kb are clearly separated and resolvable in ~90% of interphase nuclei. (Pictures A and C-F courtesy of C. Johnson and J. Lawrence).

reflection microscopy (Landegent et al., 1987). Several labs then showed a similar approach successful for fluorescence detection of single copy phage, cosmid, or YAC clones (Staunton et al., 1989; Trask et al., 1989; Lawrence et al., 1990; Lichter et al., 1990).

For genome mapping, there is a need for alternative physical mapping techniques which provide resolution in the range of 1-2 megabases and below, and allow evaluation of physical distance across a broad range to help bridge the gap between lower and higher resolution techniques. Over the last few years it has been shown that fluorescence hybridization can provide such an approach (Lawrence et al., 1988, 1990; Trask et al., 1989, 1991; Lichter et al., 1990). Rigorous characterization of the limits and versatility of this technique demonstrated that its ability to resolve and order sequences on chromosomes generally does not extend below 1-2 Mb (Lawrence et al., 1990) (Fig. 6-1, D). However, an important finding is that resolution can be greatly enhanced by analyzing the distance between two sequences in the interphase nucleus, where the chromatin is much less condensed (Lawrence et al., 1988; 1990; Trask et al., 1989; 1991). This was initially presented by a study in which one can detect two sequences within an EBV genome separated by 130 kb (Lawrence et al., 1988). Interphase distance was then shown to exhibit a strong correlation with DNA distance over the ranges examined, for both DHFR sequences in Chinese hamster (Trask et al., 1989) and for human dystrophin sequences in normal human cells (Lawrence et al., 1990) (Fig. 6-1, E and F), providing a very useful approach for determining physical order within genomes.

Another added benefit of this development is that the fluorescence *in situ* hybridization methodology can be adapted together with the traditional chromosome banding techniques, which will allow a simultaneous detection of gene probes and chromosomes locations (Viegas-Pequignot et al., 1989; Lawrence et al., 1990; Fan et al., 1990).

Mapping Tumor Suppressor Gene Candidates to Chromosomes

It is well established that within the human genome there are numerous (50-100) cytogenetic sites that are frequently involved in chromosomal rearrangements or deletion seen in cancer cells (reviewed in

Trent et al., 1989). Typically, rearrangement at specific site correlates with specific types of cancers. These sites have been believed and in some cases demonstrated to be the sites of tumor suppressor genes. One way *in situ* hybridization can potentially contribute to cancer genetics is to identify the chromosomal locus of a known gene which, based on its biochemical function, may be a putative tumor suppressor or oncogene. It can then be determined if that locus correlates with any of the known specific chromosomal changes implicated in tumors. Using *in situ* hybridization p107, a tumor suppressor gene candidate, has been mapped to chromosome 20.

p107 is a cellular protein that shares several key functional properties with RB, the product of the tumor suppressor gene Rb (Ewen et al., 1989). Hence, p107 has also been suggested as a putative tumor suppressor. Tumor-suppressor genes are a group of genes which have important functions in the regulation of normal cell proliferation and development. Loss of functions of tumor suppressor genes have been found or are suspected in many different types of cancer. A predominant example is the development of retinoblastoma (Rb), now known to involve the loss of both allelic Rb genes mapped on the long arm of chromosome 13 (q14). (Francke 1976; Friend et al., 1986; Lee et al., 1987; Horowitz et al., 1990).

A partial cDNA for human p107 has been cloned (Ewen et al., 1991). The p107 cDNA clone (4 kb) was labeled with digoxigenin and used to probe human metaphase chromosomes from normal peripheral blood lymphocytes. More than 90% of metaphase figures showed a clear signal, evident by the identical labeling of both sister chromatids of the chromosome. In most metaphase figures both homologous chromosomes were labeled, and there was no evidence of signal at other chromosomal sites. As illustrated in Fig. 6-2, A and B, hybridization could be unambiguously visualized in one cell by the identical labeling of both sister chromatids on each of the two homologous chromosomes. The labeled chromosomes consistently showed the small metacentric morphology of an F group chromosome. Banding analysis of nine metaphases, with DAPI staining of BrdU-incorporated chromosomes, has identified the labeled chromosome as chromosome 20 and localized the p107 gene to 20q11.2 using direct visual analysis of signal placement. Fig. 6-2, C illustrates the position of the chromosome signal on several enlarged

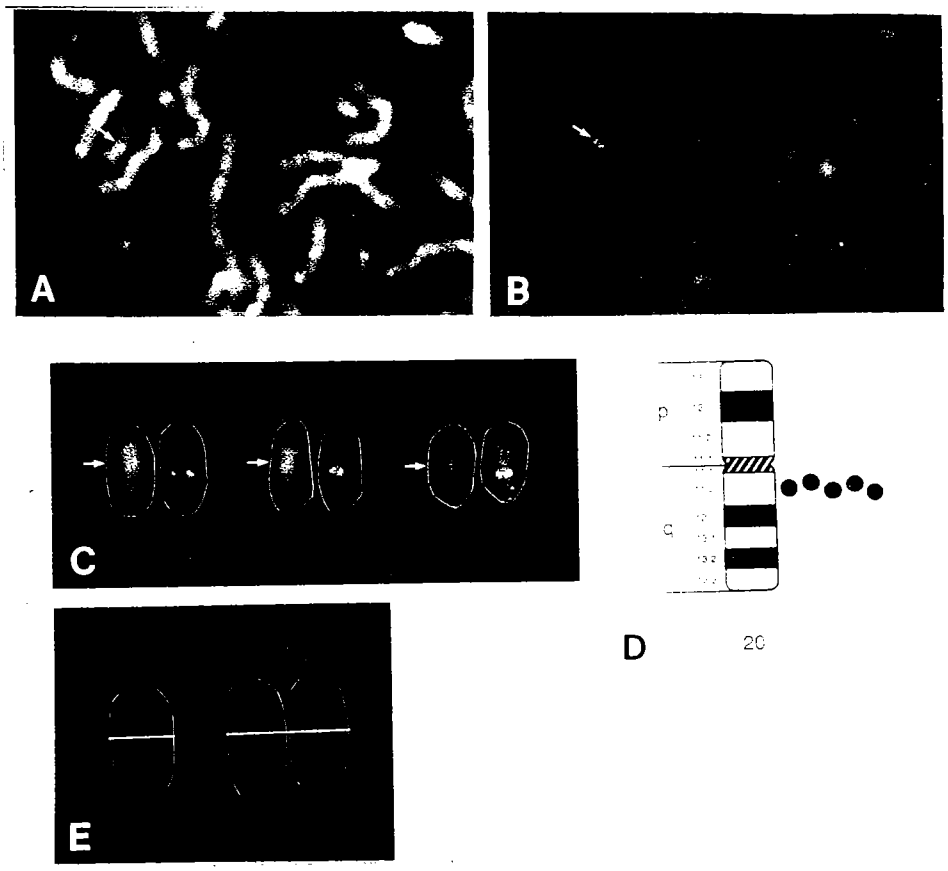

Figure 6-2. Localization of the p107 gene. (A) DAPI staining of metaphase chromosomes from normal human lymphocytes. The arrows indicate human chromosome 20. (B) Hybridization with the digoxigenin-labeled p107 cDNA probe, detected by fluoresein-conjugated anti-digoxigenin. One homolog of chromosome 20 shows two signals, one on each sister chromatid. The other homolog shows one labeled chromatid. (C) Higher magnification of several chromosomes showing alignment of the chromosome 20 signals. In each pair of chromosomal images, the DAPI fluorescein signals are on the left and the fluorescent p107 cDNA hybridization signals are on the right. (D) Ideogram of human chromosome 20 showing the placement of the p107 gene in q11.2 based on analysis of five banded metaphase chromosomes. In five more metaphase spreads, the gene was localized to this band by virtue of its placement relative to the centromere. In addition, measurements of signal placement in 27 metaphase agreed with this localization. (E) Simultaneous localization of the p107 gene proximal to the PTP1B gene on the long arm of chromosome 20. Double-label hybridization and a dual-band fluorescence filter were used to visualize green (p107) and red (PTP1B) signals in precise register. DAPI (blue) stains total DNA.

chromosomes. Fig. 6-2, D summarizes the data from five banded chromosomes, scored independently by two observers with essentially identical results. Placement of the signal was also analyzed by measurements along the total length of the chromosome. Based on the average of 27 metaphase cells, the p107 gene is also localized to q11.2.

Because of the potential importance of the assignment, the position of p107 on the long arm of chromosome 20 was confirmed and further defined by its colocalization with another gene, phosphotyrosyl phosophatase 1B (PTP1B), which was previously mapped to chromosome 20 in the region q13.1-q13.2 (Brown-Shimer et al., 1990). This was accomplished using a dual labeling approach, which allows the detection of two probes with rhodamine and fluorescein fluorescence, respectively. A dual-band epifluorescence filter made it possible to visualize both probes simultaneously in precise position with respect to one another, without any optical shift. As illustrated in fig. 6-2, E, these results clearly confirmed the assignment of the p107 gene to chromosome 20q and consistently showed that its position was proximal to the centromere relative to the PTP1B gene. All of the above cytogenetic analyses performed are in accord with the localization of p107 to chromosome 20q11.2. The localization of p107 to the 20q11.2 region was of particular interest because there is a correlation of breakpoints in this area with specific myeloid disorders such as acute nonlymphocytic leukemia and myelodysplastic syndrome. The mapping of this gene to this region provides direction to future studies which will explore the potential rearrangement of this gene in this type of leukemia.

Search for Unknown Genes at a Known Chromosomal Breakpoint

A second more directed approach for finding a gene associated with a specific cancer is to identify the DNA sequences that lie precisely at the chromosomal breakpoint associated with that cancer. This generally involves screening libraries of cosmids or yeast artificial chromosomes (YACs) from whole chromosomes or chromosome segments in order to find those clones closest to the breakpoint. Double-color fluorescence hybridization can be extremely valuable in narrowing the search and identifying sequences of an known gene at the site of deletion or breakpoint. The search would begin by

identifying two closest flanking markers for a specific deletion from previously mapped genes or restriction fragment linked polymorphisms (RFLPs). Commonly, these flanking markers will be on the order of 5-10 Mb apart, an enormous distance when looking for a single gene. The two flanking markers can both be labeled in either red or green, and then probes for unknown sequences from that chromosome differentially labeled in the opposing color. The position of the clone of interest, as being between or outside of the two flanking markers, can then be evaluated by hybridization of the three probes simultaneously to metaphase and interphase cells. This approach was found useful in search for sequences near a translocation breakpoint flanked by markers 6 centimorgans (6 Mb) apart that marked the site of the gene involved in rhabdomyosarcoma. Aided by fluorescence hybridization closer flanking markers narrowing the region to 100-300 kb were identified (Shapiro and Lawrence, in preparation).

Molecular Cytogenetic Detection of Deletions, Translocations or Other Chromosomal Rearrangements Associated with Specific Tumors

The specific genetic changes which contribute to cancer involve altered gene expression as a consequence of gene loss resulting from translocation or deletions, or smaller defects such as point mutations. The well known example of consistent chromosome change in human cancer was the Philadelphia or Ph' chromosome in chronic myelogenous leukemia (Nowell & Hungerford, 1960), which occurs as the result of a translocation between chromosome 9 and 22 [t(9,22)(q34;q11)] (Rowley et al., 1973). There are now at least 70 recurring translocations that have been detected in human malignant cells. A consistent deletion is another genetic factor frequently observed in human cancers, with deletion of a specific region correlated with a particular tumor tissue type.

In the inherited forms of retinoblastoma, the absence of genetic material inherited from one of the parents can be detected by the loss of heterozygosity for markers flanking the locus. Since similar events uncovering recessive somatic mutations occur in the sporadic forms of retinoblastoma (Cavenee et al., 1983), the consistent loss of heterozygosity at specific loci in cancers may indicate deletion of tumor suppressor genes. With

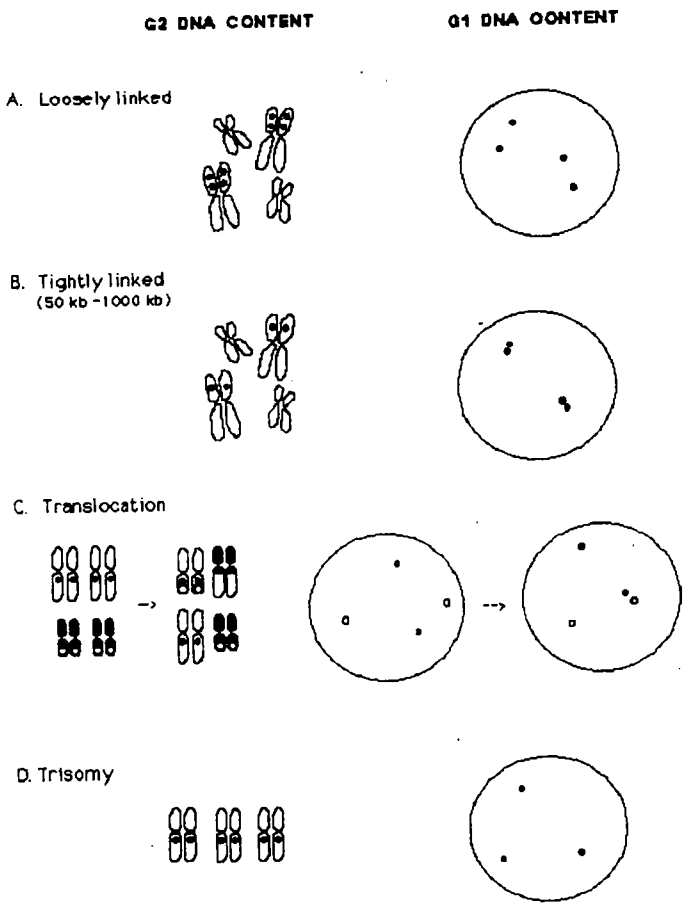

Figure 6-3. Hypothetical outcomes after hybridization of one or two single-copy probes to interphase and metaphase cells. (A) Loosely linked sequences will be resolvable along the chromosomes length and show only a distant pairing within interphase nuclei. (B) When sequences from the same chromosomal region become closer, they will no longer resolvable at metaphase but will still be clearly visualized as closely paired signals within decondensed interphase nuclei. (C) Hybridization patterns for normal (left) and translocated (right) metaphase and interphase cells. Solid and open circles represent signals from two pairs of different chromosomes. In normal cells the interphase nucleus shows a widely dispersed variable distribution of four hybridization signals. In contrast, in cells carrying the translocation, the fusion of two different chromosomes consistently gives a pair of close solid and open signals in both interphase and metaphase nuclei. (D) In the case of trisomy, three chromosomes showing sister chromatid labeling will be seen in metaphase, and three hybridization signals will be visualized at interphase.

in situ hybridization, submicroscopic deletions involving 1-2 kb or more of DNA are apparent as the total absence of signal on one homolog. The presence of signal on the other homolog serves as an internal positive control. Alternatively, hybridization can be used to detect the amplification of specific sequences.

To detect the specific translocation known to characterize particular types of cancers, chromosome libraries, specific repeats or a group of probes for a specific chromosomal region can be used. Translocations may also be detected in metaphase chromosomes by comparing the location of probes which flank the site of the breakpoint on a given chromosome, as schematically represented in fig. 6-3. For analysis of more easily obtained interphase cells, translocations may also be detected using two probes, one from each of the chromosomes involved in the translocation, which will be detected unusually close together (on the same chromosome) when the translocation is present. This was demonstrated in the case of bcr-abl fusion in chronic myelogenous leukemia, the fusion involves a translocation, t(9,22)(q34;q11), to produce the characteristic Philadelphia chromosome (Tkachuk et al., 1990).

Applications for Analysis of General Cytogenetic Aberrations

It is only recently that methodology for applying non-isotopic cytological hybridization for the analysis of cytogenetic aberrations has begun to realize its full potential. The speed, convenience, and precision of non-isotopic probe-labeling techniques make this technology applicable for diagnostic as well as research purposes. For a long time, the field of cytogenetics has been limited to the analysis of relatively gross chromosomal aberrations based on banding patterns. Standard karyotypic analysis, while allowing a survey of the complete set of chromosomes, can only discern deviations in whole chromosomes or chromosome segments containing approximately 10 Mb or more of DNA. Now it has become possible cytologically to detect specific genetic defects 1,000-10,000 fold smaller, and eventually it may be possible to detect even smaller defects. In the hunt for specific disease genes, a molecular cytogenetic defect in the gene itself might be revealed because any aberration resulting in nonidentical labeling of homologous

chromosomes is readily apparent by this technique. Clearly, the technology has value for clinical research into the etiology of genetic diseases as well as a strong potential for clinical diagnostics of these diseases.

Hybridization of chromosome libraries, chromosome-specific centromere probes, or even small single-copy sequences can all make readily apparent for monosomies or trisomies of specific chromosomes (see, for example, Fig. 6-1, C). The most common clinical abnormalities in this category are trisomies 21, 13, and 18 and the sex chromosome abnormalities XO, XXX, XXY, and XYY. Using a collection of several probes for the above chromosomes with multiple labels, it is possible to screen for several aneuploidies at once.

Chromosome libraries or specific repeats can also be used for the detection and characterization of translocations (Fig. 6-1, B). In addition, translocations that appear to be balanced can be analyzed much more precisely using a battery of probes for a specific chromosomal region. Translocations may be even more readily detected at interphase using two probes known to flank the breakpoint, which will be detected unusually close together (on the same chromosome) when the translocation is present.

Submicroscopic deletions involving a few kb or more of DNA will become easier to be detected by *in situ* hybridization. In the case of carrier detection, heterozygous gene deletions usually are difficult to be identified by southern blot analysis because heterozygosity is manifest only as the change in intensity of a band, often difficult to discern. With *in situ* hybridization, on the other hand, heterozygosity can be readily identified as the total absence of signal on one homolog.

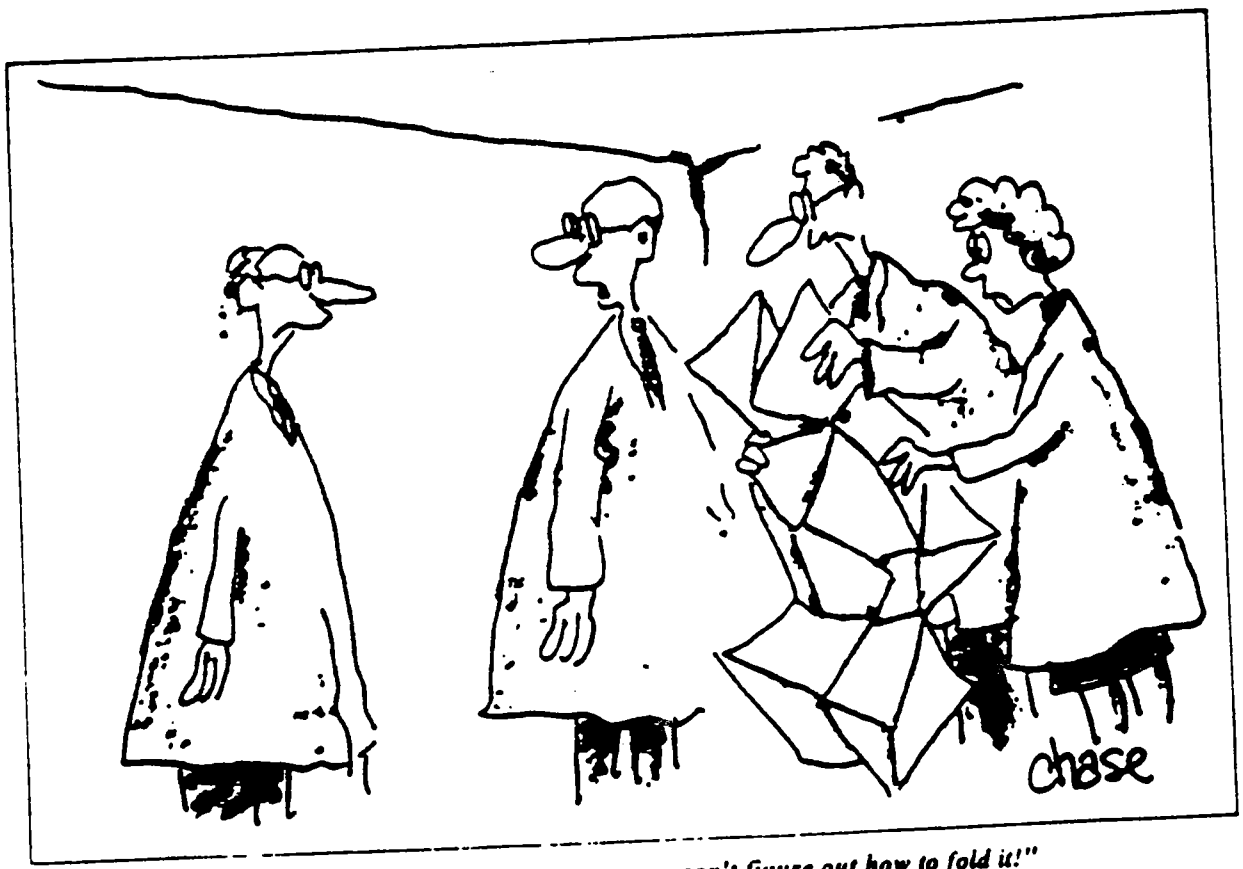

"We finished the genome map, now we can't figure out how to fold it!"

REFERENCE

Abulafia R, Ben-Ze'ev A, Hay N, and Aloni Y (1984) Control of late Simian virus 40 transcription by the attenuation mechanism and transcriptionally active termary complexes are associated with the nuclear matrix. J Mol Biol 172:467-487.

Agard DA and Sedat JW (1983) Three-dimensional architecture of a polytene nucleus. Nature 302:676-681.

Agutter PS (1988) Nucleo-cytoplasmic transport of mRNA: Its relationship to RNA metabolism, subcellular structures and other nucleocytoplasmic exchanges. Prog Mol Subcell Biol 10:15-96.

Arroua ML, Hartung M, Devictor M, Berge-Lefrnc JL and Stahi A (1982) Localisation of ribosomal genes by in situ hybridization in the fibrilar center of the nucleolus in the human spermatocyte. Biol Cell 44:337-340.

Barr M L and Carr DH (1962) Correlations between sex chromatin and sex chromosomes. Acta Cytol 6:34-45.

Barni S and Gerzeli G (1985) The use of propidium iodide in cytochemical studies of interphase chromatin structure. Bas Appl Histochem 29:215-230.

Barrack ER (1987) Steriod hormone receptor localization in the nuclear matrix: interaction with acceptor sites. J Steriod Biochem 27:115-121.

Bauman JGJ, Wiegant J, van Duijin P, Lubsen NH, Sondermeijer PJA, Hennig W and Kubli E (1981) Rapid and high resolution detection of in situ hybridization to polytene chromosomes using fluorochrome-labeled RNA. Chromosoma 84:1-18.

Baumbach LL, Stein GS and Stein JL (1987) Regulation of human histone gene expression: transcriptional and posttranscriptional control in the coupling of histone messenger RNA stability with DNA replication. Biochemistry 26:6178-6187.

Berezney R and Coffey DS (1974) Identification of a nuclear protein matrix. Biochem Biophys Res Commun 60:1410-1419.

Berezney R and Coffey DS (1977) Nuclear Matrix: Isolation and characterization of a framework structure from rat liver nuclei. J Cell Biol 73:616-637.

Berman SA, Bursztajn S, Browen B and Gilbert W (1990) Localization of an

acetylcholine receptor intron to the nuclear menbrane. Science 247:212-214.

Beyer AL and Osheim YN (1991) Visualization of RNA transcription and processing. Sem in Cell biolo 2:131-140.

Blobel G (1985) Gene gating: a hypothesis. Proc Natl Acad Sci USA 82:8527-8529.

Boyes J and Bird A (1991) DNA methylation inhibits transcription indirectly via a methyl-CpG binding protein. Cell 64:1123-1134.

Brotherton T, Zenk D, Kahanic S and Reneker J (1991) Avian nuclear matrix proteins bind very tightly to cellular DNA of the b-globin enhancer in a tissue-specific fashion. Biochemistry 30:5845-5850.

Brown C J and Willard HF (1992) Molecular and genetic studies of human X chromosome inactivation. Adv. Dev. Biol. in press.

Brown C J, Ballabio A, Rupert JL, Lafreniere RG, Grompe M, Tonlorenzi R and Willard HF (1991a). A gene from the region of the human X inactivation centre is expressed eclusively from the inactive X chromosome. Nature 349:38-44.

Brown CJ, Hendrich BD, Lafreniere RG, Rupert JL, Xing Y, Lawrence JB and Willard HF (1992) The Human XIST gene: Analysis of a 17 kb inactive X-specific RNA that contains conserved repeats and is highly localized within the nucleus. Cell 71:527-542.

Brown CJ, Lafreniere RG, Powers VE, Sebastio G, Ballabio A, Pettigrew A, Ledbetter DH, Levy E, Craig IW and Willard HF (1991b) Localization of the X inactivation centre on human X chromosome in Xq13. Nature 349:82-84.

Brown-Shimer S, Johnson KA, Lawrence JB, Johnson C, Bruskin A, Green NR and Hill DE (1990) Molecular cloning and chromosome mapping of the human gene encoding protein phosphotyrosyl phosphatase 1B. Proc Natl Acad Sci USA 87:5148-5152.

Carmo-Fonseca M, Pepperkok R, Sproat BS, Ansorge W, Swanson MS and Lamond AI (1991a) In vivo detection of snRNP-rich organelles in the nuclei of mammalian cells. EMBO J 10:1863-1873.

Carmo-Fonseca M, Tollervey D, Pepperkok R, Barabino SML, Merdes A, Brunner C, Zamore PD, Green MR, Hurt E and Lamond AI (1991b) Mammalian nuclei contain foci which are highly enriched in components of the

pre-mRNA splicing machinery. EMBO J 10:195-206.

Carmo-Fonseca M, Pepperkok R, Carvalho MT and Lamond AI (1992) Transcription-dependent colocalization of the U1, U2, U4/U6, and U5 snRNPs in coiled bodies. J Cell Biol 117:1-14.

Carter KC and Lawrence JB (1991) DNA and RNA within the nucleus: How much sequence-specific spatial organization? J Cell Biochem 47:124-129.

Carter KC, Taneja KL and Lawrence JB (1991) Discrete nuclear domains of poly(A) RNA and their relationship to the functional organization of the mammalian nucleus. J Cell Biol 115:1191-1202.

Carter KC, Bowman D, Carrington W, Fogarty K, McNeil JA, Fay FS and Lawrence JB (1993) A three-dimensional view of precursor messenger RNA metabolism within the nucleus. Science 259:1330-1335.

Cattanach BM, Pollard CE and Perez JN (1969) Controlling elements in the mouse X-chromosome 1. Interaction with the X-linked genes. Genet. Res. 14:223-235.

Cavenee WK, Dryja TP, Phillips RA, Benedict WF, Godbout R, Gallie BL, Murphree AL, Strong LC and White RL (1983) Expression of recessive alleles by chromosomal mechanisms in retinoblastoma. Nature 305:779-784.

Chelly J, Kaplan J-C, Maire P, Gautron S and Kahn A (1988) Transcription of dystrophin gene in human muscle and non-muscle tissue. Nature 333:858-863.

Ciejek EM, Nordstrom JL, Tsai M and Malley BW (1982) Ribonucleic acid presursors are associated with the chick oviduct nuclear matrix. Biochemistry 21:4945-4953.

Ciejek EM, Tsai M-J and O'Malley BW (1983) Actively transcribed genes are associated with the nuclear matrix. Nature 306:607-609.

Coleclough C and Wood D (1984) Introns excised from immunoglobulin pre-mRNAs exist as discrete species. Mol Cell Biol 4:2017-2022.

Coleman AW, Maguire MJ and Coleman JR (1981) Mithramycin-and 4'6-diamidino-2-phenylindole (DAPI)-DNA staining for fluorescence microspectrophotometric measurement of DNA in nuclei, plasmids, and virus particles. J Histochem Cytochem 29:959-968.

Comings D (1968) The rationale for an ordered arrangement of chromatin in

the interphase nucleus. Am J Hum Genet 20:440-457.

Comings D (1980) Arrangement of chromatin in the nucleus. Hum Genet 53:131-143.

Cremer T, Cremer C, Baumann H, Luedtke EK, Sperling K, Teuber and Zorn C (1982) Rabl's model of the interphase chromosome arrangement tested in Chinese Hamster cells by premature chromosome condensation and laser-UV-microbeam experiments. Hum Genet 60:46-56.

Daly RF, Patau K, Therman E and Sarto GE (1977) Structure and Barr body formation of an Xp+ chromosome with two inactivation centers. Am J Hum Genet 29:83-93.

Dambaugh T, Beisel C, Hunnel M, King W, Fennewald S, Cheung A, Heller M Raab-Traub N and Kieff E (1980) Epstein-Barr virus (B95-8) DNA VII: molecular cloning and detailed mapping. Proc Natl Acad Sci USA 77:2999-3003.

Dambaugh TK, Hennessey K, Fennewald S and Kieff E. The virus genome and its expression in latent infection. In: *The Epstein-Barr Virus: Recent Advances*, edited by Epstein, M.A. and Achong, B.G. New York: John Wiley and Sons, 1986, p. 13-45.

De Jong L, Van Driel R, Stuurman N, Meijne AML and Van Renswoude J (1990) Principles of nuclear organization. Cell Biol Int Rep 14:1051-1074.

Ewen ME, Ludlow JW, Marsilio E, DeCaprio JA, Millikan RC, Cheng S, Paucha E and Livingston DM (1989) An N-terminal transformation-governing sequence of SV40 large T antigen contributes to binding of both p110RB and a second cellular protein, p120. Cell 58:257-267.

Ewen ME, Xing Y, Lawrence JB and Livingston DM (1991) Molecular cloning, chromosomal mapping and expression of the cDNA for p107, a retinoblastoma gene product-related protein. Cell 66:1155-1164.

Fakan S, Leser G and Martin TE (1984) Ultrastructural distribution of nuclear ribonucleoproteins as visualized by immunocytochemistry on thin sections. J Cell Biolo 98:358-363.

Fakan S and Puvion E (1980) The ultrastructural visualization of nuclear and extranucleolar RNA synthesis and distribution. Int Rev Cytol 65:255-299.

Fakan S, Puvion E and Spohr G (1976) Localization and characterization of newly synthesized nuclear RNA in isolated hepatocytes. Exp Cell Res

99:155-164.

Fan KS, Davis LM and Shows TB (1990) Mapping small DNA sequences by fluorescence in situ hybridization directly on banded metaphase chromosomes. Proc Natl Acad Sci USA 87:6223-6227.

Farache G, Razin SV, Rzeszowska-Wolny J, Moreau J, Targa FR and Scherrer K (1990) Mapping of structural and transcription-related matrix attachment sites in the a-globin gene domain of avian erythroblasts and erythrocytes. Mol Cell Biol 10:5349-5358.

Ferguson M and Ward DC (1992) Cell cycle dependent chromosomal movement in pre-mitotic human T-lymphocyte nuclei. Chromosoma 101:557-565.

Fey EG, Krochmalnic G and Penman S (1986a) The non-chromatin substructures of the nucleus: the ribonucleoprotein RNP-containing and RNP-depleted matrices analyzed by sequential fractionation and resinless section electron microscopy. J Cell Biol 102:1654-1665.

Fey EG, Ornelles DA and Penman S (1986b) Association of RNA with the cytoskeleton and the nuclear matrix. J Cell Sci Suppl.5:99-119.

Fey EG, Wan KM and Penman S (1984) Epithelial cytoskeletal framework and nuclear matrix-intermediate filament scaffold: three-dimensional organizational and protein composition. J Cell Biol 98:1973-1984.

Fey EG and Penman S (1988) Nuclear matrix proteins reflect cell type of origin in cultured human cells. Proc Natl Acad Sci USA 85:121-125.

Fey EG, Bangs P, Sparks C and Odgren P (1991) The nuclear matrix: defining structural and functional roles. CRC Crit. Rev. in Euk. Gene Expression. CRC Crit Rev 1:127-143.

Francke U (1976) Retinoblastoma and chromosome 13. Cytogenet Cell Genet 16:131-135.

Friend SH, Bernard R, Rogelj S, Weinberg RA, Rapaport JM, Albert DM and Drja TP (1986) A human DNA segment with properties of the gene that predisposes to retinoblastoma. Nature 323:643-646.

Fu X-D and Maniatis T (1990) Factor required for mammalian spliceosome assembly is localized to discrete regions in the nucleus. Nature 343:437-444.

Gall JG (1991) Spliceosomes and snurposomes. Science 252:1499-1500.

Gall JG and Callan HG (1989) The sphere organelle contains small nuclear

ribonucleoproteins. Pro Natl Acad Sci USA 86:6635-6639.

Gallinaro H, Puvion E Kister L and Jacob M (1983) Nuclear matrix and hnRNP share a common structural constituent associated with premessenger RNA. EMBO J 2:953-960.

Gartler SM and Riggs AD (1983) Mammalian X-chromosome inactivation. Ann. Rev. Genet. 17:155-190.

Getzenberg RH and Coffey DS (1990) Tissue specificity of the hormonal response in sex accessory tissues is associated with nuclear matrix protein patterns. Mol Endo 4:1336-1342.

Goldman MA, Holmquist GP, Gray MC, Caston LA and Nag A (1984) Replication timing of genes and middle repetitive sequences. Science 224:686-692.

Grant S and Chapman V (1988) Mechanisms of X chromosome regulation. Ann. Rev. Genet. 22:199-233.

Green MR (1989) Pre-mRNA processing and mRNA nuclear export. Cur Opin in Cell Biol 1:519-525.

Grosveld F, van Assendilft GB, Greaves DR and Kollias G (1987) Position-independent, high-level expression of the human b-globin gene in transgenic mice. Cell 51:975-985.

Grumbach MM, Morishma A and Taylor H (1963) Human sex chromosome abnormalities in relation to DNA replication and heterochromatinization. Proc. Natl. Acad. Sci. USA 49:581-589.

Haaf T and Schmid M (1991) Chromosome topology in mammalian interphase nuclei. Exp Cell Res 192:325-332.

Hardin JH, Spocer SS and Green WB (1969) The paranucleolar structure, accessory body of Cajal, sex chromatin, and related structures in nuclei of rat trigeminal neurons: a cytochemical and ultrastructural study. Anat Rec 164:403-412.

Harris SG and Smith HC (1988) SnRNP core protein enrichment in the nuclear matrix. Bioch Biophy Res Comm 152:1383-1387.

He D, Nickerson JA and Penman S (1990) Core filaments of the nuclear matrix. J Cell Biol 110:569-580.

Henderson A, Ripley S, Heller M and Kieff E (1983) Chromosome sitee for Epstein-Barr virus DNA in a Burkitt tumor cell line and in lymphocytes growth transformed in vitro. Proc Natl Acad Sci USA 80:1987-1991.

Henikoff S (1990) Position-effect variegation after 60 years. Tren Genet 6:422-426.

Herbomel P (1990) From gene to chromosome: Organization levels defined by the interplay of transcription and replication in vertebrates. The New Biologist 2:937-945.

Herman R, Weymouth L, and Penman S (1978) Heterogeneous nuclear RNA-protein fibers in chromatin-depleted nuclei. J Cell Biol 78:663-674.

Hochstrasser M and Sedat JW (1987) Three-dimensional organization of Drosopjila melanogaster interphase nuclei. I. Tissue specific aspectos of polytene nuclear architecture. J Cell Biolo 104:1455-1470.

Horowitz JM, Park SH, Bogenmann E, Cheng JC, Yandell DW, Kaye FJ, Minna JD, Dryja TP and Weinberg RA (1990) Frequent inactivation of the retinoblastoma anti-oncogene is restricted to a subset of human tumor cells. Proc Natl Acad Sci USA 87:2775-2779.

Huang S and Spector D (1991) Nascent pre-mRNA transcripts are associated with nuclear regions enriched in splicing factors. Gene Develop 5:2288-2302.

Huang S and Spector D (1992) U1 and U2 small nuclear RNAs are present in nuclear speckles. Proc Natl Acad Sci USA 89:305-308.

Hutchinson N, and Weintraub H (1985) Localization of DNAse I-sensitive sequences to specific regions of interphase nuclei. Cell 43:471-482.

Hynes RO (1985) Molecular biology of fibronectin. Ann Rev Cell Biol 1:67-90.

Ignotz RA, Endo T and Massague J (1987) Regulation of fibronectin and type I collagen mRNA levels by transforming growth factor-B. J Biol Chem 262:6443-6446.

Jackson DA, McCready SJ and Cook PR (1981) RNA is synthesized at the nuclear cage. Nature 292:552-555.

Jackson DA and Cook PR (1985) Transcription occurs ar a nucleoskeleton. EMBO J 4:919-925.

Jackson DA and Cook PR (1986) Replication occurs at a nucleoskeleton. EMBO J 5:1403-1410.

Jackson DA (1986) Organization beyond the gene. TIBS 11:249-252.

Jackson DA and Cook PR (1988) Visualization of a filementous nucleoskeleton with a 23 nm axia repeat. EMBO J 7:3667-3677.

Jackson DA (1991) Structure-function relationships in eukaryotic nuclei. BioEssays 13:1-10.

Jackson DA, Hassan AB, Errington RJ and Cook PR (1993) Visualization of focal sites of transctiption within human nuclei. EMBO J 12:1059-1065.

Johnson CV and Lawrence JB (1991) A simple, rapid technique for precise mapping of multiple sequences in two colors using a single optical filter set. Genetic Analysis Techniques and Applications 8:75-79.

Kislauskis E, Bullock B, McNeil S and Dobner PR (1988) The rat gene encoding neurotensin and neuromedin N. J Biol Chem 263:4963-4968.

Kopczynski CC and Muskavitch MAT (1992) Introns excised from the *Delta* primary transcript are localized near sites of *Delta* transcription. J Cell Biol 119:503-512.

Koening M, Hoffman EP, Bertelson CJ, Monaco AP, Feener C and Kunkel LM (1987) Complete cloning of the Duchenne muscular dystrophy (DMD) cDNA and preliminary genomic organization of the DND gene in normal and affected individuals. Cell 50:509-517.

Korenberg JR and Rykowski M (1988) Human genome organization: Alu, Lines, and the molecular structure of metaphase chromosme bands. Cell 53:391-400.

Krystosek A and Puck TT (1990) The spatial distribution of exposed nuclear DNA in normal, cancer, and reverse-transformed cells. Proc Natl Acad Sci USA 87:6560-6564.

Landegent JE, Jansen in de Wal N, Dirks RH, Baas F, Van der Ploeg M (1987) Use of whole cosmid cloned genomic sequences for chromosomal localization by non-radioactive in situ hybridization. Hum Genet 77:366-370.

Langer PR, Waldrop AA and Ward DC (1981) Enzymatic synthesis of biotin-labeled polynucleotides: Novel nucleic acid affinity probes. Proc Natl Acad Sci USA 78:6633-6637.

Langer-Safer PR, Levine M and Ward DC (1982) Immunological method for mapping genes on Drosophila polytene chromosomes. Proc Natl Acad Sci USA 79:4381-4385.

Lawrence JB, Marselle LM, Byron KS, Sullivan JL and Singer RH (1990) Subcellular localization of low-abundance human immunodeficiency

virus nucleic acid sequences visualized by fluorescence in situ hybridization. Proc Natl Acad Sci USA 87:5420-5424.

Lawrence JB and Singer RH (1985) Quantitative analysis of in situ hybridization methods for the detecion of actin gene expression. Nucl Acids Res 13:1777-1799.

Lawrence JB and Singer RH (1986) Intracellular localization of messenger RNAs for cytoskeletal proteins. Cell 45:407-415.

Lawrence JB, Singer RH and Marselle LM (1989) Highly localized tracks of specific transcripts within interphase nuclei visualized by in situ hybridization. Cell 57:493-502.

Lawrence JB, Singer RH and McNeil JA (1990) Interphase and metaphase resolution of different distances within the human dystrophin gene. Science 249:928-932.

Lawrence JB, Villnave CA and Singer RH (1988) Sensitive high-resolution chromatin and chromosome mapping in situ: presence and orientation of two closely integrated copies of EBV in a lymphoma line. Cell 52:51-61.

Lee EYHP, To H, Shew J, Bookstein R, Scully P and Lee W (1987) Inactivation of the retinoblastoma susceptibility gene in human breast cancers. Science 241:218-221.

Levitt A, Axel R and Cedar H (1979) Nick translation of acitve genes in intact nuclei. Develop Biol 69:496-505.

Lewin B (1975) Units of transcription and translation: the relationship between hterogeneous nuclear RNA and messenger RNA. Cell 4:11-20.

Lewin B (1987a) The packaging of DNA, in Genes III, John Wiley and Sons, New York, pp497-559.

Lewin B (1987b) Reaching maturity: RNA processing, in Genes III, John Wiley and Sons, New York, pp443-496.

Lewis JD, Meehan RR, Henzel WJ, Maurer-Fogy I, Jeppesen P, Klein K and Bird A. (1992) Purification, sequence, and cellular localization of a novel chromosomal protein that binds to methylated DNA. Cell 69:905-914.

Lichter P, Cremer T, Borden J, Manuelidis L and Ward DC (1988) Delineation of individual human chromosomes in metaphase and interphase cells by in situ suppression hybridization using recombinant DNA libraries.

Hum Genet 80:224-234.

Lichter P, Tang CC, Call K, Hermanson G, Evans G, Housman D and Ward DC (1990) High-resolution mapping of human chromosome II by in situ hybridization with cosmid clones. Science 247:64-69.

Lompre A-M, Nadal-Ginard B and Mahdavi V (1984) Expression of the cardiac venticular a- and b- myosin heavy chain genes is developmentally and hormonally regulated. J Biol Chem 259:6437-6446.

Long BH, Huang C-Y and Pogo AO (1979) Isolation and characterization of the nuclear matrix in friend erythroleukemia cells: chromatin and hnRNA interactions with nuclear matrix. Cell 18:1079-1090.

Lyon MF (1971) Possible mechanisms of X chromosome inactivation. Nature N. Biol. 232:229-232.

Lyon MF (1961) Gene action in the X-chromosome of the mouse (*Mus musculus* L.) Nature 190:372-373.

Manning JE, Hershey ND, Broker TR, Pellegrini M, Mitchell HK and Davidson N (1975) A new method of in situ hybridization. Chromosoma 53:107-117.

Manuelidis L (1984a) Active nucleolus organizers are precisely positioned in adult central nervous system cells but not in neuroectodermal tumor cells. J Neuropath and Exp Neuro 43:225-241.

Manuelidis L and Borden J (1988) Reproducible compartmentalization of individual chromosome domains in human CNS cells revealed by in situ hybridization and three-dimensional reconstruction. Chromosoma 96:397-410.

Manuelidis L(1984b) Different central nervous system cell types display distinct and nonrandom arrangements of astelite DNA sequences. Proc Natl Acad Sci USA 81:3123-3127.

Manuelidis L and Ward DL (1984) Chromosomal and nuclear distribution of the Hind III 1.9 kb repeat segment. Chromosoma 91:28-38.

Mariman ECM, van Eekelen CAG, Reinders RJ, Berns AJM and van Venrooij WJ (1982) Adenoviral heterogeneous nuclear RNA is associated with the host nuclear matrix during splicing. J Mol Biol 154:103-119.

Mathog D, Hochstrasser M, Gruenbaum Y, Saumweber H and Sedat J (1984) Characteristic folding pattern of polytene chromosomes in Drosophila salivary gland nuclei. Nature 308:414-421.

Mattei, M. G., J. F. Mattei, I. Vidal, and F. Giraud. 1981. Structural anomalies of the X chromosome and inactivation center. Hum Genet 56:401-408.

Maundrell K, Maxwell ES, Puvion E and Scherrer K (1981) The nuclear matrix of duck erythroblasts is associated with globin mRNA coding sequences but not with the major proteins of 40S nuclear RNP. Exp Cell Res 136:435-445.

McBurney MW (1988) X chromosome inactivation: A hypothesis. Bio. Essays. 9:85-88.

Miller Jr. OL and Beatty BR (1969) Visualization of nucleolar genes. Science 164:955-957.

Miller TE, Huang C-Y and Pogo AO (1978) Rat liver nuclear seleton and ribonucleoprotein complexes containing hnRNA. J Cell Biol 76:675-691.

Mirkovitch J, Gasser SM and Laemmli UK (1988) Scaffold attachment of DNA loops in metaphase chromosomes. J Mol Biol 200:101-109.

Mirkovitch J, Mirault M-E and Laemmli UK (1984) Organization of the higher-order chromatin loop: specific DNA attachment sites of nuclear scaffold. Cell 39:223-232.

Murphy S, Moorefield B and Pieler T (1989) Common mechanisms of promoter recognition by RNA polymerases II and III. Trends in Genetics 5:122-126.

Nakayasu H and Berezney R (1989) Mapping replicational sites in the eucaryotic cell nucleus. J Cell Biol 108:1-11.

Nelson WG, Pienta KJ, Barrack ER and Coffey DS (1986) The role of the nuclear matrix in the organization and function of DNA. Ann Rev Biophys Chem 15:457-475.

Nevins JR (1983) The pathway of eukaryotic mRNA formation. Ann Rev Biochem 52:441-466.

Nickerson JA, Krochmalnic G, Wan KM and Penman S (1989) Chromatin architecture and nuclear RNA. Proc Natl Acad Sci ,USA 86:177-181.

Nowell PC and Hungerford DA (1960) A minute chromosome in human granulocytic leukemia. Science 132:1497-1497.

Nyman U, Hallman H, Hadlaczky G, Pettersson I, Sharp G, Ringertz NR (1986) Intranuclear localization of snRNP antigens. J Cell Biol 102:137-144.

Ogata N (1990) Preferential association of a transcriptionally active gene with

the nuclear matrix of rat fibroblasts transformed by a simian-virus-40-pBR332 recombinant plasmid. Biochem J 267:385-390.

Osheim YN, Miller Jr,OL and Beyer AL (1985) RNP particles at splice junction sequences on drosophila chorion transcripts. Cell 43:143-151.

Palmiter RD and Brinster RL (1986) Germ-line transformation of mice. Ann Rev Genet 20:465-499.

Pardoll DM, Vogelstein B and Coffey DS (1980) A fixed state of DNA replication in eucaryotic cells. Cell 19:527-536.

Pardoll DM and Vogelstein B (1980) Sequence analysis of nuclear matrix associated DNA from rat liver. Exp Cell Res 128:466-470.

Patel RS, Odermatt E, Schwarzbauer JE and Hynes RO (1987) Organization of the fibronectin gene provides evidence for exon shuffling during evolution. EMBO J 6:2565-2572.

Paulson JR and Laemmli UK (1977) The structure of histone-depleted metaphase chromosomes. Cell 12:817-828.

Pinkel D, Landegent J, Collins C, Fuscoe J, Seagraves R, Lucas J and Gray J (1988) Fluorescence in situ hybrdization with human chromosome-specific libraries: Detection of trisomy 21 and translocations of chromosome 4. Proc Natl Acad Sci USA 85:9138-9142.

Pinkel D, Straume T and Gray JW (1986) Cytogenic analysis using quantitative high-sensitivity, fluorescence hybridization. Proc Natl Acad Sci USA 83:2934-2938.

Powell A, King W and Kieff E (1979) Epstein-Barr virus-specific RNA. III. Mapping of the DNA encoding viral-specific RNA in restringently infected cells. J Virol 29:261-274.

Puckett L and Darnell JE (1976) Essential factors in the kinetic analysis of RNA synthesis in HeLa cells. J Cell Physiol 90:521-534.

Raap AK, van de Rijke FM, Dirks RW, Sol CJ, Boom R and van der Ploeg M (1991) Biocolor fluorescence in situ hybridization to intron and exon mRNA sequences. Exp Cell Biol 197:319-322.

Rabl C (1885) Uber zelltheilung. Morphologisches Jahrbuch 10:214-330.

Raska I, Andrade LEC, Ochs RL, Chan EKL, Chang C, Roos G and Tan EM (1991) Immunological and ultrastructural studies of the nuclear coiled body with autoimmune antibodies. Exp Cell Res 195:27-37.

Renz M and Kurż C (1984) A colorimetric method for DNA hybridization. Nucleic Acids Res 12:3435-3444.

Riggs AD (1990a) Marsupials and mechanisms of X chromosome inactivation. Aust J Zool 37:419-441.

Riggs AD (1990b) DNA methylation and late replication probably aid cell memory, and type I DNA reeling could aid chromosome folding and enhancer function. Phil Trans R Soc Lond 326:285-297.

Roberge M, Dahmus ME and Bradbury EM (1988) Chromosomal loop/nuclear matrix organization of transcriptionally active and inactive RNA polymerases in Hela nuclei. J Mol Biol 201:545-555.

Robinson SI, Nelkin BD and Vogelstein B (1982) The ovalbumin gene is associated with the nuclear matrix of chicken oviduct cells. Cell 28:99-106.

Robinson SI, Small D, Idzerda R, McKnight GS and Vogelstein B (1983) The association of transcriptionally active genes with the nuclear matrix of the chicken oviduct. Nucl Acids Res 11:5113-5130.

Rowley JD (1973) A new consistent chromosomal abnormality in chronic myelogeneous leukemia identified by guinicine fluorescence and Giemsa staining. Nature 243:290-293.

Russell LB (1963) Mammalian X-chromosome action: Inactivation limited in spread and in region of origin. Science 140:976-978.

Saez LJ, Gianola KM, McNally EM, Feghali R, Eddy R, Shows T and Leinwand LA (1987) Human cardiac myosin heavy chain genes and their linkage in the genome. Nucleic Acid Res 15:5443-5459.

Scheer U and Benavente R (1990) Functional and dynamic aspects of the mammalian nucleolus. Bioassays 12:14-21.

Schroder HC, Bachman M, Diehl-Siefert B and Muller W (1987) Transport of mRNA from nucleus to cytoplasm. Prog Nucl Acids Res 34:89-142.

Schwarzbauer JE, Patel RS, Fonda D and Hynes RO (1987) Multiple sites of alternative splicing of the rat fibronectin gene transcript. EMBO J 6:2573-2580.

Shermoen AW and O'Farrell PH (1991) Progreesion of the cell cycle through mitosis leads to abortion of nascent transcripts. Cell 67:303-310.

Sierra F, Lichlter A, Marashi F, Rickles R, van Dyke T, Clark S, Wells J, Stein G

and Stein J (1982) Organization of human histone genes. Proc Natl Acad Sci USA 79:1795-1799.

Skare J and Strominger JL (1980) Cloning and mapping of BamHI endonuclease fragments of DNA from the transforming B95-8 strain of Epstein-Barr virus. Proc Natl Acad Sci USA 77:3860-3864.

Small D, Nelkin B and Vogelstein B (1985) The association of transcribed genes with the nuclear matrix of Drosophila cells during heat shock. Nucleic Acid Res 13:2413-2432.

Smith HC and Berezney R (1983) Dynamic domains of DNA polymerase α in regenerating rat liver. Biochemistry 22:3042-3046.

Spector DL (1990) Higher order nuclear organization: Three-dimensional distribution of small nuclear ribonucleoprotein particles. Proc Natl Acad Sci USA 87:147-151.

Spector (1992) Differences in snRNP localization between transformed and nontransformed cells. Mol Biolo Cell 3:555-569.

Spector DL (1984) Colocalization of U1 and U2 small nuclear RNPs by immunocytochemistry. Biol Cell 51:109-112.

Spector DL; Fu X-D and Maniatis T (1991) Associations between distinct pre-mRNA splicing components and the cell nucleus. EMBO J 10:3467-3481.

Spector DL and Smith HC (1986) Redistribution of U-snRNPs during mitosis. Exp Cell Res 163:87-94.

Staunton DE, Fisher R, LeBeau M, Lawrence JB, Burton D, Franke U, Dustin M and Thorley-Lawson DA (1989) Blast-1 possesses a glycosyl-phosphatidylinositol (GPI) membrane anchor is related to LFA-3 and Ox-45, and maps to chromosome 1Q 21-24. J Exp Med 169:1087-1099.

Stein GS, Sierra F, Plumb M, Marashi F, Baumbach L, Stein JL, Carozzi N and Prokopp K (1984) Organization and expression of human histone genes, in Histone genes, John Wiley and Sons, New York, pp397-455.

Strauss WM, Dausman J, Beard D, Johnson C, Lawrence JB and Jaenisch R (1993) Germ line transmission of a yeast artificial chromosome spanning the murine α1(I) collagen locus. Science 259:1904-1907.

Tamkun JW, Schwarzbauer JE and Hynes RO (1984) A single rat fibronectin gene generates three different mRNAs by alternative splicing of a complex exon. Proc Natl Acad Sci USA 81:5140-5144.

Taneja KL, Lawrence LM, Fay FS and Singer RH (1992) Poly(A) RNA codistribution with microfilaments: Evaluation by in situ hybridization and quantitative digital imaging microscopy. J Cell Biol 119:1245-1260.

Therman E, Sarto GE and Patau K (1974) Center for Barr body condensation on the proximal part of the human Xq: a hypothesis. Chromosoma 44:361-366.

Thiry M and Thiry-Blaise L (1989) In sity hybridization at the electron microscope level: an improved method for precise localization of ribosomal DNA and RNA. Eur J Cell Biol 50:235-243.

Tkachuk DC, Westbrook CA, Andreeff M, Donlon TA, Cleary ML, Suryanarayan K, Homge M, Redner A, Gray J and Pinkel D (1990) Detection of bcl-abl fusion in chronic myelogeneous leukemia by in situ hybridization. Science 250:559-563.

Trask B, Pinkel D and Van den Engh G (1989) The proximity of DNA sequences in interphase cell nuclei is correlated to genomic distance and permits ordering of cosmids spanning 250 kilobase pairs. Genomics 5:710-717.

Trask BJ, Massa H, Kenwrick S and Gitschier J (1991) Mapping of human chromosome Xq28 by two-color fluorescence in situ hybridization of DNA sequences to interphase cell nuclei. Am J Hum Genet 48:1-15.

Trent JM, Kaneko Y and Mitelman F (1989) Human gene mapping 10: report of the committee on structural chromosome changes in neoplasia. Cell Genet 51:533-554.

Tsim KWK, Greenberg I, Rimer M, Randall WR and Salpeter MM (1992) Transcripts for the acetylcholine receptor and acetylcholine esterase show distribution differences in cultured chick muscle cells. J Cell Biolo 118:1201-1212.

Tubo RA and Berezney R (1987) Pre-replicatice association of multiple replicative enzyme activities with the nuclear matrix during rat liver regeneration. J Biol Chem 262:1148-1154.

Van Eekelen CAG and Van Venrooij WJ (1981) HnRNA and its attachment to a nuclear protein matrix. J Cell Biol 88:554-563.

van Santen V, Cheung A and Kieff E (1983) Epstein-Barr virus RNA. VII. Size and direction of transcription of virus-specific cytoplasmic RNAs in a transformed cell line. Proc Natl Acad Sci USA 78:1930-1934.

Vaughn JP, Dijkwel PA, Mullenders LHF and Hamlin JL (1990) Replication forks are associated with the nuclear matrix. Nucleic Acids Res 18:1965-1969.

Verheijen R, van Venrooij W and Ramaekers F (1988) The nuclear matrix: Structure and composition. J Cell Science 90:11-36.

Viegas-Pequignot E, Li Z, Dutrillaux B, Apion F and Parkin D (1989) Assignment of human desmin gene to bound 2q35 by non-radioactive in situ hybridization. Hum Genet 83:33-36.

Vogelstein B, Pardoll DM and Coffey DS (1980) Supercoiled loops and eukaryotic DNA replication. Cell 22:79-85.

Wang J, Cao L, Wang Y and Pederson T (1991) Localization of pre-messenger RNA at discrete nuclear sites. Proc Natl Acad Sci USA 88:7391-7395.

Weintraub H and Groudine M (1976) Chromosomal subunits in active genes have an altered conformation. Science 193:848-856.

Weisbrod S (1982) Active chromatin. Nature 297:289-295.

Weiss L (1983) The nucleus, in Histology, Elsevier Biomedical, New York, pp24-34.

Wu C, Murphy C, Callan HG and Gall JG (1991) Small nuclear ribonucleoproteins and heterogeneous nuclear ribonucleoproteins in the amphibian germinal vesicle: loops, spheres, and snurposomes. J Cell Biol 113:465-483.

Xing Y, Johnson CV, Dobner P and Lawrence JB (1993) Higher level organization of individual gene transcription and RNA splicing. Science 259:1326-1330.

Xing Y, Lawrence JB (1991) Preservation of in vivo RNA distribution within the nuclear matrix demonstrated by in situ hybridization coupled with biochemical fractionation. J Cell Biol 112:1055-1063.

Zeitlin S, Parent A, Silverstein S, Efstratiadis A (1987) Pre-mRNA splicing and the nuclear matrix. Mol Cell Biol 7:111-120.

Zeitlin S, Wilson RC and Efstratiads A (1989) Autonomous splicing and complementation of in vivo-assembled spliceosomes. J Cell Biol 108:765-777.

Zieve GM and Sauterer RA (1990) Cell biology of the snRNP particles. Critical Rev in Biochem & Mol Biolo 25:1-46.